Doctoral School of the University of Torino
PhD Program in **Technology Driven Sciences: Technologies for Cultural Heritage**
XXXVII Cycle

Development of an innovative and sustainable coating for the protection of outdoor bronze artworks

Giulia Pellis

Supervisor: Prof. Dominique Scalarone
Co-Supervisor: Prof. Paola Rizzi

UNIVERSITÀ
DI TORINO

University of Torino, Chemistry Department
PhD Program in
Technology Driven Sciences: Technologies for Cultural Heritage
XXXVII Cycle

Development of an innovative and sustainable coating for the protection of outdoor bronze artworks

Giulia PELLIS

Supervisor: Prof. Dominique Scalarone
Co-Supervisor: Prof. Paola Rizzi

PhD Program Coordinator: Prof. Vincenzo Lombardo
Academic years of enrolment: 2021-2024
Code of scientific discipline: CHIM/12 – Chemistry for the Environment and for Cultural Heritage

University of Torino
Chemistry Department
PhD Program in
Technology Driven Sciences: Technologies for Cultural Heritage
XXXVII Cycle

Development of an innovative and sustainable coating for the protection of outdoor bronze artworks

Candidate: **Giulia Pellis**
Supervisor: Prof. **Dominique Maria Scalarone**
Co-Supervisor: Prof. **Paola Rizzi**

Jury Members:

Dr. **Maria Pia Casaletto**
Istituto per lo Studio dei Materiali Nanostrutturati, CNR

Prof. **Cristina Chiavari**
Università di Bologna
Dipartimento di Beni Culturali

Prof. **Sergio Favero Longo**
Università di Torino
Dipartimento di Scienze della Vita e Biologia dei Sistemi

Università degli Studi di Torino, April 2025

“What we call the beginning is often the end
And to make an end is to make a beginning.”

T.S. Eliot

Abstract

Every outdoor bronze artwork is a one-of-a-kind creation with a distinctive history in terms of composition, production process and external exposure to the environment. However, they face a common problem: corrosion phenomena occurring over the surface promoted by degradation agents in the atmosphere. So, there is the need to choose the proper conservation method not to alter the aesthetic and the stability of these precious objects. The most widely used practice for protecting metals is applying a coating on the surface. In general, coatings for conservation are applied to avoid the contact of the metal-patina layer with the actively corroding agents present in the environment. Moreover, an ideal protective coating should prevent the object from degradation without modifying its appearance. Eventually, the properties of these treatments should assure total compatibility with the surfaces involved, good protective performance, reversibility, long-term durability and low-cost maintenance. The most frequently applied coating for bronze protection is Incralac, based on an acrylic resin, namely Paraloid ® B44, containing the inhibitor benzotriazole (BTA) as a corrosion inhibitor that has the role of slowing down the corrosion processes but also exhibits some drawbacks related to lack of stability, poor permanence on the surface and toxicity. Due to these limitations, the search for alternative products to Incralac is of great interest.

This PhD thesis presents a novel sustainable protective coating and a new system for encapsulating corrosion inhibitors that ensure long-lasting permanence over time. Additionally, a novel and easy-to-interpret chemometric approach has been developed to monitor and study the evolution of coatings.

A multi-analytical study on Paraloid® B44 formulations with 5-mercapto-1-pheniltetrazole (MPT) or 2-amino-5-ethyl-1,3,4-thiadiazol- (AEDTA) corrosion inhibitors and UV stabilizers—namely Tinuvin® 312 or Tinuvin® 5050—identified the best combination, with better performance than Incralac. Particular attention was given to the stability of corrosion inhibitors, addressed by encapsulating AEDTA in a complex with methyl-β-cyclodextrin (Me-β-CD), which improved its retention and stability. Simultaneously, an innovative chemometric approach using Principal Component Analysis (PCA) was developed, demonstrating its effectiveness as a tool for monitoring and interpreting the degradation processes of coatings.

Finally, the project explored the optimal application methods and protective properties of the newly formulated acrylic coatings on bronze patinated mock-ups. It was found out that applying two layers of Paraloid ® B44 coatings at different concentration by brush resulted in enhanced protection compared to the bare patina. Furthermore, the most effective formulation was determined to be one that included AEDTA and Tinuvin® 312.

Acknowledgments

I would like to sincerely thank my PhD supervisor, Professor Dominique Scalarone, for her unwavering support and invaluable advice throughout these years. Her mentorship has been fundamental to my scientific growth, helping me gain confidence and independence in my work.

I would like to express my gratitude to the entire InCARE project group. Without your efforts, much of this work would not have been possible. I especially want to thank Prof. Giussani and Dr. Letardi for generously sharing their expertise and for their unwavering support and willingness to help whenever I needed it.

My appreciation also goes to Dr. Emilio Cano, Dr Blanca Ramirez Barat and dr. Teresa Molina from the COPAC group at the Consejo Superior de Investigaciones Scientificas for their supervision during my PhD abroad period. Their guidance, expertise, and generous access to laboratory resources greatly supported my practical and theoretical development.

A heartfelt thank you to the professors and everyone involved in the Be-Archaeo project. I appreciate being included in this amazing project that allowed me to explore Japan and its ancient culture.

A big thank you to all my colleagues-my PhD journey mates for making this path more joyful and less heavy. I couldn’t have asked for better Panettonæ to share this incredible adventure with!

Table of Contents

Chapter 1

General Overview

One of the major topics that modern chemistry has to deal with is the one related to the conservation of Cultural Heritage: indeed, this is a relevant aspect of applied chemistry, strongly intertwined with the social and historical aspects of human life. Artworks and monuments serve as tangible footprints of societies, reflecting their histories and, at times, folklore. In this context, the conservation of Cultural Heritage acts as a bridge to the past, offering invaluable insights for discussions and studies on the reconstruction of human history.

Outdoor bronze sculptures and ornamentations are a prominent facet of Cultural Heritage, deeply embedded in urban landscapes worldwide. These artworks influence our perception of Cultural Heritage and its significance in everyday life. However, preserving outdoor sculptures poses several challenges. These artworks are often exposed to harsh environmental conditions, and maintenance can be hampered by limited funding and the public perception that sculptures can age with aesthetically pleasing corrosion products, which however, could potentially destroy the aesthetic value of the statues and influence their further corrosion. Therefore, there is the need to protect and preserve these invaluable pieces of art for future generations and this is what my PhD project wanted to contribute to.

1.1 Research objectives and methodology

This PhD thesis aimed to develop an eco-friendly and non-hazardous protective coating for outdoor bronze artworks in urban environments. This new coating is an alternative to the currently used products, particularly Incralac, which pose toxicity risks for operators and the environment.

The first step of the research focused on the formulation of the coating, with Incralac as a benchmark. Thus, the acrylic resin Paraloid® B44 was chosen as the film-forming component and, in order to improve safety, the toxic corrosion inhibitor benzotriazole was replaced with corrosion inhibitors with a more favourable toxicity profile. Furthermore, light stabilizers were added to prevent the photooxidative degradation of the acrylic resin.

The coatings were characterized using a multi-analytical approach to fully assess their physical-chemical properties. A wide range of techniques was employed, including Fourier transform infrared spectroscopy (FTIR), colorimetric measurements, differential scanning calorimetry (DSC), determination of the insoluble fraction, and pyrolysis-gas chromatography/mass spectrometry (Py-GC/MS). They were applied on inert supports and aged in a xenon arc chamber for 1000 hours. These multisets of data were studied using Principle Component Analysis (PCA). PCA was able to extract relevant information, providing easily interpretable visual results, and this helped in the selection of the optimal coatings for application on bronze mock-ups. After selecting the best coatings, the project focused on the known issue of the poor permanence of corrosion inhibitors within the coatings. The best performing corrosion inhibitor was encapsulated in green nanocontainers, namely methyl-β-cyclodextrin (Me-β-CD). A comprehensive study of the methyl-β-cyclodextrin/corrosion inhibitor complex was conducted to evaluate its potential for protecting bronze. The results demonstrated the formation of an inclusion complex with a 1:1 stoichiometry and confirmed the effectiveness of the complex in extending the retention of the corrosion inhibitor within protective acrylic coatings.

To test the anticorrosive properties of the coatings, patinated bronze coupons (88.3% of Cu, 5.7% of Sn, 3.9% of Zn, 1.6% of Pb and traces of Ni and Fe) were selected since they represent the traditionally used quaternary bronze alloy. Mock-ups were prepared by an artistic foundry in Milan (*Fonderia Artistica Battaglia*). The patina is the artistic patina "*Verde Messina*"; it was created with copper nitrate as a base layer, followed by ammonium sulphide. The selection of this kind of patina relied on the fact that it simulates a surface with significant reactivity. The coupons were characterized with non-destructive techniques within the PRIN 2022 InCARE

(Innovative Multi-Analytical Characterisation of the Influence of Patina-Coating Interaction on Anti-Corrosive Properties) project, in which I have been taking part since September 2023.

The best coatings selected in the previous steps of the research were applied on these coupons. The application method was deeply studied during a two-month research period funded by Erasmus Traineeship+ at the Laboratories of Consejo Superior de Investigaciones Cientificas in Madrid (March-May 2024).

In December 2024 patinated bronze coupons with the most promising coatings were placed in an urban marine environment at GEMS (Genoa Experimental Marine Station) for weathering in order to test their protective properties in harsh real environmental conditions.

1.2 Organization of the Thesis

Chapter 2 covers a literature review of the corrosion of outdoor bronzes, coatings science, the protective treatments currently investigated, and the strategies for evaluating their performances.

Chapter 4 contains an overview of the results of the research that are presented as a collection of four articles in Chapters 5, 6, 7 and 8. The articles are presented in the form they were submitted for publication or in the final version accepted for publication. Only Chapter 8 is a manuscript still in preparation. The articles are the following:

A) Improvement in the sustainability and stability of acrylic protective coatings for outdoor bronze artworks

G. Pellis, B. Giussani, P. Letardi, T. Poli, P. Rizzi, B. Salvadori, A. Sansonetti, D. Scalarone

Published in *Polymer Degradation and Stability* 218 (2023) 110575
DOI: 10.1016/j.polymdegradstab.2023.110575

B) Advancing preservation: a chemometric approach for monitoring the degradation of protective coatings for bronze statues

G. Pellis, M. Tiburziano, B. Giussani, P. Letardi, B. Salvadori, A. Sansonetti, D. Scalarone

Published in *Microchemical Journal* 210 (2025) 112971.

DOI:10.1016/J.microc.2025.112971

C) Enhancing permanence of corrosion inhibitors within acrylic protective coatings for outdoor bronze using green nanocontainers

G. Pellis, F. Caldera, F. Trotta, T. Biazoli de Oliveira, P. Rizzi, T. Poli, D. Scalarone

Published in *Molecules 28 (2024) 5702*
DOI: 10.3390/molecules29235702

D) Optimizing application methods of sustainable acrylic protective coatings for patinated outdoor bronze artworks

G. Pellis et al.

Manuscript in preparation

Chapter 9 includes the conclusions, as well as perspectives and suggestions for future research.

Chapter 2

State of the Art

This chapter describes the relationship between environmental factors and metal surfaces, highlighting its effects on the appearance and structural integrity of bronze artworks. Furthermore, the formation and characteristics of patinas that develop over time due to environmental exposure are explained. A section of the chapter also deals with the study of coating science, presenting the properties and mechanism of action of the most relevant kinds of coatings typically employed. This will be followed by a thorough overview of traditional coatings that have been used for decades, as well as an examination of innovative coatings that are currently being investigated. The final part of the chapter reviews the most commonly used methods for evaluating coating performance.

2.1 The effects of the outdoor environment on bronzes

Metals and their alloys have been crucial in technological advancement throughout history. In ancient times, the ability to mine and work various metals often determined the dominance and political success of one civilization over others. Metals were primarily used for making utensils and portable items and serving as key materials in constructions and decorative elements of buildings [1]. During the Bronze Age, civilizations gained a significant technological advantage by discovering that incorporating specific elements, mainly tin and arsenic, into copper strengthened the metal and reduced the release of oxygen bubbles during casting [2]. The enhancement of copper-based alloy has made it possible to create more complex shapes and allow the formation of functional tools, vessels, and artworks. Over the centuries, advancements in metallurgical technology and material availability led to various compositions of bronze alloys used in artistic endeavours. This made it challenging to classify bronze as a single material. However, different types of bronze share common properties since they have a high copper content within the alloy. In art and ornamentation, especially during the 19th century, the commonly used types of bronze included copper-lead-tin-zinc alloys or pure copper. Moving to the 20th century, silicon bronze alloys gained popularity [3] as the demand for innovative, Pb-free

alternatives increased due to environmental and health concerns associated with lead (Pb). Artistic foundries widely use silicon bronzes, such as Cu-3Si-1Mn, valued for their excellent corrosion resistance, good weldability, remarkable castability, and golden colour. This alloy is particularly employed in bearings, bells, impellers, pump and valve components, marine fittings, statuary, and monuments. [4,5]

Alloying and casting techniques have evolved over time, as well as the effects of outdoor exposure on bronze objects, which have changed significantly since the Industrial Revolution. During the third millennium BCE, the primary environmental factors influencing bronze exposure included oxygen, water, and chloride salts, particularly in coastal regions. When copper alloys come into contact with air, they develop an oxide layer known as cuprite (Cu_2O) [1,6]. This naturally occurring oxide film forms slowly, typically appearing as a thin, smooth, and compact layer that offers moderate protection in non-aggressive environments. Alloying elements significantly influence the oxidation rate of copper; for instance, tin generally slows the process, whereas nickel tends to accelerate it [3]. The oxidised surface of bronze, depending on the composition of the alloy, can exhibit colours ranging from golden to reddish to blackish-brown and in the artistic context is often called patina. (Figure 1)

Figure 1: On the left, a section of Ascanio Sobrero's statue located in Turin (1914); on the right, a detail of Napoleon as Mars Peacemaker located in Milan (1809-1811)

Over time, urban industrial environments have introduced new challenges for outdoor materials, including exposure to corrosive pollutants like sulphur dioxide (SO_2), a byproduct of fossil fuel combustion. Acid rain, resulting from the dissolution of sulphur oxides and nitrogen oxides in water, and also containing ammonia, organic compounds, and soot, has further exacerbated these challenges [7]. Concerns about the impact of acid rain impact on Cultural Heritage surged in the 1970s, leading to predictions of significant losses in sculptural details of monuments and statues by the end of millennium [8].

Clean air policies implemented in Europe and the United States have reduced SO_2 emissions, leading to shifts in the composition of corrosion products on bronze surfaces [9–13]. However, concentrations of nitrogen oxides and ozone continue to be high globally [10]. Atmospheric pollutants play a crucial role in the natural weathering of metals and their alloys, a process further intensified by climate change, which increases tropospheric reactivity [13]. Alterations in atmospheric composition—

closely linked to climate change [14]—affect the acidity, oxidation capacity, and reaction kinetics of the environment, thereby impacting on outdoor sculptures exposed to diverse conditions [13]. In the Mediterranean area, rising temperatures increase thermoclastism, a process where temperature fluctuations create thermal stress that leads to material cracking [15]. In contrast, northern Europe experiences an increase in freeze-thaw cycles and frost events, which result in more damage to metal surfaces. In these conditions, water infiltrates pores or cracks, freezes, and expands, accelerating deterioration.

Additionally, high level of atmospheric humidity and shifts in rainfall patterns are significant factors in corrosion. For instance, the dissolution and recrystallization of salts during repeated wet-dry cycles hastens degradation. Moreover, moisture promotes microbial growth, which indirectly speeds up decay by driving biochemical reactions that corrode or destabilize metal surfaces [16].

The warming of the troposphere and the increase of humidity enhance chemical reaction rates on metal surfaces, accelerating oxidation and corrosion. Changes in the chemistry of atmospheric deposition, such as shifts in pH, also affect how these substances react with metals, adding complexity to the dynamics of corrosion. However, not all climate-related effects are harmful. In areas with milder winters, reduced frost damage may improve the durability of certain materials. Additionally, increased pH levels in atmospheric deposition—caused by changes in pollution sources—can slow corrosion rates, potentially providing some protection to metal surfaces [15].

Atmospheric corrosion, though not fully understood, is recognized as an electrochemical process governed by a thin moisture film acting as a conductive medium. Within this film, metal oxidation releases ions, while dissolved oxygen reduces to form hydroxide ions. Upon evaporation, hydroxides or oxides precipitate, forming patinas on metal surface whose colours range from bluish-green to brown and black [17].

Long-term environmental exposure creates patinas that are inherently heterogeneous[1,9]. This variability is shaped by environmental factors—whether urban, marine, or industrial ones [18]—and alloying elements in the material. For instance, tin (Sn), zinc (Zn), and lead (Pb) significantly influence the patina morphology and composition. Among these, tin promotes the accumulation of insoluble products on the surface [7,19]. Moreover, differences in patina colour correspond to compositional variations, while the exposure geometry—whether

sheltered or unsheltered—affects the development of the patina. Sheltered conditions promote multilayered patinas rich in copper- and lead-based compounds, while runoff exposure creates thin, porous layers enriched in insoluble tin oxides. Additionally, copper, zinc, and lead ions can migrate and leach into the environment [4,20].

Once formed, patinas offer relative stability, acting as protective barriers under many environmental conditions. However, changing environmental factors can destabilize patinas, leading to surface discolouration and accelerated corrosion. Loose, porous corrosion products lack the protective qualities of dense, adherent layers, exposing the metal to further degradation and, without adequate preservation, eventual dissolution [21].

Urban environments introduce additional complexity. Here, sulphur-based pollutants from industrial activities, transportation, domestic heating, and other anthropogenic sources dominate, forming basic copper sulphates. Amorphous copper sulphate initially forms from cuprite, transitioning into crystalline phases depending on pollution and exposure conditions. Under specific conditions, such as a pH below 3.5 with high copper and sulphate ion concentrations, antlerite [$Cu_3(SO_4)(OH)_4$] can form, particularly in stagnant moisture layers [6,22].

In marine or chloride-rich urban environments, copper hydrochlorides like atacamite [$CuCl(OH)_3$] develop from nantokite [CuCl] precursors (Figure 2). Beyond sulphates and chlorides, minor quantities of other minerals, including gerhardite [$Cu_2NO_3(OH)_3$], and malachite [$Cu_2(CO_3)(OH)_2$], are also present. Small amounts of organic compounds, such as copper formates and acetates, are also detected. These compounds, formed by atmospheric organic acids, play a complex role in metal corrosion [23].

The stability of patinas in aggressive environments depends on the thermodynamic properties of copper salts. Graedel and colleagues[4,9] demonstrated that brochantite [$Cu_4(SO_4)(OH)_6$] is significantly more stable—100 times less soluble than chlorides or carbonates and 10,000 times less soluble than nitrates [23]. Consequently, it is commonly the most prevalent outer-layer corrosion product in bronze patinas.

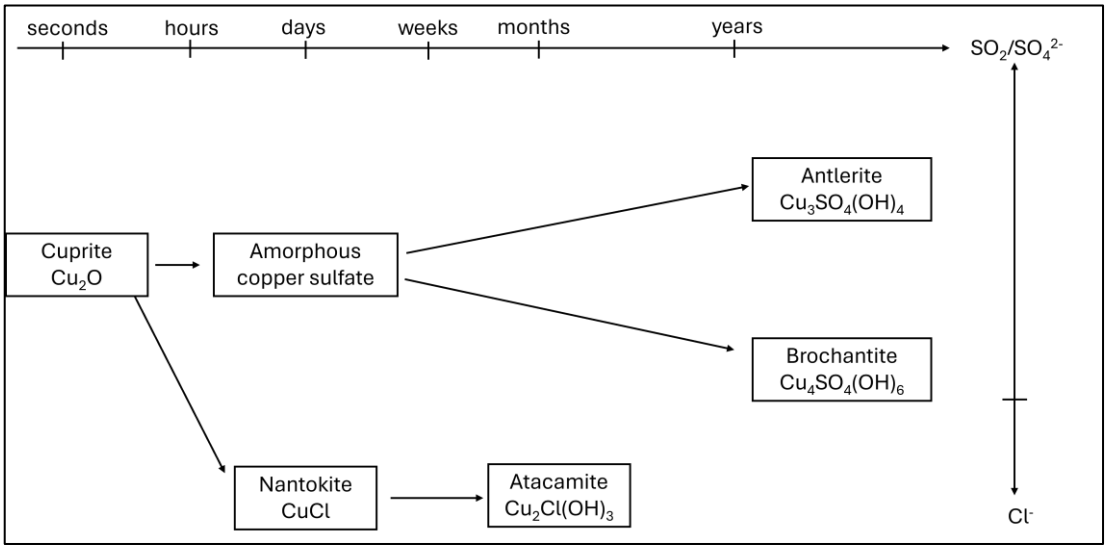

Figure 2: Scheme of corrosion products formed in sheltered conditions. Inspired by Krätschmer et al. [18]

The characteristics of the patina, including chemical stability, solubility, hygroscopic behaviour, and physical properties (density, porosity, homogeneity, and coverage), are critical in determining their protective effectiveness. While patinas formed under acid rain often exhibit disfiguring and unstable properties, with dominant minerals like cuprite, brochantite, antlerite, and atacamite, environmental conditions create visual and structural complexities. For example, copper sulphates typically render bronze surfaces light green, but environmental factors like wind, rain, and particulate deposition can lead to unsightly black crusts or streaks. Raised black areas adjacent to green spots suggest localized cathodic protection, accelerating dissolution in surrounding areas [4,24,25].

Patinas, whether naturally or artificially formed, remain central to preservation and aesthetic value of metal objects. However, understanding their protective or corrosive nature requires careful evaluation, as they are inherently porous, permeable, and prone to reforming under environmental influence. Thus, the complex interplay between patinas and their environment underscores the importance of targeted conservation efforts.

2.2 Coatings science

The issue of corrosion in bronze and copper alloys in outdoor environments primarily arises from the electrochemical conversion of metal into metal ions. For

engineers, this presents a significant metallurgical challenge: the goal is to minimize both general and localized corrosion of pure metals in applications such as bridge components, roofing, and vehicles. While aesthetic considerations are important for consumer goods like cars, they mainly focus on maintaining a like-new appearance.

One practical approach to enhance corrosion resistance in outdoor environments is using protective organic coatings. The industrial significance of these coatings has led to the development of the field known as coating science, which has attracted considerable attention from the paint and automotive industries [26]. The following overview briefly outlines some key principles and current perspectives in this area.

Adequate surface preparation is essential for achieving optimal coating performance in the coatings industry. This process begins with ensuring a clean surface with good wetting and adhesive properties suitable for the intended coating. Contaminants such as oil, dirt, and corrosion products on the metal surface can compromise the adhesion of the coating. Additionally, dirt and corrosion minerals are hygroscopic, meaning they attract moisture, which can further worsen corrosion [27].

To ensure sufficient wetting during the application of a coating, the surface tension of the coating must be lower than that of the metal surface. Cleaning the metal surface helps to lower its surface tension, allowing for better wetting. Good wetting promotes effective contact and spreading, resulting in superior adhesion and film quality. Roughening the surface can increase the surface area and potentially enhance the adhesion of the coating; however, if the surface is too rough, it may create voids underneath the coating, leading to poor wetting characteristics[28,29].

Good coating quality, defined by a relative lack of defects, is essential for effective corrosion protection. Coating defects not only impact aesthetic appearance but also diminish performance in aggressive environments. This is especially true for significant defects such as bubble holes and cracks [30].

One common issue is “pin holing”, which can occur due to solvent popping or air entrapment during application. These small holes allow air and moisture to infiltrate, potentially leading to localized corrosion pits. Another defect, known as "orange peel," occurs when the coating does not flow smoothly due to rapid solvent evaporation. This creates tensions that result in a bumpy surface as the coating dries, becoming visible in reflected light. The “orange peel” effect leads to variations in thickness at a micro-scale, affecting the coating performance by creating local differences in permeability and generating electrochemical and osmotic pressure gradients. Other common coating defects include seeds and cratering. These issues manifest as small wells and

dimples caused by dust and other contaminants on the surface during application. Like the “orange peel”, these defects lead to fluctuations in local thickness that can compromise the coating effectiveness [31].

Achieving good coating quality requires meticulous practices and technical skills. However, the application of coatings using spray or brush techniques can lead to various defects. To minimize these defects, it is generally recommended to apply multiple thin layers of coating, preferably perpendicular to each other. A thin wax topcoat may provide some benefits; however, it may not significantly increase the overall thickness of the coating. Operators should exercise caution to ensure the layers do not create undesirable thickness variations or leave residues that could result in interlayer delamination. Additionally, layering can worsen residual stresses that develop during film formation and may lead to issues such as adhesion loss, cracking, or crazing [31,32]. It is interesting to consider whether “orange peels” might also relate to stress-induced loss of adhesion or cohesion. When a coating is applied properly, its performance can vary greatly based on its inherent protective properties and stability in outdoor environments. Several characteristics are desirable for coatings to ensure good outdoor durability, including strong ultraviolet light (UV) resistance, sufficient flexibility to withstand thermal stresses, chemical compatibility with the metal surface for enhanced adhesion and chemical resistance to the environment, and relatively low permeability to oxygen and water.

High-quality pigments offer significant benefits in terms of UV protection. For clear coatings, UV protection typically comes from innate chemical stability, UV absorbers and other stabilizers, such as hindered amine light stabilizers [27]. Flexibility is not a precisely defined attribute, but some flexibility should be incorporated into the chemical and/or physical structure of coatings to prevent stress buildup during application and service, which can lead to loss of adhesion and cracking.

For example, chemical compatibility with metal can be improved in polymer coatings by including polar hydroxyl or carboxylic groups that are attracted to the oxides and hydroxides of the metal surface in their structure. However, it is important to note that these groups may increase water permeability due to a solvency effect. Low permeability is best accomplished with a high-density coating, such as those made from crosslinked polymers. Ideally, the crosslink density in the coating should be as uniform as possible. However, excessively high crosslink density can also lead to stress buildup in the film.

Unfortunately, engineering all these desirable qualities into a single coating material is challenging, if not impossible. A more effective approach is to design a coating system that combines these attributes. For instance, a three-part system can usually be employed: the primer coating ensures good adhesion to the metal, the middle coat provides durability and other desirable properties, and the topcoat enhances low permeability [3].

Developing a coating suitable for metal artworks presents several challenges, particularly regarding aesthetics and the decision of whether or not to apply it. Each artwork is a unique case, and the requirements for protective treatment can vary significantly. It is essential not to alter the original surface of the object, which is achieved by using only clear, thinly applied coatings, thereby reducing the potential for developing more performative coatings. Additionally, the formulation must be simple to prepare and apply, enabling conservators to work efficiently and effectively. Paragraph 2.3 outlines current approaches and methods in the conservation of outdoor bronzes and will discuss briefly the conservation/restoration point of view.

2.2.1 Degradation of polymeric coatings

Polymeric coatings exposed to outdoor conditions are subjected to the effects of environmental agents, pollutants, chemicals, sunlight, and thermal variations. The extent to which these factors contribute to the degradation of the polymer product is closely tied to its structure and chemical composition.

Degradation processes usually occur slowly, but even minor changes can significantly impact the properties of a coating. Small structural alterations can greatly reduce the molecular weight, which is essential for many polymer properties. Polymers are made up of long chains of carbon-carbon (C-C) bonds, and breaking even just one of these bonds can halve the molecular weight.

Exposure to solar radiation can negatively impact the integrity of coatings. Polymers may absorb ultraviolet radiation, due to impurities or their inherent chemical structure, particularly if they contain chromophore groups that are excited by light and transfer energy to the polymer chain. Typical photochemical reactions occur when carbonyl, aromatic, or double bond groups are present. If the absorbed energy is sufficient to break C-H or C-C bonds, free radicals form, which readily react with oxygen, initiating chain reactions that lead to structural rearrangements or chain scission. These changes compromise the chemical and physical properties of the polymer. In the presence of oxygen, photo-oxidative processes occur (Figure 3). The result can be the appearance of cracking, which undermines the barrier function of the

coating, reduced resistance to deformation, colour changes, and the potential loss of transparency—an essential property for protective coatings used in the conservation of Cultural Heritage. Photo-oxidative processes typically follow slower kinetics than thermos-oxidative ones.

Rising temperatures accelerate degradation, triggering reactions that may affect the main polymer chain. This can lead to either scission or cross-linking, depending on the specific chemical structure. If side groups are affected, the molecular weight might remain unchanged, but degradation products can be released. In the presence of oxygen, thermo-oxidative reactions are triggered.

The degradation mechanisms induced by temperature or UV exposure are complex and depend on the polymer structure. Generally, reactions begin with the formation of radicals via primary covalent bond dissociation or hydrogen loss. This is followed by propagation, where radicals stabilize either by reacting with oxygen to form hydroperoxides and peroxides, or by inter- or intramolecular radical transfer, leading to reduction in molecular weight and loss of small fragments, or by depolymerization, leading to the formation of monomers.

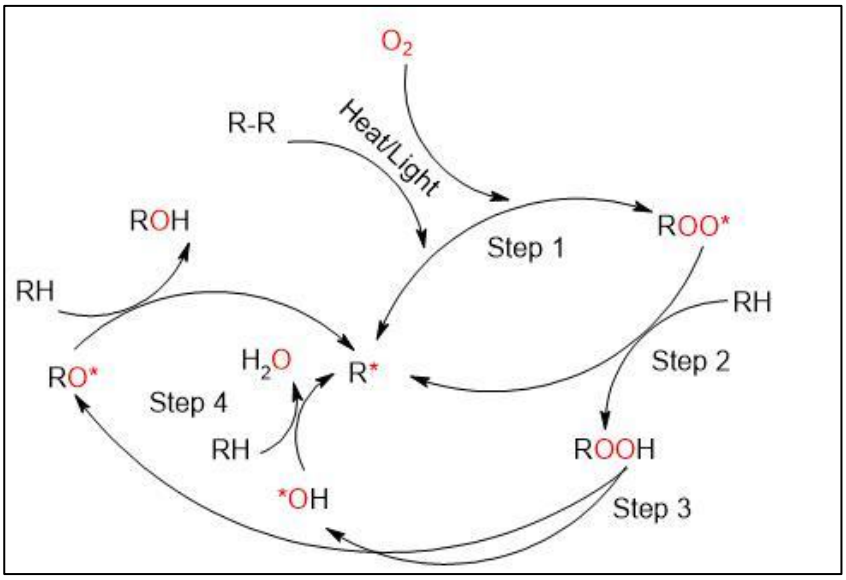

Figure 3: Typical radical oxidative degradation process of polymers

In addition, structural rearrangements (e.g., double bond formation) or extensive cross-linking may also occur, which stiffen the structure and reduce flexibility.

Acrylic and methacrylic polymers exhibit good stability and resistance to degradation. However, prolonged UV exposure combined with oxidation can trigger chain radical reactions, resulting in the formation of various functional groups, such as aldehydes, ketones, hydroxyls, anhydrides, lactones, or carboxylic acids. Degradation of acrylic or methacrylic resins is highly influenced by the alkyl side groups attached to the ester. Paraloid® B72 and B44 exhibit good resistance to oxidation and degradation due to their short side groups. Paraloid ® B72 is a copolymer of methyl acrylate/ethyl methacrylate (MA/EMA) while Paraloid ® B44 is a ethyl acrylate/methyl methacrylate copolymer(EA/MMA). In general, chain scission processes dominate, while in similar copolymers with longer side groups, cross-linking processes prevail [33,34].

2.2.2 UV stabilizers

To enhance the weather resistance of coatings intended for outdoor use, organic and inorganic additives can be incorporated into the formulation to provide light stability.

Several studies have demonstrated that organic stabilizers, such as HALS (Hindered Amine Light Stabilizers) and UVAs (Ultraviolet Absorbers), offer excellent light stability. Adding these additives can increase the weather resistance of polymer coatings by two/three times. Additionally, metal oxides nanoparticles (e.g., SiO_2, TiO_2, ZnO, ZrO_2) can absorb UV rays, thereby protecting polymers [35,36].

Among organic light stabilizers, two main categories can be identified:

- Ultraviolet Light Absorbers (UVAs)
- Hindered Amine Light Stabilizers (HALS)

UVA additives absorb ultraviolet radiation before it reaches the material to be protected, then reemit the absorbed energy as weak thermal energy. These additives exhibit a high absorption coefficient in the ultraviolet range of the electromagnetic spectrum. A noteworthy class of UVA additives consists of molecules containing phenolic groups, which enable energy dissipation by forming O–H–O bridges, such as salicylates, 2-hydroxybenzophenones, xanthones, or O–H–N bridges like 2-(2-hydroxyphenyl)benzotriazoles and 2-(2-hydroxyphenyl)-1,3,5-triazines. These intramolecular hydrogen bonds facilitate energy dissipation through a radiative mechanism where proton transfer is crucial, allowing the molecule to return to its initial configuration after releasing thermal energy.

In contrast, HALS do not absorb UV radiation but inhibit the radical degradation of the polymer. These compounds are typically derivatives of tetramethylpiperidine containing an amine group. Also known as "free radical scavengers", HALS effectively neutralize radicals present in the material. HALS stabilizers are oxidized to nitroxyl radicals, which react with free radicals to form intermediate amino ethers.

These intermediates subsequently react with peroxide radicals regenerating the original molecule, which re-enters the cycle, and producing non-radical byproducts [37,38].

2.3 Preservation challenges: current approaches and research developments

2.3.1 Current methods of protection of outdoor bronze

The evolution of coatings has progressed from using oils and varnishes in antiquity to contemporary lacquer and polymer finishes. The earliest known coatings can be traced back to the Greek and Roman time, where oils or protective varnishes derived from pine tar pitch were used to protect sculptures, enhancing their burnished appearance [39]. By the late Roman Empire, the aesthetic preferences shifted, leading to the use of waxes and black lacquers as coatings. This trend continued into the Medieval period, and by the Renaissance, red-brown translucent lacquers began to gain popularity [40]. During this period, darker lacquer coatings were also utilized to conceal casting flaws and repairs necessary to create bronze sculptures [39]. The current treatment technologies employed in conserving bronze sculptures are largely derived from traditional practices and industrial applications. However, past research has been limited in addressing how to tailor these materials and methods to meet the specific needs of conservation. As a result, conservators have widely recognized that these techniques often fall short of effectively accommodating the diverse requirements and unique conditions encountered in conservation work [18,41].

Conservation applications differ from industrial applications primarily in terms of aesthetic considerations and physical and chemical properties. Industrial coatings are intended for freshly stripped, sandblasted, and primed metal surfaces. In contrast, the surfaces of artworks and historical objects often cannot be treated in this way without causing significant damage. Conservation efforts face challenges because they typically involve applying coatings to uneven, contaminated surfaces that can be naturally or artificially corroded. This complexity makes it difficult to establish a uniform list of desirable coating properties for outdoor bronze artworks, as the

requirements can vary significantly from one piece to another. Over time, the understanding of the essential characteristics of coatings has evolved, and products developed three decades ago may lack many of the features deemed necessary today. Advances in coating technology and the broader field of coating science have further refined the development of modern protective solutions, enabling better alignment with current conservation needs [42].

The unique characteristics of heritage objects arise from a complex history that is often not completely understood. This is evident in the corrosion products that develop over years or even centuries. In many cases, these corrosion products preserve valuable information about the original shape of the object, its decoration, and manufacturing techniques. Therefore, it is essential to preserve these features [43]. Moreover, to effectively apply the principles of corrosion science to the conservation of metal heritage objects, it is essential to consider the specific metal or alloy, the manufacturing techniques, and the specific corrosion issues related to indoor (museums) or outdoor conditions, or archaeological settings [44].

The initial step of the conservation/restoration process is cleaning. The cleaning methods should specifically target removing water-soluble compounds, atmospheric particulate deposits, and hydrocarbon residues from previous treatments or unsuccessful coatings. Simultaneously, preserving the valuable patina for aesthetic, historical, and conservation purposes is crucial [44].

After cleaning, applying treatments to prevent or reduce harmful corrosion is a common practice. For outdoor bronze, this typically involves the use of coatings that prevent direct contact between the metal or patina layer and actively corroding agents in the atmosphere, such as water and corrosive ions. Additionally, corrosion inhibitors may be applied to slow down the electrochemical reactions that cause corrosion.

2.3.2 Protective treatments

When treating outdoor bronze sculptures, it is crucial to apply a protective coating to ensure the sculpture lasts over time. Without this sacrificial coating, the underlying metal is prone to corrosion, leading to physical damage and changing the sculpture's appearance from what the owner or artist originally intended [26]. So, restorers and conservators have carefully developed the conservation methods over the centuries [45].

Conservation science has developed rapidly in the early 20th century. Despite this, the conservation and restoration of metals remains one of the most complex challenges

in the field. As a result, numerous scientific investigations have been conducted to explore new conservation techniques that could serve as alternatives to traditional methods. These studies primarily focus on developing higher quality, faster, more economical preservation approaches that offer long-term anticorrosion benefits for the conservation and restoration of metals [46]. As a matter of fact, it is imperative to consider ecological, economic and social aspects while looking at the solutions offered by scientific research [47]. Despite efforts to find alternatives, wax and Incralac® remain popular choices for protecting bronze surfaces [48].

The actual conservation perspective focuses on new eco-friendly and safe treatments. Treatments applied to heritage objects should observe specific requirements. An ideal sustainable coating should prevent the object from degradation without modifying its appearance: in this view, only transparent coatings are allowed. Moreover, the application method should be straightforward, and the chemical nature of the treatments should allow their removal with a safe and non-toxic approach. Eventually, the properties of these treatments should ensure total compatibility with the surfaces involved, good protective performance, long-term durability, and low-cost maintenance [44,45].

This section will now provide a concise overview of the most commonly used coatings and highlight recent innovations in coating solutions.

2.3.2.1 Traditional coatings

2.3.2.1.1 Waxes

The earliest coatings used for outdoor bronze sculptures often included oils such as lemon oil, paraffin oil, linseed oil, castor oil, and waxes like carnauba or beeswax mixtures—tinted, clear, or natural [35]. These coatings are known to saturate matte patinas, darkening the surface and accumulating dust [45]. Drying oils can last up to one year, becoming increasingly insoluble over time. Waxes, commonly employed to provide lustre and protect surfaces, require reapplication every six months due to their limited durability. They serve as barriers against moisture and oxygen, protect the metal from handling, and are often used as topcoats to enhance the longevity and appearance of varnishes by reducing their shine. Conservators prefer waxes for their natural finish, avoiding the artificial gloss often associated with other coatings. However, natural waxes, particularly those derived from animals, can contain free acids that damage metal surfaces and are prone to acid hydrolysis. Consequently, synthetic paste waxes are preferred for outdoor applications [3].

Since the 1980s, professional conservators favoured many recipes based on microcrystalline waxes. These synthetic waxes, derived from petroleum, can be straight-chain, cyclic, or branched products. Their small crystal size allows them to be closer to the amorphous state, which is beneficial for application. Conservators often create customized formulations by mixing microcrystalline wax with other synthetic waxes, such as polyethylene wax, to achieve higher melting points and better performance. Wax coatings perform better on patinated bronzes than on untreated metal surfaces [49] and they have also shown better results when used on monuments than on artificial coupons [50]. Probably, waxes are more effective in creating a barrier in porous surfaces, being retained inside the pores. While some studies report wax durability of 23–48 months for outdoor exposure (particularly when combined with benzotriazole) [50,51], performance significantly declines in marine environments where chlorides accelerate degradation [52]. Although waxes are widely used for outdoor conservation, they are arguably better suited for indoor environments, where conditions are less aggressive. Renaissance Wax, for example, was specifically formulated for indoor use but has been adapted to broader applications despite limited supporting studies [45]. Waxes offer poor corrosion protection compared to varnishes and display limited weathering resistance, necessitating frequent renewal. Residual wax complicates future treatments, as residues can be incompatible with other conservation materials. However, they remain popular for their accessibility and ease of application. To overcome these drawbacks, waxes are sometimes used in conjunction with acrylic resins or as part of triple-layer systems (e.g., wax/acrylic polymer/wax) [44]. In such systems, wax can act as a priming layer to mitigate the effects of thermal expansion on the coating, improve reversibility, and enhance protection.

2.3.2.1.2 Acrylic coatings

Together with waxes the most representative traditionally used coatings are acrylic resins (e.g. Incralac, Paraloid® B72, Paraloid® B44) [53].

Acrylics are a class of transparent thermoplastic resins derived from acrylic and/or methacrylic polymers or copolymers, commercially introduced in the 1930s. In the 1960s and 1970s, they became widespread in the field of conservation, due to their transparency, mechanical robustness, adhesion, and chemical stability. Since then, acrylic resins have been widely used in the conservation practice as protective coatings and adhesives for many materials, including metals. Long-term research at the Canadian Conservation Institute showed that after 12–15 years of artificial light ageing

equivalent to 45 years in a museum, most acrylics exhibit good stability with minimal yellowing and only slight mechanical degradation [45,54].

Among the numerous acrylic formulations available, the Paraloid family by Rohm & Haas (formerly Acryloid in the U.S.) is one of the most used in metal conservation. As a matter of fact, Paraloid® B72, Paraloid® B44 and Incralac are the most common products in metal conservation. Other acrylics used for metal protection are Paraloid® B48-N, Paraloid® B67 and Paraloid® B82. Paraloid® B72, being considered the most stable thermoplastic resin soluble in hydrocarbon solvents, is also the most popular polymer used in conservation both as a consolidant, adhesive and protective coating [45].

Paraloid® B-48N, a copolymer of methyl methacrylate and butyl methacrylate, offers enhanced adhesion and abrasion resistance on metal surfaces. It was developed shortly after Paraloid® B44 and serves as the base resin for Permalac, another coating for metal conservation [58]. Literature on the use of other Paraloid® coatings (B67 or B82) for metal protection is quite limited. Paraloid® B67 is the less preferred due to its chemical structure, which is more susceptible to thermal and photodegradation. Polymers with longer ester groups, like butyl acrylates, are more prone to crosslinking and fragmentation reactions than other acrylics [33,34,59], which can affect their protective properties and the reversibility of the treatment.

Incralac, developed in 1964 by the International Copper Association (formerly INCRA), is the most widely used modern coating for outdoor bronzes. Its expected lifespan is around 3–5 years on outdoor bronzes and up to nine years with wax topcoats and regular maintenance [3,55]. Incralac is a combination of Paraloid® B44, benzotriazole (BTA) and other additives. Paraloid® B44, a copolymer of ethyl acrylate and methyl methacrylate, was chosen among the other acrylics because it provides the best protection, having good physical properties and corrosion resistance [56]. Over the years, several changes have been made to the initial formulation to meet the increasingly stringent requirements of environmental regulations. Its performance depends on the chemical composition of the patinas, solvents and additives. The exact formulation of this product has not always been clear and its use has involved different methodologies, substrates and application techniques [44]. The outdoor performances do not match with the conservation goals of low maintenance, good protection and easy removal; however, its use is still quite intense because there is no quantitative proof of significantly better performing substitutes [57].

Extensive studies on these materials, particularly Incralac, have provided valuable insights into their performance. Acrylic resins remain indispensable in conservation, offering a versatile and durable solution for protecting metals and other materials.

2.3.2.2 Other coatings

In the last decades, organosilanes, carboxylates, fluoropolymers and triazoles have been the most experimented coatings to protect copper and its alloys. More recently, innovative solutions, such as nanocomposites and biopolymers, have been explored [42]. An improvement of the protective ability of the coating and longer life are sought, as well as the reduction of the toxicity, among others, of the solvents needed for application [41,44].

2.3.2.2.1 Silane based coatings

Over the past 50 years, silane-based coatings have emerged as a promising alternative for protecting various metals in diverse applications. This advancement is largely attributed to the development of sol-gel coatings derived from alkoxysilanes, offering an environmentally friendly solution compared to traditional chromate- or phosphate-based chemical conversion treatments, which are highly toxic. Silane sol-gel coatings exhibit several advantageous properties, including adaptability to various application techniques, low processing temperatures, strong adhesion, and good penetration into both the metal surface and patinas. Consequently, these coatings hold significant potential for the conservation of heritage metal artefacts [45].

Initial studies on bronze protection, focused on ORMOCERs. These organic-inorganic copolymers feature a multi-component formulation incorporating a cross-linkable epoxy-functionalized alkoxysilane and one or more network modifiers [60]. Applied to both bare and patinated bronze and subjected to artificial ageing, ORMOCERs demonstrated excellent adhesion and sustained performance, especially when applied as a bilayer on patinated bronze [61]. However, they also showed limited reversibility (often requiring mechanical methods to be removed) and potential colour changes.

Among the most studied alkoxysilanes, 3-mercaptopropyl-trimethoxysilane (PropS-SH) has proven particularly promising. The thiolate bond it forms creates highly protective layers on copper, enhancing the adhesion of the coating to the substrate [62]. Studies have examined the influence of curing temperature and time on the silane layer [63], as well as its substrate affinity with copper and bronze [64]. In terms of protective efficiency, PropS-SH has given excellent results. For example, on

patinated bronze samples exposed to acid rain, a 97% inhibiting efficiency was achieved after 30 days, while Incralac obtained 89% [5]. However, some limitations were found, mainly its susceptibility to photo-oxidation and hydrolysis under UV radiation and high temperature. To overcome these problems, research has explored the addition of nanoparticles, such as TiO_2 or LaO_3, to enhance stability, as well as the encapsulation of inhibitors, such as in β-cyclodextrin, to improve protective performance [65–67].

The hydrophobicity of silane-based systems also offers advantages for heritage conservation. While TEOS (Tetraethyl orthosilicate**)** has primarily been applied to stone materials, some studies have extended its use to metals like bronze and brass. For instance, modifying TEOS with 3% SiO_2 sol solutions under alkaline conditions using hexamethyldisilazane (HMDS) resulted in coatings with good hydrophobic properties. However, their protective capabilities remain limited, as indicated by polarization resistance (Rp) values, which were higher for bare bronze than for coated samples [68].

2.3.2.2.2 Flourinated coatings

Fluorinated coatings are organic polymers in which some or all of the hydrogen atoms bonded to carbon are replaced by fluorine. These coatings are categorized into two main types: perfluorinated polymers, which consist only of C–F and C–C bonds with trace amounts of other elements, and partially fluorinated polymers, which include hydrogen or other atoms alongside fluorine and carbon. Since the 1990s advances in polymer synthesis have allowed the development of diverse fluoropolymers with properties tailored by the fluorine content and its distribution. Among these, polytetrafluoroethylene (PTFE), polyvinyl fluoride (PVF), and polyvinylidene fluoride (PVDF) are the most used in coatings, with PVDF being particularly notable for applications on outdoor metal objects due to its chemical inertness, UV resistance, and durability in aggressive environments [45]. However, PVDF inherent chemical inertness also produces poor adhesion to substrates, and for this reason, it was blended with acrylic modifiers [69].

Recent research has focused on fluorinated acrylic (FA) copolymers combined with adhesion promoters, like modified polymethyl methacrylate silane (MS) to further enhance adhesion. When applied to pre-corroded bronze, this combination has demonstrated inhibitory efficiency after 30 days of accelerated ageing, mainly when applied as a premixed product rather than in layers [70].

As research advances, these innovative fluoropolymer-based products s progress, providing practical and reversible solutions for the protection of heritage metal objects.

2.3.2.3 Environmentally-friendly coatings

Recently, research has increasingly focused on developing eco-friendly and sustainable approaches to preserve Cultural Heritage. Significant advancements have been made in developing bio-based corrosion inhibitors and green coatings. Although these novel applications are still sporadic and not yet part of established conservation methods, they can represent a promising direction for the future of conservation science. Currently, the lack of systematic investigations on the performance of these new coatings poses challenges in evaluating their effectiveness in practical conservation scenarios. Nonetheless, the prospect of "green" alternatives deserves attention [42].

A significant example in the field of biofilms is the use of fungal strains to combat corrosion processes. The potential for using fungal species on bronze arises from their ability to produce oxalic acid. This acid helps converting copper corrosion compounds into stable and less soluble products, which do not participate in the corrosion reactions. Albini et al. [71] investigated the effectiveness of a novel biological treatment utilizing a specific fungal strain of *Beauveria bassiana* as an alternative method for stabilizing copper-based alloys. This treatment demonstrated promising properties related to environmental and health concerns, given that it is already employed in organic agriculture. Results showed that the interaction between unsheltered areas of tin-enriched bronze surfaces and the treatment was effective, producing tin- and copper-based oxalates. These compounds were also found after severe runoff conditions, indicating good adhesion of the treatment [71].

Another example is polylactic acid (PLA), which is biodegradable and produced from totally renewable materials. Giuntoli et al.[72] introduced an innovative PLA-based polymer designed for the protection of metallic surfaces. They conducted the polymerization reaction without solvents, adopting a green chemistry approach, and incorporated benzotriazole (BTA) group to enhance corrosion inhibition. Their research indicated that the polymer could serve as an effective protective coating; however, additional studies are necessary to gain a deeper understanding of its anticorrosive efficiency.

Giuliani et al. [73] evaluated the protective effectiveness of chitosan on copper-based alloys. Chitosan, a natural polymer derived from the partial deacetylation of chitin through alkaline treatment or enzymatic hydrolysis, was used by the authors to embed to BTA and 2-mercaptobenzothiazole (MTB) as corrosion inhibitors, with the

aim of minimizing the leaching of these toxic compounds into the environment. They developed a long-lasting, transparent, eco-friendly and biodegradable protective film. The research highlighted that the preparation of the coating is crucial for effective protection. Specifically, a plasticizing agent, such as glycerol, is necessary to achieve the best film quality. The results indicate that the application of the chitosan-based coating can enhance the protective barrier against environmental agents, providing superior performance compared to using BTA alone.

Biopolymers and molecules stand out as interesting materials for the protection of bronze artistic artefacts, however their stability over time must be investigated more in depth.

Table 1: List of the cited coatings

Coating	Additives or other layers	Substrate	Application	Weathering	Testing	Year	Ref
Microcrystalline waxes		Bronze, clean		Matural urban and marine envirnment	EIS	2001	[74]
MC Reinessance wax		Bronze Steel	Cloth on warm panel	Artificial, climatic chamber, Natural, outdoor exposure	EIS	2015	[75]
Incralac	Wax	Bronze, cast	Spray	Artificial, climatic chamber, salt fog	EIS	2004	[76]
Incralac	None, waxes	Bronze, clean Bronze monument	Brush	Natural, marine environment	EIS	2004	[77]
Incralac		Bronze	Brush	Natural, outdoor	EIS	2015	[78]
Incralac		Bronze statue	Brush	Natural, outdoor	EIS	2016	[79]
Incralac	Soter wax	Bronze, clean, patinated	Brush		EIS, FTIR, color, SEM-EDS	2018	[80]
Paraloid B44		Bronze, cast, patinated		Artificial, immersion	EIS	2003	[35]
Paraloid B44	Inhibitors	Bronze, patinated	Brush	Artificial, immersion tests, climatic chamber	EIS, SEM, Raman	2010	[81]
Paraloid B44		Bronze	Brush	Natural, outdoor	EIS	2015	[78]
Paraloid B48		Bronze	Brush	Natural, outdoor	EIS	2015	[78]
Paraloid B67		Bronze	Brush	Natural, outdoor	EIS	2015	[78]
Paraloid B72		Bronze	Brush	Natural, outdoor	EIS	2015	[78]
ORMOCERs		Bronze, clean, patinated	Spray Brush	Artificial; climatic chamber, SO_2	GPC, FTIR, viscosity, thickness	1997	[61]
PropS-SH		Gilded bronze, clean	Immersion	Artificial; acid rain, NaCl solution	EIS, FTIR, EDS/SEM, Raman	2012	[63]
PropS-SH		Gilded bronze, clean, patinated	Immersion	Artificial, acid rain, wet and dry cycles	EIS, GF-AAS, color, EDS/SEM, Raman	2013	[64]

PropS-SH	CeO_2 , TiO_2, La_2 O_3 nanoparticles	Bronze, clean	Immersion	Natural Artificial, UV/condensation cycles	SEM, EDS, micro-Raman, AAS, FTIR, XRD	2015	[65]
PropS-SH	CeO_2 , TiO_2, La_2 O_3 nanoparticles	Bronze, clean	Immersion	Artificial; acid rain, NaCl solution	EIS, EDS/SEM, ICP-OES, AAS	2020	[66]
PropS-SH	Inhibitors, MPT, β-CD	Bronze, clean	Immersion Spray	Artificial; acid rain	EIS, NMR, FTIR, ESI, DOSY	2019	[67]
TEOS + SiO 2	Modifying agents, TMCS, HMDS	Copper, clean	Immersion	Artificial; UV/condensation cycles	EIS, AFM, SEM, Contact angle	2014	[82]
TEOS + SiO 2	Modifying agents, HMDS	Bronze, clean Brass, clean	Immersion	Artificial; UV/condensation cycles	EIS, AFM, SEM, Contact angle	2016	[83]
PLA	BTA	Bronze		Artificial, thermo hygrometric, photochemical	NMR, FTIR, UV-Vis, GPC, DSC, Colorimetry, SEM-EDS	2014	[72]
Fungal strain S6 *Beauviera baussiana*		Bronze naturally aged	Spray		FTIR,SEM. EIS	2018	[71]
Chitosan	BTA or MBT	Bronze	Drop-casting	Artificial, accelerate corrosion test	FTIR, SEM-EDS	2018	[73]

2.3.3 Corrosion inhibitors

Corrosion inhibitors are one of the methods for conservation-restoration professionals to protect and prolong the life of metallic Cultural Heritage. Corrosion inhibitors are chemical substances that, when present in a corrosion system at the appropriate concentration, reduce the corrosion rate without significantly altering the concentration of any corrosive agent [85]. In general, corrosion inhibitors are effective at low concentrations, with their effectiveness increasing as the concentration increases. It is common practice to combine different inhibitors in commercial formulations to leverage their synergistic effects. This approach enhances protection while minimizing the dosage of inhibitors, thereby reducing potential health and environmental risks. Although no inhibitors have been specifically developed for conservation purposes, those from industrial applications are often adapted for use in particular environments and with specific alloys. Consequently, in the conservation field inhibitors are intentionally and, sometimes, empirically used.

Usually, a valid strategy for protecting metal substrates is the addition of a corrosion inhibitor to the coating material, making it an active coating consisting of a passive polymer matrix loaded with chemically active compounds [54]. Unlike the

direct application of corrosion inhibitors onto a surface, incorporating them into the polymer matrix offers two significant advantages. First, it allows the use of smaller amounts of inhibitors. Second, it helps to immobilize these inhibitors within the coating, reducing their leaching into the environment and creating long-lasting protective films [73,86,87].

1H-Benzotriazole (BTA) (Figure 4) is recognized as one of the most effective and extensively studied corrosion inhibitor for copper and its alloys, used in both industrial applications and heritage conservation.

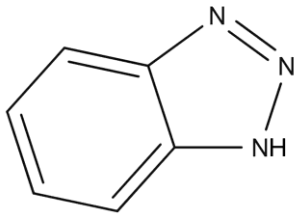

Figure 4: Structure of BTA

Initial studies demonstrated that BTA forms a polymeric complex with copper that acts as a chemically resistant, thin barrier to corrosion [88]. Subsequent research confirmed the efficacy of BTA in protecting copper against aqueous and gaseous environments polluted with sulphur dioxide, hydrogen sulphide, and salt mist. The inhibition mechanism involves BTA chemical adsorption onto the copper surface, displacing water and forming Cu(I) and Cu(II) complexes. Its effectiveness has been studied in various corrosive environments, including acidic, neutral, and alkaline solutions containing ions such as chlorides, sulphates, and ammonia. The use of BTA for heritage conservation gained popularity in the mid-20th century. In 1967, Madsen proposed BTA as a treatment for bronze disease, recommending immersion in a 3% BTA solution, either in ethanol under vacuum or in a heated aqueous solution [89]. Ethanol was preferred due to its lower surface tension, which allowed a deeper penetration into corrosion layers. This treatment became a standard practice and it was often followed by an additional Incralac coating to enhance protection. However, concerns about its long-term effectiveness emerged, as BTA-treated objects sometimes showed signs of reactivated corrosion, particularly in heavily corroded artefacts with low pH microenvironments. Studies comparing the performance of BTA on pure copper versus copper alloys revealed variations in the efficacy. Complex bronze alloys containing elements like tin, zinc, and lead, showed weaker metal–

triazole bonding, potentially reducing inhibition efficiency[90]. From the 2010s, the European Union health directives highlighted the problem of using BTA for conservation purposes [91]. As reported by Lafuente and Cano [90], concerns were raised regarding the toxicity of BTA (benzotriazole) early in its application. Oddy and Sease have highlighted specific precautions for using this compound [93,94]. The environmental and health risks associated with it remain a hotly debated issue. While some researchers claim that BTA is carcinogenic and poses significant dangers to plant and animal life [63], others argue that it is only mildly toxic. Recent toxicological studies indicate that BTA exhibits low acute toxicity and shows no signs of antiestrogenic effects *in vivo* [94]. Concerns about its safety remain. Over the past three decades, there has been a growing need to replace it with non-toxic inhibitors, shifting research towards eco-sustainable chemicals. [42].

Different solutions to reduce BTA toxicity have been proposed by Casaletto et al. by encapsulating BTA in nanocarriers of halloysite or β-cyclodextrins. Both are naturally available, biocompatible, low-cost, and environmentally friendly. Halloysite is a natural cylindrical clay and it can be easily processed with many polymeric materials. It has given promising results in terms of both surface coverage and selective release of BTA during the corrosion process [47]. β-cyclodextrins are toroidal-shaped macrocyclic oligosaccharides composed of at least six α-D-glucopyranose units linked via α(1->4) glycosidic bonds. The study of their performances as nanocarriers for BTA is still ongoing, but they also promise to give good results [95].

Other corrosion inhibitors with a safer toxic profile have been proposed [21,43,90,96]. Up to now, the most efficient alternative inhibitors of bronze corrosion are azoles and particularly triazoles, tetrazoles, imidazoles and thiadiazole [97].

Azoles are five-membered heterocyclic organic molecules composed of one or more nitrogen atoms with free electron pairs that are potential sites for bonding copper and that enable corrosion inhibition. Moreover, phenyl, thiol groups, or other heteroatoms can enhance their protective efficiency, providing additional potential active sites.

The surface chemistry of azoles is not well understood. It is thought that the inhibition by these substances starts with adsorption onto the metal substrate [73]. Chemisorption was found to occur through the electron lone pairs in nitrogen atoms and/or through delocalized π-electrons in aromatic rings favoured by the concomitant presence of other heteroatoms with donor nature like sulphur, either in the ring or in functional groups [98]. Moreover, alkyl chain substituents generally improve the

inhibition efficiency promoting the electron-donor effect of azoles. Group position is also essential; 2- and 5- positions are shown to be more convenient [99]. Therefore, heteroatoms such as nitrogen, sulphur, and phosphorous in the compound improve its action as a copper corrosion inhibitor [73,90].

Among azoles, imidazoles contain two nitrogen atoms within the five-membered aromatic ring: one nitrogen atom is pyrrolic, while the other is pyridinic. The imidazole structure offers two sites for complex formation with the metal surface: the nitrogen atom with a free sp^2 lone pair and the aromatic ring [100].

Tetrazoles, on the other hand, are synthetic azoles containing four nitrogen atoms. Some studies have evaluated the efficiency variation based on the presence of different groups attached to the tetrazole nucleus, including amino, phenyl, and mercapto groups. According to Zucchi [101], protective properties are significantly enhanced by introducing a phenyl group ($-C_6H_5$) at the fifth position of the tetrazole ring. This result may be attributed to an increased molecular surface area or hydrophobicity of the substituted molecule. Similarly, the effect of introducing an amino group at the same position can be associated with its electron-donor properties or the ability to form salts (e.g., with sodium). An alternative is to place a thiol group at the fifth position and replace the hydrogen atom in the first position with a benzene or methyl group. The derivative, 5-mercapto-1-methyltetrazole, exhibits lower inhibition efficiency and stability compared to 5-mercapto-1-phenyltetrazole. This difference could be attributed to the smaller surface area or possibly to the electronic effect of the methyl group. Subsequent research by Mihit [102] have confirmed and compared the potential of tetrazole derivatives as corrosion inhibitors. Specifically, the following molecules were characterized: tetrazole (TTZ), 1-phenyl-tetrazole (PT), 5-amino-tetrazole (AT), and 5-mercapto-1-phenyl-tetrazole (MPT). (Table 1)

Table 2: Structure of tetrazole derivatives

Name	Structure
Tetrazole (TTZ)	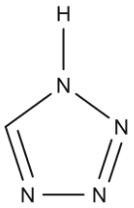
1-phenyl-tetrazole (PT)	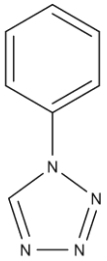
5-amino-tetrazole (AT)	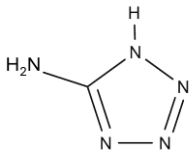
5-mercapto-1-phenyl-tetrazole (MPT)	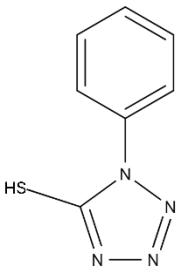

The four compounds exhibit different effects on the kinetics of copper corrosion, with the MPT derivative achieving the highest efficiency. The -SH group and the aromatic ring contribute a synergistic inhibitory effect [102].

Like BTA, these inhibitors form protective barriers consisting of polymeric complexes where the azole acts as a bridge between two or more Cu(I) ions, which are inert, insoluble, and long-lasting on the Cu_2O substrate. Cu(I) is formally bound to the nitrogen or sulphur atoms of the inhibitor, significantly reducing ion diffusion. (Figure 5) The result is a thermally stable coating that effectively inhibits the corrosion mechanism.

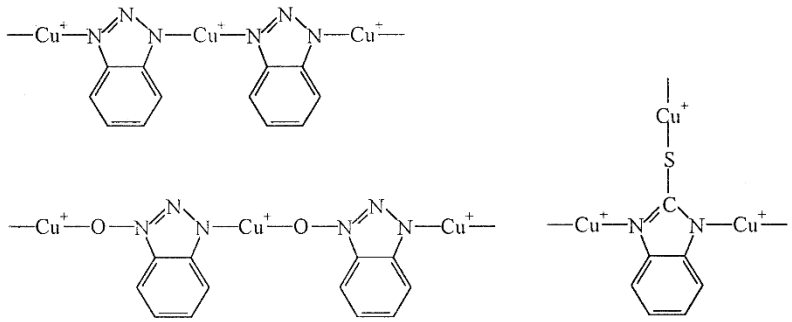

Figure 5: Several polymeric complexes formed by azoles [88]

A more in-depth study conducted by Ye on the formation mechanism of the Cu(I)-MPT complex reveals that the coordination complex stabilizes Cu(I) ions and inhibits the electrochemical reaction of the substrate. According to the results, it appears more likely that the inhibitor reacts with copper oxide, and that the Cu(I)-MPT layer forms above the Cu_2O one. Thus, the copper surface treated with MPT can likely be described as a structure composed of overlapping layers of Cu-MPT/Cu_2O/Cu. Each MPT molecule acts as a bridge between two or more Cu(I) ions through bonds with nitrogen and sulphur. The hydrophobic portion of the MPT in the complex prevents hydrated corrosive ions from contacting the metal surface, effectively inhibiting corrosion [103].

Thiadiazoles, such as AEDTA (2-amino 5-ethyl 1,3,4 thiadiazole) [103], AEDT (2-amino-5-ehthyltio-1,3,4 thiadiazole) and PTAT (5-phenyl-4H-1,2,3-triazole-3-thiole) have also proved to be good mixed-type copper corrosion inhibitors with an inhibition efficiency increasing with concentration. These three molecules strongly absorb copper, forming complexes with copper ions and preventing the formation of Cu chloride and oxychloride complexes [99]. Furthermore, they are neither toxic nor noxious to humans and the environment [2].

In recent years, another very active area of research concerns the so-called "green inhibitors," i.e. inhibitors obtained from natural plant extracts. These inhibitors present several advantages, such as biodegradability, easy availability, and non-toxic nature, but also disadvantages, such as the very complex nature and high variability of the extracts (depending on the exact origin of the plant). Their application to Cultural Heritage is quite limited, even though efforts are being made to use these products as substitutes for unhealthy compounds [90].

2.3.3.1 Nanocarriers

The most common method for protecting metals is the incorporation of corrosion inhibitors into coatings. However, detrimental interactions between the active species and the matrix within which they are dispersed may occur, such as loss of the inhibition and degradation of the coating. Furthermore, the addition itself may be limited by solubility issues, a decrease in barrier properties and adherence to the substrate [105]. Recently, researchers have focused on improving anti-corrosion properties of coatings by encapsulating corrosion inhibitors using suitable carriers [26,27]. According to this strategy, a good compatibility between the carrier and the coating matrix is crucial to ensure the proper dispersion of the carrier. This is important for maintaining the expected barrier performance of the protective coating [26]. Various carrier types have been explored, including inhibitor-filled porous particles and nanocapsules coated with polyelectrolytes[106–108], as well as layered anion-exchange particles that contain intercalated anionic corrosion inhibitors [109]. The polyelectrolyte-coated carriers can release inhibitor molecules in response to the local pH variations in solution, which are linked to the onset of corrosion phenomena. In contrast, carriers with intercalated anionic inhibitors restrict the access of aggressive anions, such as chlorides, to the metal substrate and release corrosion-inhibiting species through ion-exchange processes.

In addition to these carriers, cyclodextrins (CDs) have also been used to host corrosion inhibitors due to their ability to complex small organic molecules[110]. CDs are produced through the enzymatic degradation of starch by cyclodextrin glucanotransferase (CGTase). The outer surface of the molecule is hydrophilic, which makes it water-soluble, while the inner cavity is hydrophobic, creating a favourable environment for non-polar compounds [111]. The "native" CDs are αCD, ßCD, γCD. α-, ß-, γ-, cyclodextrins are cyclic oligosaccharides composed of 6, 7 or 8 monomers of D-(+) glucopyranose, respectively joined together by an α,1-4 glucosidic bond [112]. (Figure 6)

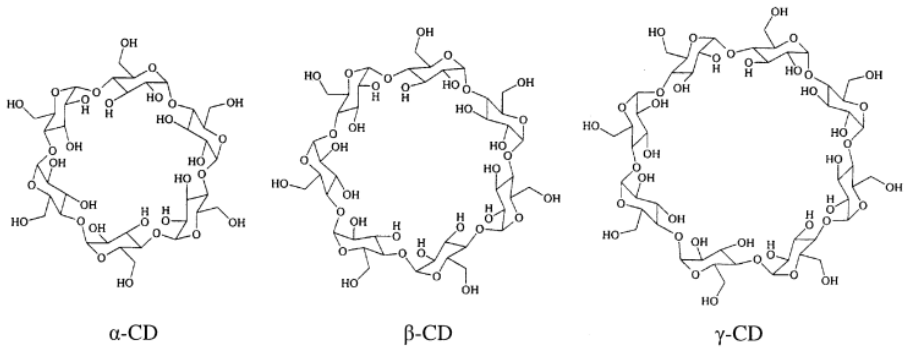

Figure 6: αCD, ßCD, γCD. [113]

Given the different numbers of glucose monomers in cyclodextrins the size of cavities varies: 4.7-5.3 Å for α-cyclodextrin (αCD), ranges from 6.0-6.5 Å for β-cyclodextrin (βCD), and 7-8.3 Å for γ-cyclodextrin (γCD). Due to the chair conformation of the glucopyranoside units, cyclodextrins exhibit a three-dimensional truncated cone shape. The hydroxyl groups are oriented towards the exterior part of the cone, with primary hydroxyl groups located at the convergent part and secondary hydroxyl groups at the divergent part of the cone. [114]. Despite the hydrophilic nature of cyclodextrins and their complexes, their solubility in water is relatively limited, particularly for βCD. Additionally, βCD and γCD tend to form intramolecular hydrogen bonds between their secondary hydroxyl groups, which reduces the availability of these groups for hydrogen bonding with surrounding water molecules. To address this issue, hydroxyl groups are often modified to enhance solubility, resulting in cyclodextrins with more hydrophobic substituents, such as methoxy or ethoxy groups. [115,116] As a matter of fact, various derivatives of CDs, such as hydroxypropyl-β-CD and methyl-β-CD, have been developed to enhance their performance, including improved complexation efficiency and controlled release properties [117]. CDs are widely used in the pharmaceutical, biomedical, and food industry due to their unique ability to form inclusion complexes with guest molecules. This capability allows for improved solubility, stability, and bioavailability of these molecules. Numerous studies have highlighted the potential of CDs to host corrosion inhibitors with the aim of improving their retention within protective coatings. This is important because corrosion inhibitors often leach out of the coating, which diminishes their effectiveness. By incorporating these inhibitors into carriers like CDs, these issues can be addressed [118]. Research has demonstrated that CDs are effective carriers for this purpose. For example, β-cyclodextrin has successfully encapsulated 5-mercapto-1-phenyl-tetrazole, leading to improved corrosion resistance in bronze [67]. Additionally, α- and β-cyclodextrin complexes with dibenzylthiourea (DBT) have

enhanced corrosion protection for carbon steel by improving the solubility of DBT [119].

Furthermore, β- and γ-cyclodextrins complexed with various organic inhibitors have shown improved corrosion resistance for aluminum alloys and zinc [110–122]. In another case, β-cyclodextrin complexes with 2-phosphonobutane-1,2,4-tricarboxylic acid provided enhanced corrosion protection for carbon steel [123]. Lastly, hydroxypropyl-β-cyclodextrin complexes with octadecylamine (ODA) have improved anticorrosion properties for steel due to increased solubility of the guest compound [124].

2.3.4 Testing coatings

Many projects focus on developing new treatments for copper alloy artworks; however, the lack of standardized testing methods for new coatings makes it difficult to compare different studies. Each study employs varying choices in terms of alloy, application methods, testing techniques, and weathering conditions used to assess the longevity of coatings, which complicates the comparison with the results that are typical of the coating industry [44]. Nonetheless, researchers emphasize several important issues that require careful consideration when studying conservation treatments. These treatments perform differently depending on whether they are applied on bare metals or on patinated or corroded surfaces [126]. This highlights the necessity of conducting reliable tests only on protective treatments applied to coupons that accurately represent heritage surfaces. Furthermore, the application methods of the coatings play a significant role in determining the effectiveness of these treatments [127]. Consequently, laboratory investigations, instrumental analyses, and electrochemical methods can determine the intrinsic performance characteristics of coatings based on a defined set of variables. However, these methods do not provide a quantitative evaluation of real-time *in situ* performance in outdoor environments. To conduct comprehensive analytical studies of new protective treatments, coupons with homogeneous surfaces are necessary for comparison across different parameters [128,129]. Nevertheless, producing coupons that accurately replicate the surface structure of outdoor bronze statues can be challenging. Simple polished copper coupons are increasingly being replaced with alloys featuring diverse compositions and natural patinas, as well as artificial patination techniques typically used in artistic foundries [42].

A multi-analytical approach is highly recommended for characterising the different properties of patinas and conservation treatments on coupons [20]. Visual

appearance, chemical composition, corrosion rate and surface texture are some of the relevant parameters to consider.

Colour measurements are essential for monitoring aesthetic appearance and quantifying colour differences [130,131]. Portable digital microscopy has been utilized for in situ documentation of surface morphology. Electrochemical techniques are effective in characterizing the barrier properties of organic coatings, and the use of such measurements has increased over the past few decades [19,43,132–135]. Fourier transform infrared spectroscopy (FTIR) in reflectance mode has proven valuable for analysing the chemical composition of both coatings and patina, whether using coupons or in field measurements [80,136]. Additionally, portable surface roughness measurements, as well as Raman and X-ray fluorescence (XRF), are valuable techniques for gathering information to better understand the effectiveness of protective treatments on complex outdoor bronze surfaces and to inform better conservation practices [44].

The growing availability of portable, non-destructive techniques enhances the possibility of comparing the surface properties of test coupons with those of outdoor exposed bronze artworks exposed outdoors, although this opportunity has yet to be fully exploited.

In fact, there is still a lack of evaluation protocols for investigating the characteristics of coatings on metal artworks and monitoring their performance [45,127]. Indeed, identifying the most relevant surface properties, the most suitable techniques to analyse them, the appropriate number of measurement points are goals that the heritage science community should pursue to optimise investigation times and costs. At the international level, the need for shared evaluation protocols is particularly felt, as witnessed by the inclusion of this issue in various European projects. In this context, some progress has been made, but the large number of variables involved in testing real surfaces and the difficult task of correlating them still leaves the question open. Moreover, the complex and evolving interplay between climate change and atmospheric composition underscores the need for updated conservation approaches [44]. Laboratory ageing tests must be refined to reflect these changing environmental scenarios, particularly in regions such as Southern Europe, where these effects are most pronounced. By closing the gap between controlled experiments and real-world conditions, these adaptations will ensure more precise predictions of degradation processes and support the development of effective preservation strategies for outdoor Cultural Heritage materials [15].

Chapter 3

References

[1] D.A. Scott, Copper and bronze in art: corrosion, colorants, conservation, Getty publications, 2002.

[2] L. Muresan, S. Varvara, E. Stupnišek-Lisac, H. Otmačić, K. Marušić, S. Horvat-Kurbegović, L. Robbiola, K. Rahmouni, H. Takenouti, Protection of bronze covered with patina by innoxious organic substances, Electrochim Acta 52 (2007) 7770–7779. https://doi.org/10.1016/j.electacta.2007.02.024.

[3] L.B. Brostoff, Coating strategies for the protection of outdoor bronze art and ornamentation, Universiteit van Amsterdam Amsterdam, Netherlands, 2003. PhD Thesis.

[4] C. Chiavari, C. Martini, A. Balbo, C. Monticelli, C. Velino, G. Masi, E. Bernardi, Atmospheric corrosion of Cu-Si-Mn bronze for contemporary art under simulated runoff and continuous immersion conditions, Corros Sci 205 (2022). https://doi.org/10.1016/j.corsci.2022.110442.

[5] G. Masi, C. Josse, J. Esvan, C. Chiavari, E. Bernardi, C. Martini, M.C. Bignozzi, C. Monticelli, F. Zanotto, A. Balbo, E. Svara Fabjan, T. Kosec, L. Robbiola, Evaluation of the protectiveness of an organosilane coating on patinated Cu-Si-Mn bronze for contemporary art, Prog Org Coat 127 (2019) 286–299. https://doi.org/10.1016/j.porgcoat.2018.11.027.

[6] T.E. Graedel, Copper patinas formed in the atmosphere—II. A qualitative assessment of mechanisms, Corros Sci 27 (1987) 721–740.

[7] C. Chiavari, A. Colledan, A. Frignani, G. Brunoro, Corrosion evaluation of traditional and new bronzes for artistic castings, Mater Chem Phys 95 (2006) 252–259. https://doi.org/10.1016/j.matchemphys.2005.06.034.

[8] R.A. Livingston, Acid rain attack on outdoor sculpture in perspective, Atmos Environ 146 (2016) 332–345. https://doi.org/10.1016/j.atmosenv.2016.08.029.

[9] K.P. FitzGerald, J. Nairn, G. Skennerton, A. Atrens, Atmospheric corrosion of copper and the colour, structure and composition of natural patinas on copper, Corros Sci 48 (2006) 2480–2509. https://doi.org/https://doi.org/10.1016/j.corsci.2005.09.011.

[10] J. Tidblad, V. Kucera, M. Ferm, K. Kreislova, S. Brüggerhoff, S. Doytchinov, A. Screpanti, T. Grøntoft, T. Yates, D. de la Fuente, O. Roots, T. Lombardo, S. Simon, M. Faller, L. Kwiatkowski, J. Kobus, C. Varotsos, C. Tzanis, L. Krage, M. Schreiner, M. Melcher, I. Grancharov, N. Karmanova, Effects of Air Pollution on Materials and Cultural Heritage: ICP Materials Celebrates 25 Years of Research, International Journal of Corrosion 2012 (2012) 496321. https://doi.org/https://doi.org/10.1155/2012/496321.

[11] T.E. Graedel, K. Nassau, J.P. Franey, Copper patinas formed in the atmosphere—I. Introduction, Corros Sci 27 (1987) 639–657. https://doi.org/https://doi.org/10.1016/0010-938X(87)90047-3.

[12] E. Basso, F. Pozzi, M.C. Reiley, The Samuel F. B. Morse statue in Central Park: scientific study and laser cleaning of a 19th-century American outdoor bronze monument, Herit Sci 8 (2020). https://doi.org/10.1186/s40494-020-00426-8.

[13] E. Sesana, A.S. Gagnon, C. Ciantelli, J. Cassar, J.J. Hughes, Climate change impacts on cultural heritage: A literature review, WIREs Climate Change 12 (2021) e710. https://doi.org/https://doi.org/10.1002/wcc.710.

[14] E. von Schneidemesser, P.S. Monks, J.D. Allan, L. Bruhwiler, P. Forster, D. Fowler, A. Lauer, W.T. Morgan, P. Paasonen, M. Righi, K. Sindelarova, M.A. Sutton, Chemistry and the Linkages between Air Quality and Climate Change, Chem Rev 115 (2015) 3856–3897. https://doi.org/10.1021/acs.chemrev.5b00089.

[15] A. Timoncini, E. Brattich, E. Bernardi, C. Chiavari, L. Tositti, Safeguarding outdoor cultural heritage materials in an ever-changing troposphere: Challenges and new guidelines for artificial ageing test, J Cult Herit 59 (2023) 190–201. https://doi.org/10.1016/j.culher.2022.12.003.

[16] C.M. Grossi, P. Brimblecombe, I. Harris, Predicting long term freeze–thaw risks on Europe built heritage and archaeological sites in a changing climate, Science of The

Total Environment 377 (2007) 273–281. https://doi.org/https://doi.org/10.1016/j.scitotenv.2007.02.014.

[17] C. Leygraf, T. Chang, G. Herting, I. Odnevall Wallinder, The origin and evolution of copper patina colour, Corros Sci 157 (2019) 337–346. https://doi.org/https://doi.org/10.1016/j.corsci.2019.05.025.

[18] A. Kraetschmer, I. Odnevall Wallinder, C. Leygraf, The evolution of outdoor copper patina, Corros Sci 44 (2002) 425–450. www.elsevier.com/locate/corsci.

[19] C. Chiavari, K. Rahmouni, H. Takenouti, S. Joiret, P. Vermaut, L. Robbiola, Composition and electrochemical properties of natural patinas of outdoor bronze monuments, Electrochim Acta 52 (2007) 7760–7769. https://doi.org/10.1016/j.electacta.2006.12.053.

[20] G. Masi, J. Esvan, C. Josse, C. Chiavari, E. Bernardi, C. Martini, M.C. Bignozzi, N. Gartner, T. Kosec, L. Robbiola, Characterization of typical patinas simulating bronze corrosion in outdoor conditions, Mater Chem Phys 200 (2017) 308–321. https://doi.org/10.1016/j.matchemphys.2017.07.091.

[21] S. Varvara, R. Bostan, L. Gəinə, L.M. Muresan, Thiadiazole derivatives as inhibitors for acidic media corrosion of artificially patinated bronze, Materials and Corrosion 65 (2014) 1202–1214. https://doi.org/10.1002/maco.201307072.

[22] J. Tétreault, E. Cano, M. van Bommel, D. Scott, M. Dennis, M.-G. Barthés-Labrousse, L. Minel, L. Robbiola, Corrosion of Copper and Lead by Formaldehyde, Formic and Acetic Acid Vapours, Studies in Conservation 48 (2003) 237–250. https://doi.org/10.1179/sic.2003.48.4.237.

[23] C. Petiti, L. Toniolo, L. Berti, S. Goidanich, Artistic and Laboratory Patinas on Copper and Bronze Surfaces, Applied Sciences 13 (2023). https://doi.org/10.3390/app132111873.

[24] C. Chiavari, E. Bernardi, C. Martini, F. Passarini, F. Ospitali, L. Robbiola, The atmospheric corrosion of quaternary bronzes: The action of stagnant rain water, Corros Sci 52 (2010) 3002–3010. https://doi.org/10.1016/j.corsci.2010.05.013.

[25] E. Bernardi, C. Chiavari, B. Lenza, C. Martini, L. Morselli, F. Ospitali, L. Robbiola, The atmospheric corrosion of quaternary bronzes: The leaching action of acid rain, Corros Sci 51 (2009) 159–170. https://doi.org/10.1016/j.corsci.2008.10.008.

[26] M.F. Montemor, Functional and smart coatings for corrosion protection: A review of recent advances, Surf Coat Technol 258 (2014) 17–37. https://doi.org/10.1016/j.surfcoat.2014.06.031.

[27] F. Zhang, P. Ju, M. Pan, D. Zhang, Y. Huang, G. Li, X. Li, Self-healing mechanisms in smart protective coatings: A review, Corros Sci 144 (2018) 74–88. https://doi.org/10.1016/j.corsci.2018.08.005.

[28] W. Funke, U. Zorll, B.G. Murthy, Interfacial effects in solid paint films related to some film properties, Journal Paint Technology (1969).

[29] W.J. Zeno W., J. Frank N., P. S. Peter, W. Douglas A., Organic Coatings: Science and Technology, Wiley, 2007. ISBN, 0470079061

[30] P.E. Pierce, C.K. Schoff, Coating film defects, Federation of Societies for Coatings Technology, 1994.

[31] C.H. Hare, Internal stress-related coating system failures, Journal of Protective Coatings and Linings 13 (1996) 99–113.

[32] S.G. Croll, The origin of residual internal stress in solvent-cast thermoplastic coatings, J Appl Polym Sci 23 (1979) 847–858. https://doi.org/https://doi.org/10.1002/app.1979.070230319.

[33] O. Chiantore, M. Lazzari, Characterization of acrylic resins, International Journal of Polymer Analysis and Characterization 2 (1996) 395–408. https://doi.org/10.1080/10236669608033358.

[34] M. Lazzari, O. Chiantore, Thermal-ageing of paraloid acrylic protective polymers, Polymer, 41 (2000) 6447–6455. https://doi.org/10.1016/S0032-3861(99)00877-0

[35] G. Bierwagen, T.J. Shedlosky, K. Stanek, Developing and testing a new generation of protective coatings for outdoor bronze sculpture, in: Prog Org Coat, 2003: pp. 289–296. https://doi.org/10.1016/j.porgcoat.2003.07.004.

[36] T.V. Nguyen, T.A. Nguyen, T.H. Nguyen, The synergistic effects of SiO2 nanoparticles and organic photostabilizers for enhanced weathering resistance of acrylic polyurethane coating, Journal of Composites Science 4 (2020) 23. https://doi.org/10.3390/jcs4010023

[37] C. Maier, T. Calafut, Polypropylene: the definitive user's guide and databook, William Andrew, 1998. ISBN 9780815518716

[38] E. Yousif, A. Hasan, Photostabilization of poly (vinyl chloride)–Still on the run, Journal of Taibah University for Science 9 (2015) 421–448. https://doi.org/10.1016/j.jtusci.2014.09.007

[39] P.D. Weil, Patina: historical perspective on artistic intent and subsequent effects of time, nature, and man, in: Sculptural Monuments in an Outdoor Environment: A Conference Held at the Pennsylvania Academy of Fine Arts, Philadelphia, November 2, 1983, 1985: pp. 21–27.

[40] H. Strandberg, Perspectives on Bronze Sculpture Conservation. Modelling Copper and Bronze Corrosion, (1997). PhD Thesis

[41] G. Masi, E. Bernardi, C. Martini, I. Vassura, L. Skrlep, E. Švara Fabjan, N. Gartner, T. Kosec, C. Josse, J. Esvan, M.C. Bignozzi, L. Robbiola, C. Chiavari, An innovative multi-component fluoropolymer-based coating on outdoor patinated bronze for Cultural Heritage: Durability and reversibility, J Cult Herit 45 (2020) 122–134. https://doi.org/10.1016/j.culher.2020.04.015.

[42] A. Artesani, F. Di Turo, M. Zucchelli, A. Traviglia, Recent advances in protective coatings for cultural heritage-an overview, Coatings 10 (2020). https://doi.org/10.3390/coatings10030217.

[43] E. Cano, D.M. Bastidas, V. Argyropoulos, S. Fajardo, A. Siatou, J.M. Bastidas, C. Degrigny, Electrochemical characterization of organic coatings for protection of historic steel artefacts, Journal of Solid State Electrochemistry 14 (2010) 453–463. https://doi.org/10.1007/s10008-009-0907-1.

[44] P. Letardi, Testing New Coatings for Outdoor Bronze Monuments: A Methodological Overview, Coatings 11 (2021). https://doi.org/10.3390/coatings.

[45] M.T. Molina, E. Cano, B. Ramírez-Barat, Protective coatings for metallic heritage conservation: A review, J Cult Herit 62 (2023) 99–113. https://doi.org/10.1016/j.culher.2023.05.019.

[46] E. Kiele, J. Lukseniene, A. Griguceviciene, A. Selskis, J. Senvaitiene, R. Ramanauskas, R. Raudonis, A. Kareiva, Methyl–modified hybrid organic-inorganic coatings for the conservation of copper, J Cult Herit 15 (2014) 242–249.

[47] M.P. Casaletto, C. Cirrincione, A. Privitera, V. Basilissi, A Sustainable Approach to the Conservation of Bronze Artworks by Smart Nanostructured Coatings, Proceedings of Metal 2016, the 9th Interim Meeting of the ICOM-CC Metals Working Group, September 26-30, 2016 New Delhi, India, edited by Raghu Menon, Claudia Chemello, Achal Pandya, pp. 144-152, ISBN: 978-92-9012-418-4

[48] M. Mihelčič, M. Gaberšček, M. Salzano de Luna, M. Lavorgna, C. Giuliani, G. Di Carlo, A.K. Surca, Effect of silsesquioxane addition on the protective performance of fluoropolymer coatings for bronze surfaces, Mater Des 178 (2019). https://doi.org/10.1016/j.matdes.2019.107860.

[49] V. Otieno-Alego, D. Hallam, A. Viduka, G. Heath, D. Creagh, Electrochemical impedance studies of the corrosion resistance of wax coatings on artificially patinated bronze, in: METAL 98: Proceedings of the International Conference on Metals Conservation (Draguignan-Figanières, 27-29 May 1998), 1998: pp. 315–319.

[50] P. Letardi, Laboratory and field tests on patinas and protective coating systems for outdoor bronze monuments, in: METAL 2004. Proc. Interim Meeting ICOM-CC Metal WG, Camberra, Australia, 2004.

[51] C. Price, D. Hallam, G. Heath, D. Creagh, J. Ashton, An electrochemical study of waxes for bronze sculpture, in: METAL 95: Proceedings of the International Conference on Metals Conservation (Semur En Auxois, 25-28 September 1995), 1997: pp. 233–241.

[52] M. Albini, L. Comensoli, L. Brambilla, E. Domon Beuret, W. Kooli, L. Mathys, P. Letardi, E. Joseph, Innovative biological approaches for metal conservation, Materials and Corrosion 67 (2016) 200–206. https://doi.org/10.1002/maco.201408168

[53] R. Bostan, S. Varvara, L. Găină, T. Petrisor, L.M. Mureşan, Protective effect of inhibitor-containing nitrocellulose lacquer on artificially patinated bronze, Prog Org Coat 111 (2017) 416–427. https://doi.org/https://doi.org/10.1016/j.porgcoat.2016.08.004.

[54] J.L. Down, Adhesive testing at the Canadian Conservation Institute, past and future, Studies in Conservation 29 (1984) 18–21.

[55] B. Ramírez Barat, A. Crespo, E. García, S. Díaz, E. Cano, An EIS study of the conservation treatment of the bronze sphinxes at the Museo Arqueológico Nacional

(Madrid), J Cult Herit 24 (2017) 93–99. https://doi.org/https://doi.org/10.1016/j.culher.2016.10.010.

[56] J. Wolfe, R. Grayburn, A review of the development and testing of Incralac lacquer, Journal of the American Institute for Conservation 56 (2017) 225–244. https://doi.org/10.1080/01971360.2017.1362863.

[57] D. Watkinson, Preservation of Metallic Cultural Heritage, Corrosion Management (2010) 3307–3340.

[58] J. Wolfe, R. Grayburn, H. Khanjian, A. Heginbotham, A. Phenix, Deconstructing Incralac: A formulation study of acrylic coatings for the protection of outdoor bronze sculpture, in: ICOM-CC 18th Triennal Conference, 2017. https://www.researchgate.net/publication/319717768.

[59] O. Chiantore, L. Trossarelli, M. Lazzari, Photooxidative degradation of acrylic and methacrylic polymers, Polymer (Guildf) 41 (2000) 1657–1668. https://doi.org/https://doi.org/10.1016/S0032-3861(99)00349-3.

[60] M. Pilz, H. Römich, A new conservation treatment for outdoor bronze sculptures based on ORMOCER®, in: METAL 95: Proceedings of the International Conference on Metals Conservation (Semur En Auxois, 25-28 September 1995), 1997: pp. 245–250.

[61] M. Pilz, H.R.¨ Omich, Sol-Gel Derived Coatings for Outdoor Bronze Conservation, Kluwer Academic Publishers, 1996.

[62] F. Zucchi, V. Grassi, A. Frignani, G. Trabanelli, Inhibition of copper corrosion by silane coatings, Corros Sci 46 (2004) 2853–2865. https://doi.org/https://doi.org/10.1016/j.corsci.2004.03.019.

[63] A. Balbo, C. Chiavari, C. Martini, C. Monticelli, Effectiveness of corrosion inhibitor films for the conservation of bronzes and gilded bronzes, Corros Sci 59 (2012) 204–212. https://doi.org/10.1016/j.corsci.2012.03.003.

[64] C. Chiavari, A. Balbo, E. Bernardi, C. Martini, M.C. Bignozzi, M. Abbottoni, C. Monticelli, Protective silane treatment for patinated bronze exposed to simulated natural environments, Mater Chem Phys 141 (2013) 502–511. https://doi.org/https://doi.org/10.1016/j.matchemphys.2013.05.050.

[65] C. Chiavari, A. Balbo, E. Bernardi, C. Martini, F. Zanotto, I. Vassura, M.C. Bignozzi, C. Monticelli, Organosilane coatings applied on bronze: Influence of UV radiation and

thermal cycles on the protectiveness, Prog Org Coat 82 (2015) 91–100. https://doi.org/https://doi.org/10.1016/j.porgcoat.2015.01.017.

[66] C. Monticelli, F. Zanotto, V. Grassi, M. Seyedi, A. Balbo, Improving the protectiveness of 3-Mercaptopropyl-Trimethoxysilane coatings on bronze by addition of oxidic nano-andmicroparticles, Coatings 10 (2020). https://doi.org/10.3390/coatings10030225.

[67] C. Monticelli, G. Fantin, G. Di Carmine, F. Zanotto, A. Balbo, Inclusion of 5-mercapto-1-phenyl-tetrazole into β-cyclodextrin for entrapment in silane coatings: An improvement in bronze corrosion protection, Coatings 9 (2019). https://doi.org/10.3390/coatings9080508.

[68] E. Kiele, J. Senvaitiene, A. Griguceviciene, R. Ramanauskas, R. Raudonis, A. Kareiva, Application of sol–gel method for the conservation of copper alloys, Microchemical Journal 124 (2016) 623–628. https://doi.org/https://doi.org/10.1016/j.microc.2015.10.003.

[69] R.A. Iezzi, S. Gaboury, K. Wood, Acrylic-fluoropolymer mixtures and their use in coatings, Prog Org Coat 40 (2000) 55–60. https://doi.org/https://doi.org/10.1016/S0300-9440(00)00117-X.

[70] T. Kosec, L. Škrlep, E. Švara Fabjan, A. Sever Škapin, G. Masi, E. Bernardi, C. Chiavari, C. Josse, J. Esvan, L. Robbiola, Development of multi-component fluoropolymer based coating on simulated outdoor patina on quaternary bronze, Prog Org Coat 131 (2019) 27–35. https://doi.org/10.1016/j.porgcoat.2019.01.040.

[71] M. Albini, P. Letardi, L. Mathys, L. Brambilla, J. Schröter, P. Junier, E. Joseph, Comparison of a bio-based corrosion inhibitor versus benzotriazole on corroded copper surfaces, Corros Sci 143 (2018) 84–92. https://doi.org/10.1016/j.corsci.2018.08.020.

[72] G. Giuntoli, L. Rosi, M. Frediani, B. Sacchi, B. Salvadori, S. Porcinai, P. Frediani, Novel coatings from renewable resources for the protection of bronzes, Prog Org Coat 77 (2014) 892–903. https://doi.org/10.1016/j.porgcoat.2014.01.021.

[73] C. Giuliani, M. Pascucci, C. Riccucci, E. Messina, M. Salzano de Luna, M. Lavorgna, G.M. Ingo, G. Di Carlo, Chitosan-based coatings for corrosion protection of copper-based alloys: A promising more sustainable approach for cultural heritage

applications, Prog Org Coat 122 (2018) 138–146. https://doi.org/10.1016/j.porgcoat.2018.05.002.

[74] P. Letardi, Outdoor bronze protective coatings: Characterisation by a new contact-probe electrochemical impedance measurements technique. The Science of Art, 2002, 173-178.

[75] N. Swartz, T.L. Clare, on the protective nature of wax coatings for culturally significant outdoor metalworks: microstructural flaws, oxidative changes, and barrier properties. *Journal of the American Institute for Conservation*, *54*(3), (2015) 181–201. https://doi.org/10.1179/1945233015Y.0000000012

[76] L. A. Ellingson , T. J. Shedlosky, G. P. Bierwagen, E. R. de la Rie, L.B. Brostoff. The Use of Electrochemical Impedance Spectroscopy in the Evaluation of Coatings for Outdoor Bronze. *Studies in Conservation*, *49*(1), (2004) 53–62. https://doi.org/10.1179/sic.2004.49.1.53

[77] P. Letardi Laboratory and field tests on patinas and protective coating systems for outdoor bronze monuments. In Proceedings of the International Conference on Metals Conservation, Canberra, Australia October 2004 (Vol. 48, p. 379387).

[78] B. Ramírez-Barat, E. Cano, In situ assessment of protective coatings for metallic cultural heritage using electrochemical impedance spectroscopy, Ge- Conservacion 8 (2015) 6–13, doi: 10.37558/gec.v8i0.278

[79] B. Ramírez Barat, A. Crespo, E. García, S. Díaz, E. Cano, An EIS study of the conservation treatment of the bronze sphinxes at the Museo Arqueológico Nacional (Madrid), J. Cult. Herit. 24 (2017) 93–99, doi: 10.1016/j.culher.2016. 10.010

[80] B. Salvadori, A. Cagnini, M. Galeotti, S. Porcinai, S. Goidanich, A. Vicenzo, C. Celi, P. Frediani, L. Rosi, M. Frediani, G. Giuntoli, L. Brambilla, R. Beltrami, S. Trasatti, Traditional and innovative protective coatings for outdoor bronze: Application and performance comparison, J Appl Polym Sci 135 (2018). https://doi.org/10.1002/app.46011.

[81] H.O. Ćurković, T. Kosec, A. Legat, E. Stupnišek-Lisac, Improvement of corrosion stability of patinated bronze, Corros. Eng. Sci. Technol. 45 (2010) 327–333, doi:10.1179/147842210X12710800383684

[82] E. Kiele, J. Lukseniene, A. Griguceviciene, A. Selskis, J. Senvaitiene, R. Ramanauskas, R. Raudonis, A. Kareiva, Methyl-modified hybrid organic-inorganic

coatings for the conservation of copper, J. Cult. Herit. 15 (2014) 242–249, doi: 10.1016/j.culher.2013.06.002

[83] E. Kiele, J. Senvaitiene, A. Griguceviciene, R. Ramanauskas, R. Raudonis, A. Kareiva, Application of sol-gel method for the conservation of copper alloys, Microchem. J. 124 (2016) 623–628, doi: 10.1016/j.microc.2015.10.003

[84] F. Faraldi, E. Angelini, C. Riccucci, A. Mezzi, D. Caschera, S. Grassini, Innovative diamond-like carbon coatings for the conservation of bronzes, Surface and Interface Analysis 46 (2014) 764–770. https://doi.org/10.1002/sia.5367.

[85] International Standard BS EN ISO 8044:2015 Corrosion of metals and alloys. Basic terms and definitions, 2015.

[86] K. Marušić, H.O. Ćurković, H. Takenouti, Corrosion Inhibition of Bronze and Its Patina Exposed to Acid Rain, J Electrochem Soc 160 (2013) C356–C363. https://doi.org/10.1149/2.063308jes.

[87] S. Zhou, Z. Zhao, H. Mao, L. Wang, J. Chen, J. Chen, X. Huang, Bronze preservation by using composite hydrogel coating-loaded corrosion inhibitors, Herit Sci 10 (2022). https://doi.org/10.1186/s40494-022-00747-w.

[88] I. Dugdale, J.B. Cotton, An electrochemical investigation on the prevention of staining of copper by benzotriazole, Corr Sci 3 (1963) 69-74. https://doi.org/10.1016/S0010-938X(63)80001-3

[89] H.B. Madsen. A preliminary note on the use of benzotriazole for stabilizing bronze objects. Stud. Conserv., 12 (1967), pp. 163-167 https://doi.org/10.1179/sic.1967.017

[90] E. Cano, D. Lafuente, Corrosion inhibitors for the preservation of metallic heritage artefacts, in: Corrosion and Conservation of Cultural Heritage Metallic Artefacts, Elsevier Ltd, 2013: pp. 570–594. https://doi.org/10.1533/9781782421573.5.570.

[91] ECHA site. Available online: https://echa.europa.eu/it/substance-information/-/substanceinfo/100.002.177#:~:text=According%20to%20the%20classification%20provided,swallowed%20and%20causes%20skin%20irritation (accessed on March 2025)

[92] C. Sease, Benzotriazole: A Review for Conservators. Studies in Conservation 23 (2) (1978): 76–85. https://doi.org/10.2307/1505798.

[93] W. A. Oddy, Toxicity of Benzotriazole. Studies in Conservation, 19(3), (1974) 188–189. https://doi.org/10.1179/sic.1974.016

[94] C. A. Harris, E. J. Routledge, C. Schaffner, J. V. Brian, W. Giger, J. P. Sumpter, Benzotriazole is antiestrogenic in vitro but not in vivo, Environmental Toxicology and Chemistry, 26(11), (2007), 2367–2372, https://doi.org/10.1897/06-587R.1

[95] M.P. Casaletto, V. Figà, A. Privitera, A. Mazzaglia, A. Scala, R. Zagami, Sustainable corrosion inhibition of Copper-based alloys by smart β-Cyclodextrin/Benzotriazole complexes, in: Proceedings of the 5th European Cyclodextrin Conference, Lisbon, Portugal, 2017: pp. 3–6.

[96] L.T. Popoola, Organic green corrosion inhibitors (OGCIs): A critical review, Corrosion Reviews 37 (2019) 71–102. https://doi.org/10.1515/corrrev-2018-0058.

[97] S. Varvara, L.M. Muresan, K. Rahmouni, H. Takenouti, Evaluation of some non-toxic thiadiazole derivatives as bronze corrosion inhibitors in aqueous solution, Corros Sci 50 (2008) 2596–2604. https://doi.org/10.1016/j.corsci.2008.06.046.

[98] C. Monticelli, A. Balbo, J. Esvan, C. Chiavari, C. Martini, F. Zanotto, L. Marvelli, L. Robbiola, Evaluation of 2-(salicylideneimino) thiophenol and other Schiff bases as bronze corrosion inhibitors by electrochemical techniques and surface analysis, Corros Sci 148 (2019) 144–158. https://doi.org/10.1016/j.corsci.2018.12.017.

[99] M.M. Antonijevic, M.B. Petrovic, Copper Corrosion Inhibitors. A review, Int. J. Electrochem. Sci 3 (2008) 1–28. https://doi.org/10.1016/S1452-3981(23)15441-1

[100] K. Marušić, H. Otmačić Ćurković, E. Supnišek Lisac, H. Takenouti, Two imidazole based corrosion inhibitors for protection of bronze from urban atmospheres, Croatica Chemica Acta 91 (2018) 435–446. https://doi.org/10.5562/cca3440

[101] F. Zucchi, G. Trabanelli, M. Fonsati, Tetrazole derivatives as corrosion inhibitors for copper in chloride solutions, Corros Sci 38 (1996) 2019–2029. https://doi.org/10.1016/S0010-938X(96)00094-7

[102] M. Mihit, L. Bazzi, R. Salghi, B. Hammouti, S. El Issami, Some tetrazolic compounds as corrosion inhibitors for copper in nitric acid medium, International Scientific Journal for Alternative Energy and Ecology 62 (2008) 173–182.

[103] X.R. Ye, X.Q. Xin, J.J. Zhu, Z.L. Xue, Coordination compound films of 1-phenyl-5-mercaptotetrazole on copper surface, Appl Surf Sci 135 (1998) 307–317. https://doi.org/10.1016/S0169-4332(98)00301-8

[104] E.M. Sherif, S.M. Park, 2-Amino-5-ethyl-1,3,4-thiadiazole as a corrosion inhibitor for copper in 3.0% NaCl solutions, Corros Sci 48 (2006) 4065–4079. https://doi.org/10.1016/j.corsci.2006.03.011.

[105] H. Shi, Z. Wang, G. Chu, Z. Li, H. Zhang, L. Song, Y. Wang, L. Sun, Z.C. Cao, F. Ma, pH-responsive corrosion protection coating with chitosan encapsulated halloysite nanotubes for active protection of copper, Mater Chem Phys 331 (2025). https://doi.org/10.1016/j.matchemphys.2024.130182.

[106] D.G. Shchukin, M. Zheludkevich, K. Yasakau, S. Lamaka, M.G.S. Ferreira, H. Möhwald, Layer-by-Layer Assembled Nanocontainers for Self-Healing Corrosion Protection, Advanced Materials 18 (2006) 1672–1678. https://doi.org/https://doi.org/10.1002/adma.200502053.

[107] A.H. Jafari, S.M.A. Hosseini, E. Jamalizadeh, Investigation of Smart Nanocapsules Containing Inhibitors for Corrosion Protection of Copper, Electrochim Acta 55 (2010) 9004–9009. https://doi.org/https://doi.org/10.1016/j.electacta.2010.07.065.

[108] M. Mahmoudian, E. Nozad, M.G. Kochameshki, M. Enayati, Preparation and investigation of hybrid self-healing coatings containing linseed oil loaded nanocapsules, potassium ethyl xanthate and benzotriazole on copper surface, Prog Org Coat 120 (2018) 167–178. https://doi.org/https://doi.org/10.1016/j.porgcoat.2018.03.014.

[109] M.L. Zheludkevich, S.K. Poznyak, L.M. Rodrigues, D. Raps, T. Hack, L.F. Dick, T. Nunes, M.G.S. Ferreira, Active protection coatings with layered double hydroxide nanocontainers of corrosion inhibitor, Corros Sci 52 (2010) 602–611. https://doi.org/10.1016/j.corsci.2009.10.020..

[110] E.M.M. Del Valle, Cyclodextrins and their uses: A review, Process Biochemistry 39 (2004) 1033–1046. https://doi.org/10.1016/S0032-9592(03)00258-9.

[111] A. Matencio, G. Hoti, Y.K. Monfared, A. Rezayat, A.R. Pedrazzo, F. Caldera, F. Trotta, Cyclodextrin monomers and polymers for drug activity enhancement, Polymers 13 (2021). https://doi.org/10.3390/polym13111684.

[112] S. S. Jambhekar, P. Breen, Cyclodextrins in pharmaceutical formulations I: Structure and physicochemical properties, formation of complexes, and types of complex, Drug Discovery Today, 21(2), (2016) 356–362 https://doi.org/10.1016/j.drudis.2015.11.017

[113] Biwer, A., Antranikian, G. & Heinzle, E. Enzymatic production of cyclodextrins. Applied Microbiology and Biotechnology 59, (2002) 609–617 doi: https://doi.org/10.1007/s00253-002-1057-x

[114] W. Saenger, J. Jacob, K. Gessler, T. Steiner, D. Hoffmann, H. Sanbe, K. Koizumi, S. M. Smith, T. Takaha, Structures of the common cyclodextrins and their larger analogues - beyond the doughnut, Chemical Reviews, 98 (5) (1998) 1787–1802 DOI: https://doi.org/10.1021/cr9700181

[115] T. Loftsson, M. E. Brewster, Pharmaceutical applications of cyclodextrins. 1. Drug solubilization and stabilization, Journal of Pharmaceutical Sciences, 85 (10) (1996) 1017–1025. DOI: https://doi.org/10.1021/js950534b

[116] T. Loftsson and M. E. Brewster, Pharmaceutical applications of cyclodextrins: Basic science and product development, Journal of Pharmacy and Pharmacology, 62 (11) (2010) 1607–1621. DOI: https://doi.org/10.1111/j.2042-7158.2010.01030.x

[117] A. Figueiras, J.M.G. Sarraguça, R.A. Carvalho, A.A.C.C. Pais, F.J.B. Veiga, Interaction of omeprazole with a methylated derivative of β-cyclodextrin: Phase solubility, NMR spectroscopy and molecular simulation, Pharm Res 24 (2007) 377–389. https://doi.org/10.1007/s11095-006-9161-8.

[118] E. Berdimurodov, I. Eliboyev, K. Berdimuradov, A. Kholikov, K. Akbarov, O. Dagdag, M. Rbaa, B. El Ibrahimi, D.K. Verma, R. Haldhar, N. Arrousse, Green β-cyclodextrin-based corrosion inhibitors: Recent developments, innovations and future opportunities, Carbohydr Polym 292 (2022). https://doi.org/10.1016/j.carbpol.2022.119719.

[119] T.M. de Souza, R.F.B. Cordeiro, G.M. Viana, L.C.S. Aguiar, L.F. de Senna, L.F.B. Malta, E. D'Elia, Inclusion compounds of dibenzylthiourea with hydroxypropylated-cyclodextrins for corrosion protection of carbon steel in acidic medium, J Mol Struct 1125 (2016) 331–339. https://doi.org/https://doi.org/10.1016/j.molstruc.2016.06.072.

[120] A.N. Khramov, N.N. Voevodin, V.N. Balbyshev, M.S. Donley, Hybrid organo-ceramic corrosion protection coatings with encapsulated organic corrosion inhibitors,

Thin Solid Films 447–448 (2004) 549–557. https://doi.org/https://doi.org/10.1016/j.tsf.2003.07.016.

[121] A.N. Khramov, N.N. Voevodin, V.N. Balbyshev, R.A. Mantz, Sol-gel-derived corrosion-protective coatings with controllable release of incorporated organic corrosion inhibitors, Thin Solid Films 483 (2005) 191–196. https://doi.org/10.1016/j.tsf.2004.12.021.

[122] S. Amiri, A. Rahimi, Anticorrosion behavior of cyclodextrins/inhibitor nanocapsule-based self-healing coatings, J Coat Technol Res 13 (2016) 1095–1102. https://doi.org/10.1007/s11998-016-9824-2.

[123] C.J. Zou, Q.W. Tang, P.W. Zhao, E.D. Guan, X. Wu, H. Ye, Further study on the inclusion complex of 2-phosphonobutane-1,2,4-tricarboxylic acid with B-cyclodextrin: A new insight of high inhibition efficiency for protecting steel corrosion, J Pet Sci Eng 103 (2013) 29–35. https://doi.org/10.1016/j.petrol.2013.02.013.

[124] M.S. De Luna, G. Buonocore, G. Di Carlo, C. Giuliani, G.M. Ingo, M. Lavorgna, Protection of bronze artefacts through polymeric coatings based on nanocarriers filled with corrosion inhibitors, in: AIP Conf Proc, American Institute of Physics Inc., 2016. https://doi.org/10.1063/1.4949623.

[125] M. Salzano de Luna, G.G. Buonocore, C. Giuliani, E. Messina, G. Di Carlo, M. Lavorgna, L. Ambrosio, G.M. Ingo, Long-Lasting Efficacy of Coatings for Bronze Artwork Conservation: The Key Role of Layered Double Hydroxide Nanocarriers in Protecting Corrosion Inhibitors from Photodegradation, Angewandte Chemie 130 (2018) 7502–7506. https://doi.org/10.1002/ange.201713234.

[126] T. Kosec, A. Legat, I. Milošev, The comparison of organic protective layers on bronze and copper, Prog Org Coat 69 (2010) 199–206. https://doi.org/10.1016/j.porgcoat.2010.04.010

[127] M.T. Molina, E. Cano, B. Ramírez-Barat, Testing protective coatings for metal conservation: the influence of the application method, Herit Sci 11 (2023). https://doi.org/10.1186/s40494-023-00937-0.

[128] G. Masi, M. Aufray, A. Balbo, E. Bernardi, M.C. Bignozzi, C. Chiavari, J. Esvan, N. Gartner, V. Grassi, C. Josse, T. Kosec, C. Martini, C. Monticelli, L. Škrlep, W. Sperotto, E. Švara Fabjan, E. Tedesco, F. Zanotto, L. Robbiola, B-IMPACT project: eco-friendly and non-hazardous coatings for the protection of outdoor bronzes, in: IOP

Conf Ser Mater Sci Eng, IOP Publishing Ltd, 2020. https://doi.org/10.1088/1757-899X/949/1/012097.

[129] M. Pilz, H. Römich, Sol-gel derived coating for outdoor bronze conservation, J Solgel Sci Technol 8 (1997) 1071–1075. https://doi.org/10.1007/BF02436986.

[130] G. Chiavari, A. Colucci, R. Mazzeo, M. Ravanelli, Organic content evaluation of corrosion patinas in outdoor bronze monuments, Chromatographia 49 (1999) 35–41. https://doi.org/10.1007/BF02467184.

[131] C. Petiti, L. Toniolo, D. Gulotta, B. Mariani, S. Goidanich, Effects of cleaning procedures on the long-term corrosion behavior of bronze artifacts of the cultural heritage in outdoor environment, Environmental Science and Pollution Research 27 (2020) 13081–13094. https://doi.org/10.1007/s11356-020-07814-4.

[132] E. Cano, D. Lafuente, D.M. Bastidas, Use of EIS for the evaluation of the protective properties of coatings for metallic cultural heritage: A review, Journal of Solid State Electrochemistry 14 (2010) 381–391. https://doi.org/10.1007/s10008-009-0902-6.

[133] T. Kosec, H.O. Ćurković, A. Legat, Investigation of the corrosion protection of chemically and electrochemically formed patinas on recent bronze, Electrochim Acta 56 (2010) 722–731. https://doi.org/10.1016/j.electacta.2010.09.093.

[134] P. Letardi, Electrochemical measurements in the conservation of metallic heritage artefacts: An overview, in: Corrosion and Conservation of Cultural Heritage Metallic Artefacts, Elsevier Ltd, 2013: pp. 126–148. https://doi.org/10.1533/9781782421573.2.126.

[135] L.A. Ellingson, T.J. Shedlosky, G.P. Bierwagen, E.R. de la Rie, L.B. Brostoff, The use of electrochemical impedance spectroscopy in the evaluation of coatings for outdoor bronze, Studies in Conservation 49 (2004) 53–62. https://doi.org/10.1179/sic.2004.49.1.53.

[136] P. Letardi, B. Salvadori, M. Galeotti, A. Cagnini, S. Porcinai, A. Santagostino Barbone, A. Sansonetti, An in situ multi-analytical approach in the restoration of bronze artefacts, Microchemical Journal 125 (2016) 151–158. https://doi.org/10.1016/j.microc.2015.11.018

Chapter 4

Overview of the articles

The decision to structure my PhD thesis as a collection of four articles is based on the fact that, from an academic perspective, a consistent number of publications is often a key requirement for advancement. Moreover, by publishing my results in international journals, I reached a broader academic audience and received valuable feedback on my work. This process of submission, review, and revision has improved the methodological and theoretical basis of my research.

Structuring my research into four distinct but interconnected papers made the writing and the project process more efficient and effective. It allowed me to focus on specific aspects of my overall research question while maintaining a coherent narrative throughout the thesis: the first paper (**Article A**) aims to identify the best formulation based on the physicochemical properties, without the variable of the bronze substrate. This approach saved material and enabled me to pay closer attention to potential drawbacks related only to coating science. In this study, I employed a canonical approach, which involved a qualitative comparison of the multi-analytical results, enabling a comprehensive examination of the coatings performance. To go deeper into data interpretation, I decided to use chemometrics (**Article B**). This method enables the handling of correlated variables by considering their interconnections and dependencies. Given that my data was multivariate, I believed that employing chemometrics would be beneficial. Principal Component Analysis (PCA) enabled the studying of coating aging and helped to confirm the selection of the optimal formulation. Once I identified the most performative formulation, I aimed to improve it by addressing the issue of the leaching of corrosion inhibitor from the coating. After discovering that cyclodextrins could be an ideal nanocontainer, I incorporated them into the formulation, which resulted in an improved coating (**Article C**). Finally, it was necessary to test the formulation on the target surface. I first determined how to apply the formulations and assessed their compatibility with the bronze patinated surface (**Article D**). Once this was established, the coated bronze mock-ups were exposed to outdoor weathering in a marine environment.

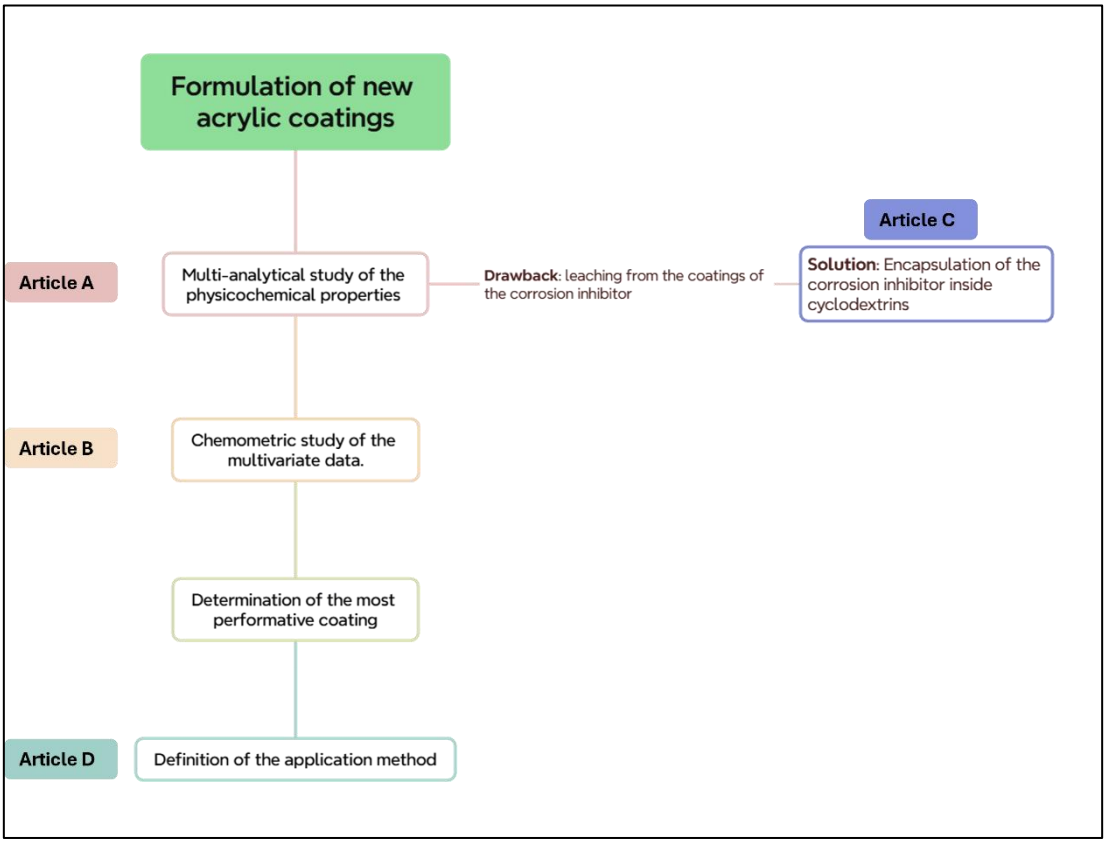

Scheme 1: Workflow of the presented results

4.1 Article A: Improvement in the sustainability and stability of acrylic protective coatings for outdoor bronze artworks

Article A presents the main results of the first part of the PhD project. This paper concerns the development of new coatings and the selection of the best performing ones through an extensive analysis of their physical-chemical properties.

The formulations were designed based on Incralac, the most widely employed product for protecting copper alloys. The acrylic resin Paraloid® B44, which is the film-forming component of Incralac, was considered thanks to its peculiar properties of being transparent and versatile, exhibiting strong adhesion, stability, and reversibility. Instead, the harmful benzotriazole was replaced with other corrosion inhibitors with a safer toxicity profile. As alternatives to benzotriazole, 5-mercapto-1-pheniltetrazole (MPT) and 2-amino-5-ethyl-1,3,4-thiadiazol- (AEDTA) were chosen since they had already proven to be effective inhibitors of copper corrosion [104], but never been employed inside an acrylic resin.

The formulation was completed with a light stabilizer, to inhibit the photodegradation of the resin, and a green solvent. The two light stabilizers are Tinuvin® 312, a UV absorber (i.e. ethandiamide N'-(2-ethoxyphenyl)-N-(2-ethylphenyl)oxamide), and Tinuvin® 5050, composed of a mixture of UV absorber (i.e. 2-(2-hydroxyphenyl) benzotriazole) and HALS—Hindered Amine Light Stabilizer. The two kinds of Tinuvin were chosen because they have different mechanisms for hampering photodegradation phenomena, allowing us to determine which was better suited for the new system.

To comprehensively study the contribution of every single component, formulations with only corrosion inhibitor, light stabiliser, and acrylic resin, together with the ones with all the components, were formulated for a total of 21 formulations. They were applied on inert supports to avoid any variable given by the substrate and to evaluate the intrinsic stability of the coatings, before investigating their protective and anticorrosive properties. The prepared samples underwent artificial solar ageing and were monitored over time using a multi-analytical approach to examine their chemical and physical-mechanical properties simultaneously. Their structural and compositional changes were monitored by Fourier transform infrared spectroscopy (FTIR). Colour stability was evaluated by colorimetric measurements. Differential scanning calorimetry (DSC) was used to determine the glass transition temperature (Tg) and to estimate other properties of the coatings, such as resistance and flexibility. Reversibility was assessed by determining the insoluble fraction of the coatings after ageing. Moreover, the persistence of corrosion inhibitors in the coatings was studied by pyrolysis-gas chromatography/mass spectrometry (Py-GC/MS). All the results were compared with those of pure Incralac.

Interesting outcomes resulted after 1000 hours of exposure to artificial solar light. The presence of both light stabilizers and corrosion inhibitors in the formulations yielded the best results. All coatings exhibited colour changes below the perceptibility threshold ($\Delta E = 3$), with slight darkening (negative ΔL^*) and yellowing (positive Δb^*). Formulations containing MPT demonstrated less colour stability than those with AEDTA, and Incralac was the one that changed the most. Both stabilizers improved the colour stability of coatings. MPT and AEDTA increased the glass transition temperature (Tg), making the coatings brittle over time. However, the stabilizers mitigated this effect, with both types of Tinuvin reducing the Tg increase over time. Regarding reversibility, coatings with only the corrosion inhibitors showed increased insoluble fraction, while the use of light stabilizers minimized the formation of insoluble fraction, improving the removability of the coatings. FTIR analyses revealed that Paraloid® B44 exhibited good photo-oxidative stability, while AEDTA and MPT

corrosion inhibitors were released in the environment over time. Tinuvin® 312 extended the AEDTA persistence in the coating, whereas Tinuvin® 5050 showed low stability. Py-GC/MS showed that MPT undergoes a significant fragmentation, indicating instability when exposed to light stress. In summary, AEDTA performs better than MPT, as it does not exhibit colour change over time and demonstrates photochemical stability. Light stabilizers are required to enhance the chemical and thermo-mechanical properties of the coatings, with Tinuvin® 312 showing greater stability than Tinuvin® 5050.

This first phase of the research identified the best formulations for use on bronze mock-ups. However, it also revealed the need for further improvements as the corrosion inhibitors still tended to leach out over time. Article C addresses this issue.

4.2 Article B: Advancing preservation: a chemometric approach for monitoring the degradation of protective coatings for bronze statues

Article B investigates the potential of chemometrics as an effective tool to study degradation and identify the most efficient coatings through the simultaneous analysis of various types of data. Given the considerable challenges that researchers face during the monitoring of the evolution of coatings over time, this paper aimed to determine whether Principal Component Analysis (PCA) could provide additional insights and validate the traditional visual comparison methods.

The dataset was constructed using the spectroscopic data already reported in Article A, along with benchtop UV-Vis data. This choice was ideal because the data had already been analysed through visual comparison, allowing us to validate the PCA results since all obtained results were consistent with the previous observations. Additionally, it facilitated the examination of benchtop UV-Vis data that were challenging to interpret due to a high baseline. The paper proposes a methodology based on spectroscopic techniques and chemometric data analysis. The methods used proved to be effective, and the research work highlights the complementary and similar insights they provide. A monitoring system based on the principal component analysis was introduced, which distinguishes between various types of coatings in terms of corrosion inhibitor and light stabiliser, and simplifies the interpretation of differences in the decay as formulations age. This approach allows for an easy selection of optimal formulations using simple, interpretable two-dimensional graphs, without needing specific expertise in spectrum interpretation.

The results obtained confirmed those published in article A. The colorimetric data indicated that MPT coatings are more prone to degradation, whereas benchtop UV-Vis analysis revealed that Tinuvin® 5050 experiences more substantial changes over time. This complementary information, easily interpreted through the proposed chemometric approach, led to the selection of AEDTA and Tinuvin® 312 as the optimal additives to the acrylic protective coating. These results clearly show that the proposed approach for decay studies is effective and robust.

4.3 Article C: Enhancing permanence of corrosion inhibitors within acrylic protective coatings for outdoor bronze using green nanocontainers

Article C reports the method proposed to address the problem of the short permanence of the additives inside coatings. Leaching out of corrosion inhibitors from coatings is a known significant limitation. This paper explores the use of nanocarriers to slow the release into the environment of 2-amino-5-ethyl-1,3,4-thiadiazol- (AEDTA), the inhibitor that gave the best results.

Cyclodextrins were selected to host the inhibitor, due to their capability to form complexes incorporating small organic molecules. Among the different types of cyclodextrins, methyl-β-cyclodextrin (Me-β-CD) was chosen because its methoxy groups in place of primary hydroxyls offer better compatibility with acrylic resins than the unsubstituted β-CD. The complexes of Me-β-CD and AEDTA were prepared with a straightforward and green reaction: water, cyclodextrin, and corrosion inhibitor were the only reagents. A multi-analytical study of the Me-β-CD /AEDTA complex was carried out.

The results demonstrated the formation of an inclusion complex with a 1:1 stoichiometry, in which AEDTA interacts with the internal cavity of the cyclodextrin through the -NH_2 side group. This was proved by Fourier transform infrared spectroscopy, X-ray diffraction and nuclear magnetic resonance spectroscopy. Then, acrylic coatings at different Me-β-CD/AEDTA complex concentration were prepared. The efficacy of the complex in extending the retention of the inhibitor within the protective acrylic coatings was evaluated by thermally aging the coatings at 80 °C and monitoring the release of AEDTA in both uncomplexed and complexed forms every 24 hours. To evaluate the volatilization of the corrosion inhibitor, solid phase microextraction-gas chromatography/mass spectrometry (SPME-GC/MS) and thermal desorption-GC/MS (TD-GC/MS) analyses were performed. The results were

compared to those of pure AEDTA and Incralac. Chromatographic and FTIR results indicated that the coatings containing Me-β-CD/AEDTA complexes retain the corrosion inhibitor longer than the coatings with AEDTA alone and Incralac.

The new formulations may be promising candidates for developing new coatings with enhanced stability and prolonged retention of AEDTA. These coatings also possess valuable properties such as cost-effectiveness, environmental compatibility, and ease of handling. Ongoing investigations are examining the anticorrosive properties of these protective coatings: they have been applied to bronze patinated coupons, which are currently weathering at the marine station in Genoa, Italy.

4.4 Article D: Optimizing application methods of sustainable acrylic protective coatings for outdoor patinated bronze artworks- draft

The results discussed in this article conclude the research carried out during the PhD. Here, the method of coating application was studied and preliminary results on the protective properties of the newly developed formulations applied on patinated bronze coupons were obtained. This research was performed during my period abroad as visiting PhD student at the "Centro Nacional de Investigaciones Metalurgicas" of the Spanish National Research Council in Madrid.

This work evaluated application methods for the formulations developed and selected in the previous phases of the research. The coatings were those prepared with Paraloid ® B44, 5% w/w of corrosion inhibitor, namely 5-mercapto-1-pheniltetrazole (MPT) and 2-amino-5-ethyl-1,3,4-thiadiazol- (AEDTA), and Tinuvin® 312 as light stabilizer.

To investigate the possible role of Paraloid® B44 concentration in the solution, a test was performed to compare the covering capability of two layers of coating: the first with 10% w/w Paraloid for each layer and the second consisting of a layer at 5% w/w followed by another at 10% w/w. Whatever the concentration of Paraloid® B44 in solution, the concentration of corrosion inhibitors was kept constant. The brush application method was chosen because it is widely adopted in conservation practices. The formulations were applied in two crisscrossed layers one week apart. The coated coupons were characterized using electrochemical impedance spectroscopy (EIS) to evaluate the protective properties of the coatings, colorimetry and macrophotography to verify the appearance of the patina, and Eddy Current measurements to assess the

thickness of the layers. All measurements were conducted on the bare patina and one week after the application of both the first and second layer.

Results showed that the best application method was the one with Paraloid concentration of 5% w/w for the first layer and 10% w/w for the second. This ensured a better protection, namely higher polarization resistance (Rp) values, at the same thickness and colour changes. The formulations with 2-amino-5-ethyl-1,3,4-thiadiazol- (AEDTA) gave higher protection. They also produced the higher colour change in the patina surface, but within acceptable limits.

Before exposing the coatings to natural weathering, a thermohygrometric artificial ageing was conducted to verify the results obtained after the application. The colorimetric and FTIR results showed that all the coatings remained stable over time. Additionally, Principal Component Analysis was applied to the FTIR data, confirming that the most effective coatings were those with the lowest concentration of acrylic resin in the first layer. Therefore, this application method was chosen to coat other sets of coupons currently exposed to weathering in a marine-industrial environment so as to evaluate and compare the long-term effectiveness of the new formulations with bare Paraloid® B44 and Incralac.

Chapter 5

Improvement in the sustainability and stability of acrylic protective coatings for outdoor bronze artworks

G. Pellis[1], B. Giussani[2], P. Letardi[3], T. Poli[1], P. Rizzi[1], B. Salvadori[4], A. Sansonetti[5], D. Scalarone[1]

(1) Department of Chemistry, University of Torino, Via Pietro Giuria 7, Torino, Italy

(2) Science and High Technology Department, Università degli Studi dell'Insubria, Via Valleggio 9, Como, Italy

(3) Institute of Anthropic Impacts and Sustainability in the Marine Environment, CNR, Via De Marini 6, Genova, Italy

(4) Institute of Heritage Science, CNR, Via Madonna del Piano 10, Sesto Fiorentino, Italy

(5) Institute of Heritage Science, CNR, Via Roberto Cozzi 53, Milan, Italy

5.1 Abstract

Outdoor bronze artworks are an entrenched part of our urban landscape. They are usually covered by a patina resulting from their exposition to the environment. This patina plays an important aesthetic role and may provide some passivation on the surface, nonetheless it does not prevent the degradation processes promoted by external factors such as pollution, light and humidity. One of the strategies to slow down these unwanted processes is the application of protective coatings. The products currently available have some limitations due to the loss of effectiveness over time and poor environmental sustainability. With the aim of proposing more performing alternatives, coatings based on Paraloid® B44 modified with corrosion inhibitors and light stabilizers were prepared and characterized. Two non-toxic corrosion inhibitors

were studied, 5-mercapto-1-pheniltetrazole (MPT) and 2-amino-5-ethyl-1,3,4-thiadiazol- (AEDTA), comparing them with the traditional benzotriazole (BTA). The approach used aimed to identify the blend providing the most stable coatings. The chemical and physical properties of the coatings, such as colour, solubility, glass transition and composition, were studied and monitored over time. All coatings have shown adequate visual properties; however, corrosion inhibitors degrade some other properties of the coatings and need to be used in conjunction with light stabilizers. The permanence of corrosion inhibitors in the coatings over time was also studied by investigating the role of the support. The establishment of specific interactions between inhibitors and the bronze surface lengthens their permanence in the coatings compared to what happens with inert supports. Especially for AEDTA, the inhibitor retention within the coating and at the coating-bronze interface is better than for BTA and MPT.

The effect of each of the additives on the photooxidation stability of the coating was evaluated and the most promising inhibitor and stabilizer combination was identified.

5.2 Introduction

The conservation of metal art objects is a complex and demanding task, especially for those placed outdoors and exposed to atmospheric agents and reactive compounds present in the environment [1, 2]. Rain, abrasive agents such as windblown sand and debris, air pollution, and human contact are just few of the main responsible for the degradation of metal artworks [3, 4]. In particular, the complex nature of the surfaces of outdoor bronze artworks is a major challenge for their conservation, and proper methodologies should be adopted to address the interaction with the environment so as to preserve them for future generations [4, 5]. The most difficult task is in balancing the preservation of the so called “noble patina” surface layer and to protect the surface of the bronze artwork from detrimental interaction with the environment. Indeed, “noble patina”, with its pleasant appearance, is part of the heritage aesthetic value and slows down the corrosion rate with respect to bare metal. Unfortunately, this kind of patina is not stable enough in the changing environment, with pollutants and physical-chemical parameters which may lead to remarkable alteration of the composition and appearance of the surface layer [6]. As a matter of fact, the most widespread common practice for the protection of outdoor bronze monuments consists in the application of coatings on the surface [7] which should be renewed when the protective properties become too weak. In general, coatings for conservation are applied to avoid the contact between the metal-patina layers and the actively corroding agents present in the

environment. Treatments applied to heritage assets must meet specific requirements [4, 8]. An ideal sustainable coating should prevent the object from degradation without modifying its appearance: in this view, only transparent colourless coatings are allowed. Moreover, the chemical nature of the treatments should permit their removal with a safe and non-toxic approach. Eventually, the properties of these treatments should assure a total compatibility with the surfaces involved, a good protective effectiveness, long-term durability and low-cost maintenance [1, 8]. Nowadays, the most used protective products are waxes and Incralac®, but both present problems: Incralac ® contains benzotriazole (BTA)[2, 9, 10], a harmful corrosion inhibitor, suspected of being carcinogenic and which is released into the environment over time, while waxes are easily deteriorated by the environment they are supposed to protect the artworks from [11, 12]. The actual conservation perspective focuses on new eco-friendly and safe treatments to overcome the drawbacks of Incralac® or waxes, even though the latter are still considered very attractive options. In the last 20 years, the most tested protective coatings for copper and its alloys have been functional coatings with triazoles, silanes and fluoropolymers [11, 12, 13, 14, 15]. More recently, other innovative solutions have been taken into account as well, like nano-composites and biopolymers [4, 7]. Finally, preliminary studies outlined promising results concerning the application of different inorganic coatings based on calcium oxalates [16] and diamond-like carbon, applied by plasma-enhanced chemical vapour deposition [18]. Although the initial outcomes are encouraging, several aspects related to effectiveness and durability must be further explored to implement tailored applications of these systems as protective coatings for Cultural Heritage.

In this research, Paraloid® B44-based coatings containing a non-toxic corrosion inhibitor and a light stabilizer are investigated. The choice of Paraloid® B44 relies on its peculiar properties of being transparent, versatile, exhibiting strong adhesion, stability and long term reversibility making it an ideal protective coating specifically recommended for metal protection [19]. Two types of commercially available corrosion inhibitors have been studied: 5-mercapto-1-pheniltetrazole (MPT) and 2-amino-5-ethyl-1,3,4-thiadiazol-. (AEDTA) [15, 17]. They have already been tested for bronze protection, providing encouraging results, but so far they have been rarely used as components for polymer coatings. Their toxicity profile is safer than that of BTA, involving less restrictions on their usage [35]. However, a limitation of corrosion inhibitors is represented by their light-sensitivity and their poor persistence within the coating [20, 21] . Consequently, light stabilisers were added aiming at preventing the corrosion inhibitors and the acrylic resin from photooxidative degradation. Two stabilizers were chosen based on their different mechanisms of action: the UV absorber Tinuvin® 312, (i.e. N'-(2-ethoxyphenyl)-N-(2-ethylphenyl)oxamide) and Tinuvin®

5050, a mixture of UV absorber (i.e. 2-(2-hydroxyphenyl) benzotriazole) and a HALS-Hindered Amine Light Stabilizer. The solvent used to solubilize the various components and prepare the coatings is 1-methoxypropan-2-ol, a solvent with low toxicity [22].

The proposed coatings were characterized by applying a multi-analytical protocol to investigate their intrinsic properties and the feasibility of their application on bronze specimen simulating artworks. Furthermore, the same multi-analytical protocol was applied on Incralac® films which were used as a reference product. To assess the coating stability over time, the prepared specimens underwent artificial solar ageing and their structural and compositional changes were monitored by Fourier Transformed Infrared Spectroscopy (FTIR). Colour stability was evaluated by colorimetric measurements. Differential Scanning Calorimetry (DSC) was used to determine the glass transition temperature (Tg) and to estimate other properties of the coatings such as adhesion, mechanical resistance and flexibility. Reversibility was assessed by determining the insoluble fraction of the coatings after ageing. Moreover, the persistence of corrosion inhibitors in the coatings was studied by Pyrolysis-Gas Chromatography /Mass Spectroscopy (Py-GC/MS). Finally, four coatings were selected and applied by brush on bronze mock ups. Their chemical changes during artificial solar light irradiation were monitored through μFTIR in reflection mode.

5.3 Experimental

5.3.1 Materials

The components of the coatings prepared and analysed in this research are listed in Table 1. Paraloid® B44 (ethyl acrylate/methyl methacrylate copolymer) was purchased from Sinopia s.a.s. The corrosion inhibitor 5-mercapto-1-pheniltetrazole (MPT) was purchased from Alfa Aesar and 2-amino-5-ethyl-1,3,4-thiadiazol-(AEDTA) from Sigma Aldrich. Tinuvin® 312 (N'-(2-ethoxyphenyl)-N-(2-ethylphenyl)oxamide) and Tinuvin® 5050 (a mixture of 2-(2-hydroxyphenyl) benzotriazole and a HALS) were obtained from BASF. The solvent used to solubilize the various components and prepare the coatings was 1-methoxypropan-2-ol purchased from Sigma Aldrich (Table 1). The solutions were prepared by adding the various ingredients in a vial in the following order: acrylic resin, additives and finally the solvent. They were stirred for 24 hours until complete solubilization. The solutions were applied with a brush or poured with the aid of a pipette on different flat supports and left to dry until complete solvent evaporation and formation of a thin solid film. Glass slides, silicon wafers, a white ceramic tile and bronze discs were used as

supports, depending on the type of analysis to be performed, as summarised in Table 2. The bronze discs are made of Cu-Sn-Pb-Zn and comply with the SAE 660 standard. Their diameter is 4 cm. To ensure maximum reproducibility of the characteristics of the coatings, they were applied on the various supports in a controlled way: for FTIR analysis on silicon wafers the thickness of the coatings was controlled by assuring that the absorbance of the most intense peak was between 0.7 and 1; for coatings prepared on glass slides the quantity of solid coating per surface unit was kept constant by adjusting the volume of solution spread on the glass; for coatings applied by brush, the same brush was used both for white tile and bronze discs. On the white tile the application was performed by two strokes in the same direction while for bronze discs two strokes were made orthogonally, to ensure the whole covering of the surface.

The inhibitors were tested in three different concentrations, while a fixed concentration was used for light stabilizers. The composition of the prepared solutions and of the dried coatings obtained after solvent evaporation are reported in Table 3 and 4, respectively.

Table 1: Structures of the coating components

Name	Structure
Paraloid® B44 ethyl acrylate/methyl methacrylate copolymer	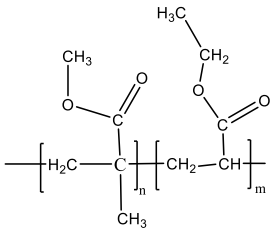
MPT 5-mercapto-1-phenyltetrazole	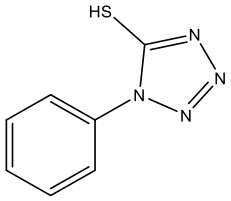
AEDTA 2-amino-5-ethyl-1,3,4-thiadiazol-	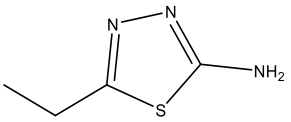
TIN312 Tinuvin® 312	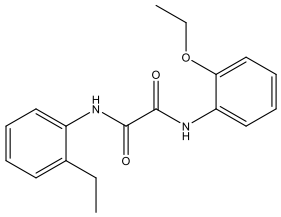
TIN5050 Tinuvin® 5050	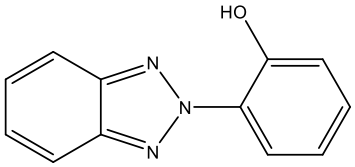 + HALS
1-methoxypropan-2-ol	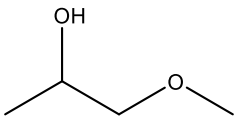

Table 2: Application method of the coating and type of support used depending on the analysis

Application method of the coating and type of support	Techniques					
	Colorimetry	**FT-IR**	**µFTIR**	**Py-GC/MS**	**DSC**	**Insoluble fraction**
Poured on glass slide				X	X	X
Poured on silicon wafer		X				
By brush on white ceramic tile	X					
By brush on bronze discs			X			

Table 3: Composition of the solutions [%w/w]

	Sample number																				
	1	**2**	**3**	**4**	**5**	**6**	**7**	**8**	**9**	**10**	**11**	**12**	**13**	**14**	**15**	**16**	**17**	**18**	**19**	**20**	**21**
B44	10	10	10	10	10	10	10	10	10	10	10	10	10	10	10	10	10	10	10	10	10
AEDTA	/	/	/	/	/	/	/	/	/	/	/	/	1.0	0.5	0.1	1.0	0.5	0.1	1.0	0.5	0.1
MPT	/	/	/	1.0	0.5	0.1	1.0	0.5	0.1	1.0	0.5	0.1	/	/	/	/	/	/	/	/	/
TIN312	/	0.3	/	/	/	/	0.3	0.3	0.3	/	/	/	/	/	/	0.3	0.3	0.3	/	/	/
TIN5050	/	/	0.3	/	/	/	/	/	/	0.3	0.3	0.3	/	/	/	/	/	/	0.3	0.3	0.3
1-methoxypropan-2-ol	90.0	89.7	89.7	89	89.5	89.9	88.7	89.2	89.6	88.7	89.2	89.6	89	89.5	89.9	88.7	89.2	89.6	88.7	89.2	89.6

Table 4: Composition of dry coatings [%w/w]

Sample number		**1**	**2**	**3**	**4**	**5**	**6**	**7**	**8**	**9**	**10**	**11**	**12**	**13**	**14**	**15**	**16**	**17**	**18**	**19**	**20**	**21**
Coating Label		B	BT3	BT5	B M9	B M5	B M1	B M9 T3	B M5 T3	B M1 T3	B M9 T5	B M5 T5	B M1 T5	B A9	B A5	B A1	B A9 T3	B A5 T3	B A1 T3	B A9 T5	B A5 T5	B A1 T5
Composition (% w/w)	**B44**	100	97	97	91	95	99	88	92	96	88	92	96	91	95	99	88	92	96	88	92	96
	AEDTA	/	/	/	/	/	/	/	/	/	/	/	/	9	5	1	9	5	1	9	5	/
	MPT	/	/	/	9	5	1	9	5	1	9	5	1	/	/	/	/	/	/	/	/	1
	TINUVIN 312	/	3	/	/	/	/	3	3	3	/	/	/	/	/	/	3	3	3	/	/	/
	TINUVIN 5050	/	/	3	/	/	/	/	/	/	3	3	3	/	/	/	/	/	/	3	3	3

The coatings were aged for 1000 hours in a Q-Sun Xe-1 Xenon Test Chamber (Q-Lab Corporation, UK), at constant temperature of 50 °C, irradiance set at 0.68 W/m^2 at 340 nm and Daylight Q filter (cut-on at 295 nm), simulating exposure to direct sunlight. They were regularly monitored by colorimetric measurements and FTIR spectroscopy, while DSC, Py-GC/MS and the determination of the insoluble fraction were performed before and after aging. The same analyses were also carried out on Incralac®.

5.3.2 Characterization

5.3.2.1 Colour measurements

Colour measurements were performed to assess colour stability of the coatings over time. The change of colour (ΔE^*_{ab}) was calculated for each area comparing the colour coordinates L*, a*, b* obtained before and after aging.The colour difference has been computed according to the parameter ΔE^*_{ab}, which represents the Euclidean distance between the two colours (CIELAB1976):

$$\Delta E^*_{ab} = \sqrt{(\Delta a^*)^2 + (\Delta b^*)^2 + (\Delta L^*)^2}$$

In the three-dimensional CIELAB colour space L* defines the lightness and it goes from 0 (black) to 100 (white), a* is a chromatic scale in the green (negative values) - red (positive values) direction and b* is the chromatic scale blue (negative values) to yellow (positive values).Thin coatings were applied by brush on a white tile and analysed by a Portable Spectrophotometer CM-700d KONICA Minolta in SCI (Specular Component Included) mode; For each mock-up, colour coordinates L*, a* and b* were acquired for a total of 15 measurements (5 sites of measure, 3 measurements for each site) then the average values were calculated.

5.3.2.2 Fourier Transform Infrared Spectroscopy (FTIR)

FTIR was used for chemical characterization and to monitor chemical changes over time. All coatings were applied on silicon supports and analysed in transmission mode with a Perkin Elmer Spectrum 100 spectrometer equipped with a DTS detector. Each analysis was performed carrying out 16 scans in a range from 450 cm^{-1} to 4500 cm^{-1}, with a resolution of 4 cm^{-1}. For reflectance micro-FTIR analyses on bronze discs a Spotlight FTIR Perkin Elmer microscope with a MCT detector was used collecting 32 scans per spectrum, at 2 cm^{-1} resolution in the range between 650 cm^{-1} to 4000 cm^{-1}.

5.3.2.3 Differential Scanning Calorimetry (DSC)

DSC provided the glass transition temperature of the coatings. The samples needed for the analysis were taken with a scalpel by scratching the coatings applied on glass slides. The analyses were performed with a Q200 (TA Instruments) Differential Scanning Calorimeter (DSC) and were carried out on 8 mg of sample (unaged and aged), setting a heat-cool-heat cycle from -40°C to 110°C with a ramp of 10°C/min under nitrogen flow.

5.3.2.4 Insoluble fraction

The insoluble fraction was determined to get information on the coating reversibility. The coatings were prepared on microscope slides in six replicas. Three of them were aged and the others were used to determine the percentage of insoluble fraction before ageing. The microscope slides were weighted before and after the application of the coating, during and after the artificial ageing. The insoluble fraction was determined after having soaked the films in tetrahydrofuran and having collected it with a vacuum filtration system on pre-weighted PTFE membrane filters (0.45 µm). Data reported are the average of the three replicas.

5.3.2.5 Pyrolysis-gas chromatography/mass spectrometry (Py-GC/MS)

Py-GC/MS analyses were used to assess the stability of corrosion inhibitors and their persistence in the coatings over time. The analyses were performed in double-shot mode with a micro-furnace Multi-Shot Pyrolyzer EGA/Py-3030D (Frontier Lab, Japan) coupled to a GC/MS system. Samples were taken with a scalpel by scratching the coatings applied on glass slides and were placed into a stainless-steel cup and inserted into the micro-furnace. For the first shot the pyrolysis temperature was set at 250 °C and kept for 1 minute. In the second shot the sample was pyrolyzed at 500 °C for 12 seconds. The interface temperature of the pyrolizer was 280 °C and the temperature of the GC injector was kept at 280 °C. The GC was equipped with a methylphenyl-polysiloxane cross-linked 5% phenyl methyl silicone (30 m, 0.25 mm i.d., 0.25 µm film thickness) capillary column. The carrier gas was helium (1.0 mL/min) and split ratio was 1/20 of the total flow. The following temperature program was used for the gas chromatographic separation: isotherm of 2 minutes at 50 °C, ramp of 10 °C/min up to 300 °C, isotherm at 300 °C for 10 minutes. An Agilent 8860 Gas Chromatograph and a 5977B Mass Selective Detector (Agilent Technologies, USA)

were used. Mass spectra were recorded under electron impact at 70 eV, scan range 45-800 m/z. All instruments were controlled by Agilent Mass Hunter Workstation (ver. 10.1.49) software. The mass spectra assignment was done by mass library searches (NIST2008), by comparison with literature data and interpretation of fragmentation paths of mass spectra.

5.4 Results and Discussion

Since one of the most important prerequisites of coatings for the protection of bronze sculptures and objects is preserving the aspect of the artwork, a colorimetric study was performed in order to evaluate whether the application of the coatings could influence the appearance of the works of art. Figure 1 shows the colour changes of the different coatings applied by brush on a white tile after 1000 hours of ageing under artificial solar light. The results obtained were encouraging, as they highlight that the colour change (ΔE) of all coatings is below the threshold of perceptibility for the human eye (ΔE=3, in red) [23]. In detail, although the variations are slight, all the samples show negative values of ΔL* and positive values of Δb*, respectively suggesting a darkening and a yellowing of the surface. The most negative ΔL* values occur in Incralac® and Paraloid® B44, alone or with MPT, while blends containing MPT always have more positive Δb* values than blends with AEDTA (see Table 1S on Supplementary Material). According to Figure 1, blends with MPT show much less colour stability with respect to AEDTA; in general, higher concentration of inhibitor corresponds to somehow greater colour change, although MPT do not strictly follow this trend. Also, the influence of light stabilisers is not the same for the two tested inhibitors: Tinuvin® 5050 provides a slightly better colour stability for both AEDTA and MPT at all tested concentrations, while Tinuvin® 312 increases the colour change upon weathering for AEDTA blends and shows the opposite effect for the MPT blends. It is worth noting that Incralac® showed a ΔE higher than or equal to all the other tested coatings except Paraloid® B44 with 9% w/w of MPT, while the blends with AEDTA show a much better colour stability with respect to both Incralac® and Paraloid® B44 alone.

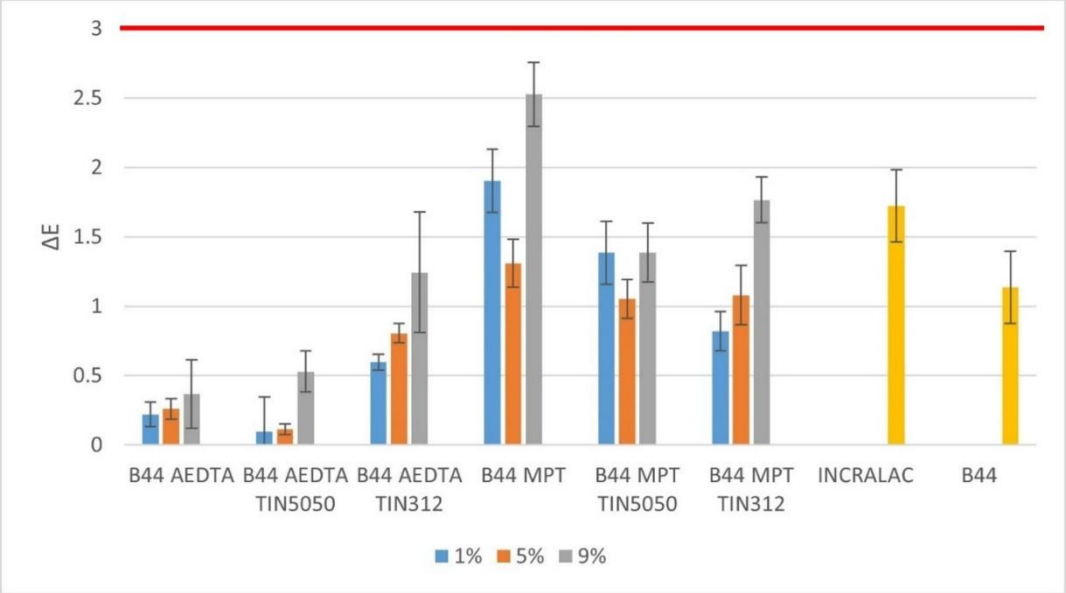

Figure 1. Colour change of the dry coatings after artificial ageing. The blue, orange and grey bars refer to the concentration of the corrosion inhibitors MPT and AEDTA at 1, 5 and 9% w/w, respectively. Error bars refer to standard deviation.

To evaluate the possible effect of the additives on the thermal and mechanical stability of the coatings, the glass transition temperature (Tg) of the differently formulated coatings were compared. Flexibility or stiffness, strength or brittleness depend on the glass transition temperature, which in turn affects both the adhesion to the surfaces and the integrity and continuity of the coatings. Specifically, an increase in Tg caused by radical cross-linking reactions of the polymer during photooxidative degradation [24, 25, 26] could result in a greater brittleness of the coating, with formation of cracks and loss of adhesion.

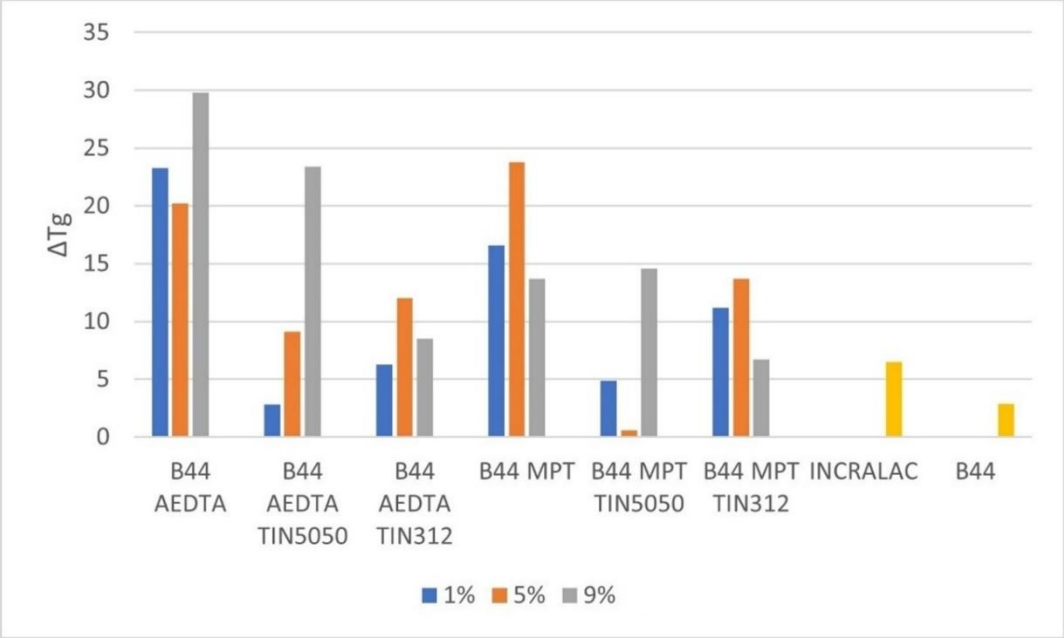

Figure 2. ΔTg values before and after ageing of the coatings. The blue, orange and grey bars refer to the concentration of the corrosion inhibitors MPT and AEDTA at 1, 5 and 9% w/w, respectively.

The increase in the Tg values of the coatings after ageing with respect to Tg of the as prepared samples are reported in Figure 2. Although well-defined trends are not always identified, it is nonetheless possible to make some general observations. As expected, the Tg of Paraloid® B44 has a limited increase during aging. Both MPT and AEDTA cause an increase in Tg and therefore a stiffening and embrittlement of the coatings during ageing. However, the addition of light stabilizers reduces the increase of the Tg and ensures greater stability of the thermal and mechanical properties. This stabilizing effect was observed for both types of Tinuvin®.

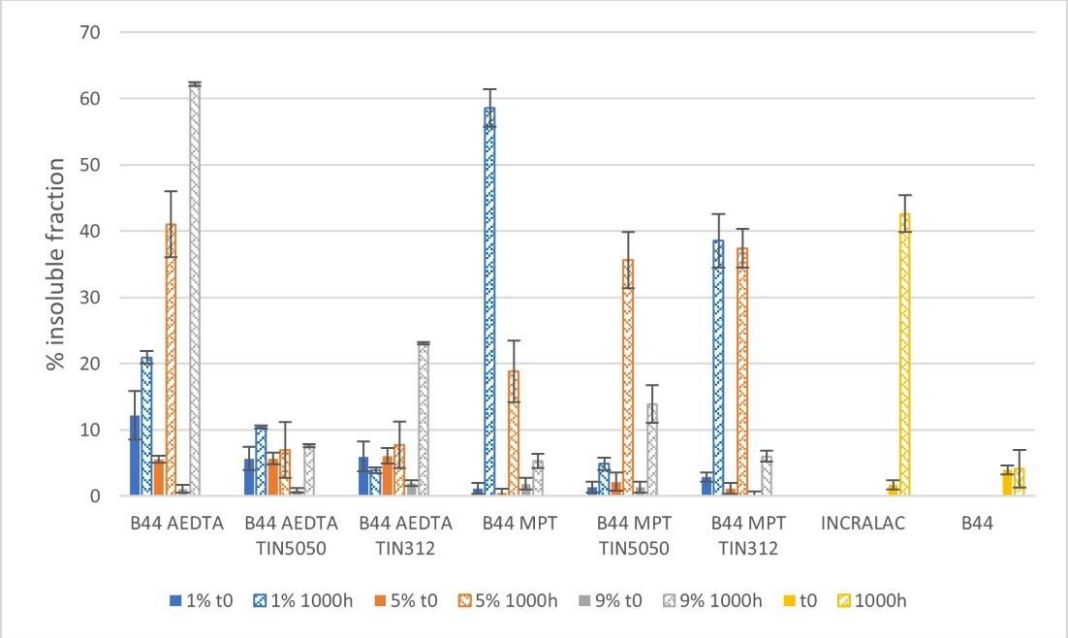

Figure 3. Insoluble fraction of Paraloid® B44 coatings modified with corrosion inhibitors AEDTA and MPT. The blue, orange and grey bars refer to the concentration of the corrosion inhibitors MPT and AEDTA at 1, 5 and 9% w/w, respectively. Plain bars indicate 0 hours of aging, while striped bars indicate 1000 hours of aging. Error bars refer to standard deviation.

Tg data are well correlated with the amount of insoluble cross-linked fraction present in the aged coatings (Figure 3). Both MPT and AEDTA cause an increase in the insoluble fraction, which makes the removability of the coatings more problematic in case it becomes necessary. However, the trend in the formation of insoluble fraction as a function of the concentration of inhibitor is opposite: the amount of insoluble fraction of MPT-coatings increases inversely proportional to the concentration of the inhibitor, becoming particularly relevant at minimum concentration of MPT, whereas AEDTA increases the amount of insoluble fraction proportionally to its concentration. Moreover, regardless of the type of inhibitor, light stabilizers inhibit the degradation reactions that cause the formation of cross-linked and insoluble acrylic fractions, confirming the effect already demonstrated by the study of the glass transition temperature of the coatings. From this point of view, the coatings containing AEDTA and a light stabilizer are the ones with the best performances, since their solubility and removability remain unchanged.

To chemically characterize the coatings, ATR-FTIR analyses of the coatings and of their single components were carried out. All the assignments were done referring to literature data. Paraloid® B44 absorptions are the main peaks in all spectra: the CH_3 asymmetric stretching at about 2988 cm^{-1}, the CH_2 asymmetric stretching at 2952 cm^{1}, the C=O stretching at about 1732 cm^{-1}, the CH_3 and CH_2 asymmetric bending at 1478 and 1449 cm^{-1} respectively, the CH_3 symmetric bending and CH_2 wagging at 1386 cm^{-1} and the C-O-C stretching vibrations in the range between 1300 and 1100 cm^{-1} [22,23,24](Figure 4, red curve).

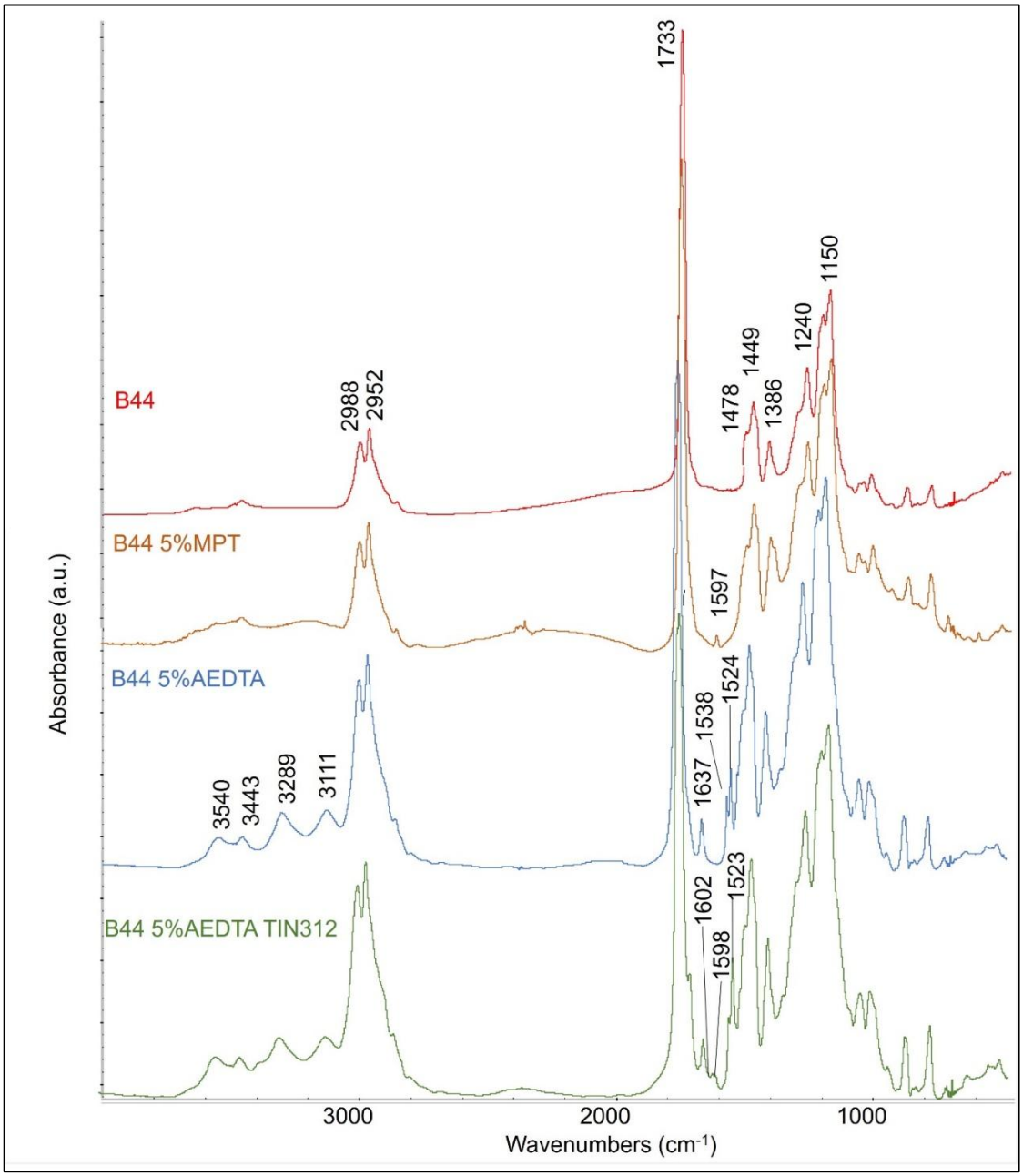

Figure 4. FTIR spectra of coatings made of Paraloid® B44, Paraloid B44 and 5% w/w MPT, Paraloid® B44 and 5% w/w AEDTA, Paraloid® B44 added with 5% w/w AEDTA and Tinuvin® 312 coatings.

FTIR peaks of the anticorrosive agent AEDTA are detected in the range from 3400 cm^{-1} to 3000 cm^{-1}, due to NH stretching, at 1637 cm^{-1}, due to N-H deformation

vibration of the primary amine, at 1538 and 1524 cm^{-1}, due to characteristic vibrations of the thiazole ring (Figure 4, blue curve).

The characteristic peaks of Tinuvin® 312 are visible at 1602, 1591 and 1523 cm^{-1} (Figure 4, green curve), while no specific signals of Tinuvin® 5050 can be identified in the FTIR spectra of the coatings (Figure 1A-addendum). The only visible signal of the anticorrosive agent MPT is the peak at 1597 cm^{-1}, assigned to the C=C stretching (Figure 4, yellow curve).

Thus, specific peaks of Paraloid® B44 and the corrosion inhibitors were identified, allowing for the monitoring of structural changes and persistence of the additives during the accelerated light aging of the coatings. This was undertaken by studying the spectral variations over the entire spectral range after normalization of the spectra, assuming that the absorption of the CH_3 bending vibration at 1385 cm^{-1} remained constant over time [30]. Following this procedure, no significant variations in the absorptions of the acrylic component of the coatings were observed, which indicates a good photo-oxidative stability of Paraloid® B44, as such and with additives. (Figure 2A 3A-addendum)

To shed a light on the fate of corrosion inhibitors over time, the change in intensity of their characteristic peaks in FTIR spectra were monitored. Figure 5 shows a detail of the spectra of the coatings with 5% w/w of corrosion inhibitors AEDTA and MPT. The red boxes in the figure highlight the range of wavenumbers in which the corrosion inhibitors absorb.

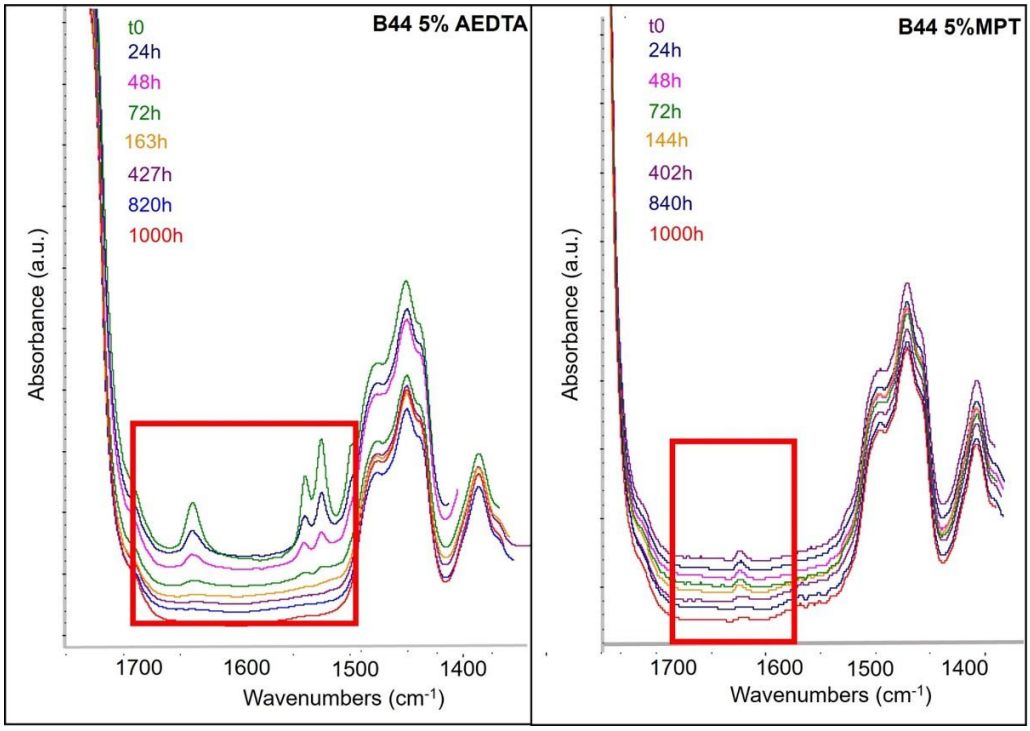

Figure 5. Detail of Paraloid® B44 coatings with 5% w/w AEDTA (left) and 5% w/w MPT (right). Red boxes highlight corrosion inhibitors absorption peaks.

Both characteristic peaks of AEDTA in the spectral range 3100-3600 cm^{-1} and the peaks at 1638, 1538 and 1524 cm^{-1} disappear over time (Figure 5, left) indicating a decrease of the corrosion inhibitor likely due to its degradation or migration to the coating surface and volatilization. The same also happens in coatings containing MPT whose characteristic peak at 1597 cm^{-1} also decreases during aging (Figure 5, right).

The possible effect of light stabilizers on the persistence of corrosion inhibitors was also investigated. The persistence of AEDTA was found to be increased in coatings containing the UV absorber Tinuvin® 312. As a matter of fact, AEDTA characteristic peak at 1632 cm^{-1} is observed also at 1000 hours of ageing (Figure 1S, Supplementary Material). On the contrary, Tinuvin® 5050 seems to have no effect on the persistence of AEDTA which after a while disappears from the coating or at least is no longer detectable by FTIR. Similarly, Tinuvin® 5050 did not provide any improvement to the persistence of MPT in the acrylic coatings (Figure 4A and 5A-addendum).

On the other hand, FTIR spectra could not clarify if Tinuvin® 312 is able to increase the stability of MPT because the characteristic FTIR peaks of MPT and Tinuvin® 312 absorb exactly in the same range of wavenumbers preventing any conclusion on possible effects of the UV absorber on the amount of corrosion inhibitor retained in the coating. So, according to FTIR analyses, Paraloid® B44 is stable to light ageing, whereas the corrosion inhibitors tend to leave the coating over time. In addition, Tinuvin® 5050 is not able to extend the permanence of the inhibitors in the coatings.

To further investigate the stability of corrosion inhibitors, double-shot Py-GC/MS analyses were performed on unaged and aged coatings. The double shot approach allowed a clearer distinction and identification of additives from the acrylic component: according to this method, the first shot consists in the thermal desorption and detection of the volatile fraction of the sample, while, during the second shot at higher temperature, the polymeric component is pyrolyzed and analysed. This helped in a better understanding of the stability and persistence of the additives in the coatings. Both coatings containing only corrosion inhibitors and those including corrosion inhibitors and light stabilisers were investigated and compared to Incralac®.

Table 5 reports the assignments of the main chromatographic peaks eluted after thermal desorption and Table 6 resumes the main peaks identified during the pyrolysis step of double-shot Py-GC/MS analyses of Paraloid® B44 coatings modified with AEDTA, MPT and light stabilisers.

Table 5: Assignment of the chromatographic peaks detected in the thermal desorption step of the double-shot Py-GC/MS analyses. (See Table 4 for coating labels)

		DESORPTION STEP																			
			t0										1000h								
Peak nr	**Tr (min)**	**Assignment**	**B A9 T3**	**B A5 T3**	**B A9 T5**	**B A5 T5**	**B A5**	**B M9 T3**	**B M5 T3**	**B M9 T5**	**B M5 T5**	**B M5**	**B A9 T3**	**B A5 T3**	**B A9 T5**	**B A5 T5**	**B A5**	**B M9 T3**	**B M5 T3**	**B M9 T5**	**B M5 T5**	**B M5**
1	1.28	1-methoxypropan-2-ol	X	X	X	X	X	X	X	X	X	X	X	X	X	X	X	X	X	X	X	X
7	6.47	Isocyanatobenzene						X	X	X	X	X						X	X	X	X	X
8	6.85	Aniline						X	X	X	X	X						X	X	X	X	X
9	9.80	1-ethyl-2-isocyanatobenzene						X										X	X			
10	9.98	2-ethylaniline	X	X									X	X								
11	10.70	Isothiocyanatobenzene						X	X	X	X	X						X	X	X	X	X
12	10.98	(methyltrisulfanyl)methane						X	X	X									X			
13	11.23	2-ethoxyaniline	X	X				X	X				X	X					X			
14	11.78	Sesquimer EA/MMA	X		X	X	X	X	X	X	X	X			X	X						
16	12.38	Methyl(phenyl)cyanamide						X	X	X	X	X								X		X
18	12.52	Dimer EA	X	X	X	X	X	X	X	X	X	X	X	X	X	X						
19	12.98	3-methylquinoline																X			X	
20	13.73	Phenylcyanamide						X	X	X	X							X	X	X	X	

21	13.96	2-amino-5-ethyl-1,3,4-thiadiazol-	X	X	X	X	X						X	X	X	X	X					
22	14.96	2,6-di*tert*-butyl-4-methylphenol	X	X	X	X	X															
24	15.44	1-phenyltetrazole								X								X		X	X	
25	15.50	m/z 57,70, 74, 129, 156, 157, 185													X							
26	16.1	1,3-benzothiazol-2-amine						X	X	X								X	X	X		
27	16.46	Dimethyl decandioate			X	X					X				X	X				X		
28	17.23	1-methyl-4-phenyltetrazole -5-thione						X	X	X	X	X										
29	17.83	Trimer EA MMA MMA	X	X	X	X	X	X	X	X	X	X		X	X	X					X	
30	18.01	Trimer EA MMA MMA	X	X	X	X	X	X	X	X	X	X			X	X						
32	18.60	Trimer EA	X	X	X	X	X	X	X	X	X	X			X	X						
33	18.81	m/z 57, 70, 74, 129, 156, 157, 185											X	X	X	X						
35	20.96	Octathiocane						X	X	X	X	X										
36	23.50	bis(2,2,6,6-tetramethylpiperidin-4-yl) decanedioate			X	X				X	X				X	X						
37	24.70	N,N'-bis(2-phenylethyl)oxamide	X	X				X	X				X	X				X	X			

38	24.78	Bis(1,2,2,6,6-pentamethylpiperidin-4-yl) decanedioate			X	X				X	X											
39	25.7	N'-(2-ethoxyphenyl)-N-(2-ethylphenyl)oxamide	X	X				X	X				X	X				X	X			
40	26.64	N,N’-bis(2-ethoxyphenyl)oxamide	X	X				X	X				X	X				X	X			
41	29.35	Marker of Tinuvin® 5050			X	X				X	X				X	X						
42	31.31	Marker of Tinuvin® 5050			X	X				X	X											
43	32.72	Marker of Tinuvin® 5050			X	X				X	X				X	X				X	X	
44	33.35	Marker of Tinuvin® 5050			X	X				X	X				X	X				X	X	
45	33.70	Marker of Tinuvin® 5050			X	X				X	X				X	X				X	X	
46	34.00	Marker of Tinuvin® 5050			X	X				X	X				X	X				X	X	

Table 6: Assignment of the chromatographic peaks detected in the pyrolysis step of the double-shot Py-GC/MS analyses. (See Table 4 for coating labels)

		PYROLYSIS STEP																			
			t0										1000h								
Peak nr	**tr (min)**	**Assignment**	**B A9 T3**	**B A5 T3**	**B A9 T5**	**B A5 T5**	**B A5**	**B M9 T3**	**B M5 T3**	**B M9 T5**	**B M5 T5**	**B M5**	**B A9 T3**	**B A5 T3**	**B A9 T5**	**B A5 T5**	**B A5**	**B M9 T3**	**B M5 T3**	**B M9 T5**	**B M5 T5**	**B M5**
2	2.10	Methyl prop-2-enoate (MA)	X	X	X	X	X	X	X	X	X	X	X	X	X	X	X	X	X	X	X	X
3	2.71	Ethyl prop-2-enoate (EA)	X	X	X	X	X	X	X	X	X	X	X	X	X	X	X	X	X	X	X	X
4	2.88	Methyl 2-methylprop-2-enoate (MMA)	X	X	X	X	X	X	X	X	X	X	X	X	X	X	X	X	X	X	X	X
5	3.83	Ethyl 2-methylprop-2-enoate (EMA)	X	X	X	X	X	X	X	X	X	X	X	X	X	X	X	X	X	X	X	X
6	9.04	Dimethyl 2-methylidenebutanedioate	X	X	X	X	X	X	X	X	X	X	X	X	X	X	X	X	X	X	X	X
9	9.80	1-ethyl-2-isocyanatobenzene	X	X				X	X				X	X				X	X			
14	11.78	Sesquimer EA-MMA	X	X	X	X	X	X	X	X	X	X	X	X	X	X	X	X	X	X	X	X
17	12.40	m/z 169, 154, 141, 125, 109, 81, 73	X	X	X	X	X	X	X	X	X		X	X	X	X	X	X	X	X	X	X
18	12.52	EA dimer	X	X	X	X	X	X	X	X	X	X	X	X	X	X	X	X	X	X	X	X
23	14.95	2,6-di*tert*-butyl-4-methylphenol	X	X									X									

29	17.83	Trimer EA-EA-MMA	X	X	X	X	X	X	X	X	X	X	X	X	X	X	X	X	X	X	X	X
30	18.01	Trimer EA-EA-MMA	X	X	X	X	X	X	X	X	X	X	X	X	X	X	X	X	X	X	X	X
31	18.20	m/z 200, 167, 153, 135, 127, 107, 95	X	X	X	X	X	X	X	X	X	X	X	X	X	X	X	X	X	X	X	X
32	18.60	Trimer EA	X	X	X	X	X	X	X	X	X	X	X	X	X	X	X	X	X	X	X	X
34	18.82	m/z 268, 255, 200, 149, 121, 93	X	X	X	X	X	X	X	X	X	X	X	X	X	X	X	X	X	X	X	X
37	24.70	N,N'-bis(2-phenylethyl)oxamide	X	X				X	X				X	X				X	X			
39	25.7	N'-(2-ethoxyphenyl)-N-(2-ethylphenyl)oxamide	X	X				X	X				X	X				X	X			
40	26.64	N,N’-bis(2-ethoxyphenyl)oxamide	X	X				X	X				X	X				X	X			

In Figure 6 the chromatograms of the thermal desorption step of the coating containing Paraloid® B44, 5% w/w AEDTA and 3% w/w Tinuvin ® 312 (BA5T3 in Table 4) before (a) and after 1000 hours of light aging (b) are compared. In both chromatograms AEDTA is detected in its molecular unaltered form at elution time of about 13.96 min (peak 21); neither degradation products nor pyrolytic fragments are observed. This highlights AEDTA stability under thermal and UV stress. Tinuvin® 312, namely N'-(2-ethoxyphenyl)-N-(2-ethylphenyl)oxamide, is eluted at 25.70 min (peak 39), and other marker peaks, all by-products due Tinuvin® 312 fragmentation in the desorption step, are detected at 11.25 min (i.e 2-ethoxyaniline, peak 13), at 24.70 min (i.e. N,N'-bis(2-phenylethyl)oxamide, peak 37) and at 26.63 min (i.e. N,N'-bis(2-ethoxyphenyl)oxamide, peak 40). These markers are detected both at time zero and after 1000 hours of ageing, confirming the light stability of Tinuvin® 312.

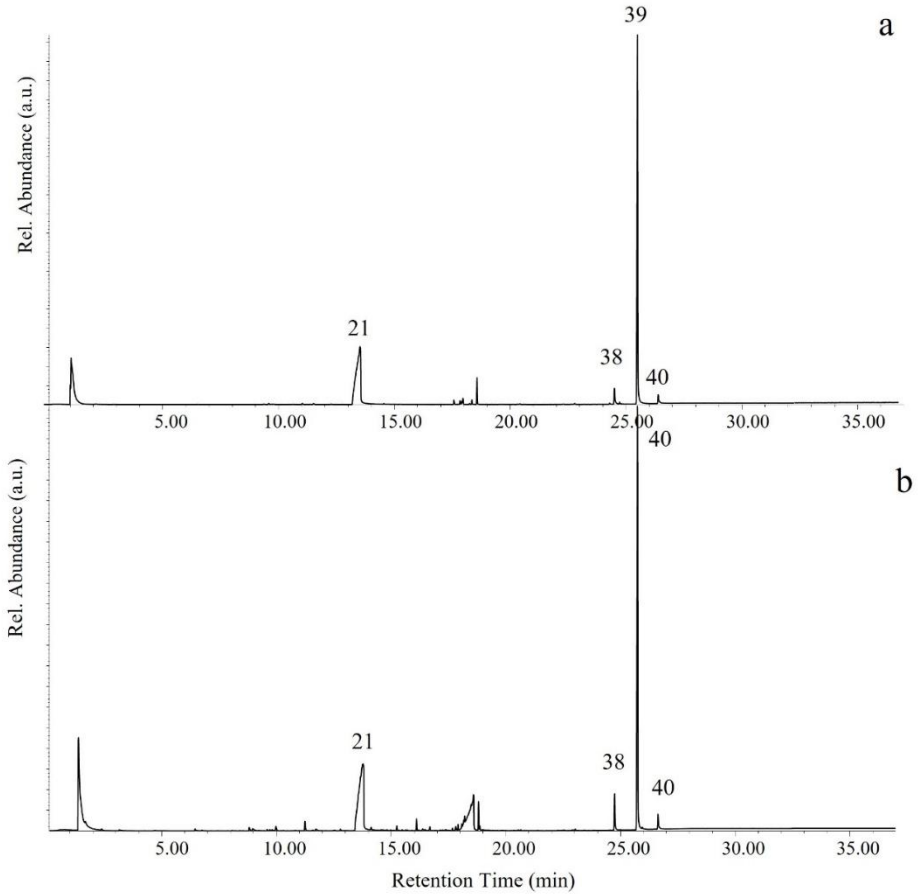

Figure 6. Desorption step of double-shot Py-GC/MS of Paraloid® B44 coatings with 5% w/w AEDTA and Tinuvin® 312, unaged (a) and after 1000h of ageing (b).

In Figure 7 the chromatograms obtained in the desorption step of unaged and aged Paraloid® B44 coatings with 5% w/w AEDTA and 3% w/w Tinuvin® 5050 (BA5T5 in Table 4) are shown. Again, AEDTA is detected at 13.96 min (peak 21) in both chromatograms, while the main marker peaks of Tinuvin® 5050, that are bis(2,2,6,6-tetramethylpiperidin-4-yl) decanedioate (peak 36), bis(1,2,2,6,6-pentamethylpiperidin-4-yl) decanedioate (peak 38) and peaks 41 and 42, are not detected or have very different intensity in the aged coatings, indicating a poor stability of Tinuvin ® 5050 under UV stress.

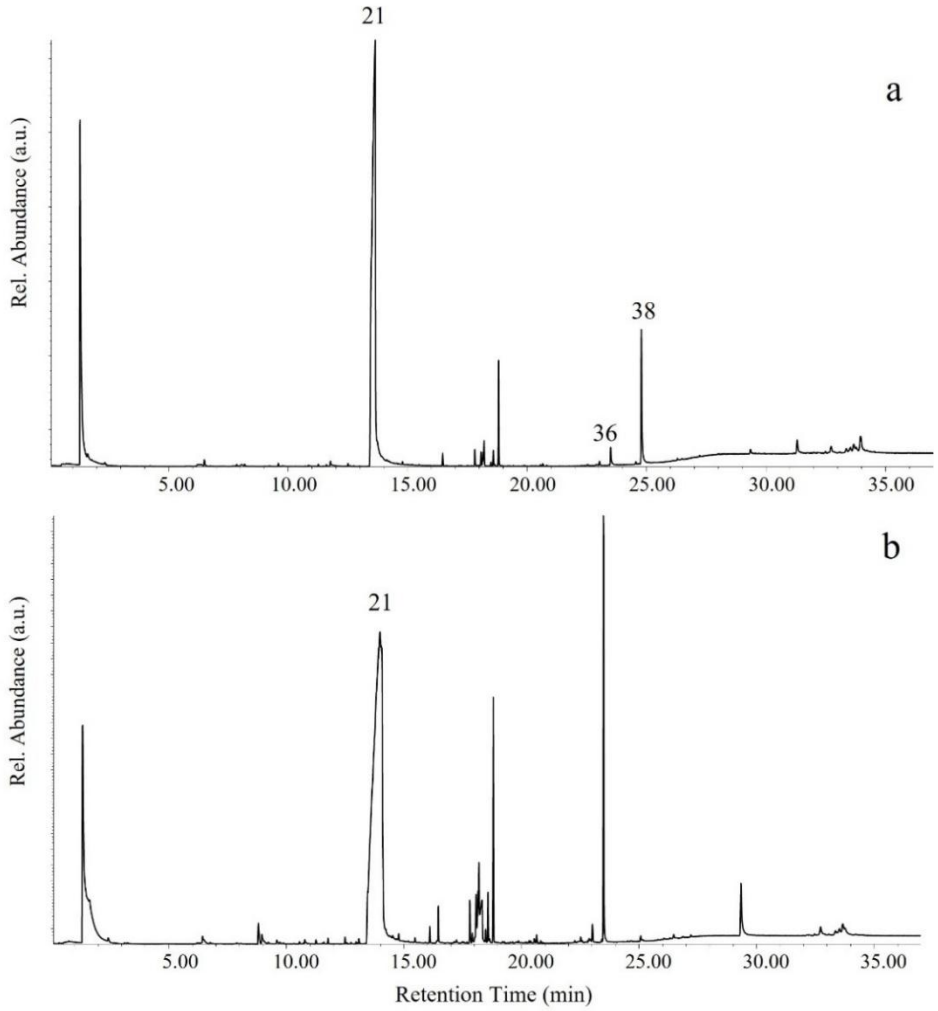

Figure 7. Desorption step of double-shot Py-GC/MS of Paraloid® B44 coatings with 5% w/w AEDTA and Tinuvin® 5050 coatings, unaged (a) and after 1000h of ageing (b).

Differently from AEDTA, MPT is affected by a consistent fragmentation during the desorption step (Figure 8). In fact, even in the unaged sample, MPT is not detected as such, but in the form of fragments and molecular adduct: isocyanatobenzene (peak 7) at 6.47 min, aniline (peak 8) at 6.85 min, isothiocyanatobenzene (peak 11) at 10.70 min, methyl(phenyl)cyanamide at 12.38 (peak 16), phenylcyanamide at 13.73 (peak 20) and methylated MPT at 17.23 min (peak 28). Fragments 7, 8, 11, 16 and 20 can be also found in the aged samples but relatively less abundant in comparison to the other components. Conversely methylated MPT disappears during aging and is replaced by 1-phenyltetrazole at about 15.44 min (peak 25). Overall, the changes observed in the MPT marker peaks following exposure to artificial sunlight indicate that this inhibitor is not stable to photooxidative aging. The behaviour of the two light stabilizers in the presence of MPT is confirmed, i.e. Tinuvin® 312 is stable under the artificial aging conditions adopted, while Tinuvin® 5050 is no longer found in aged coatings.

Similarly, the analyses carried out on Incralac® also highlighted the almost complete disappearance of BTA in the aged coatings (Table 2S and Figure 2S, Supplementary Material), confirming what is known about the poor persistence of benzotriazole in Incralac® [31].

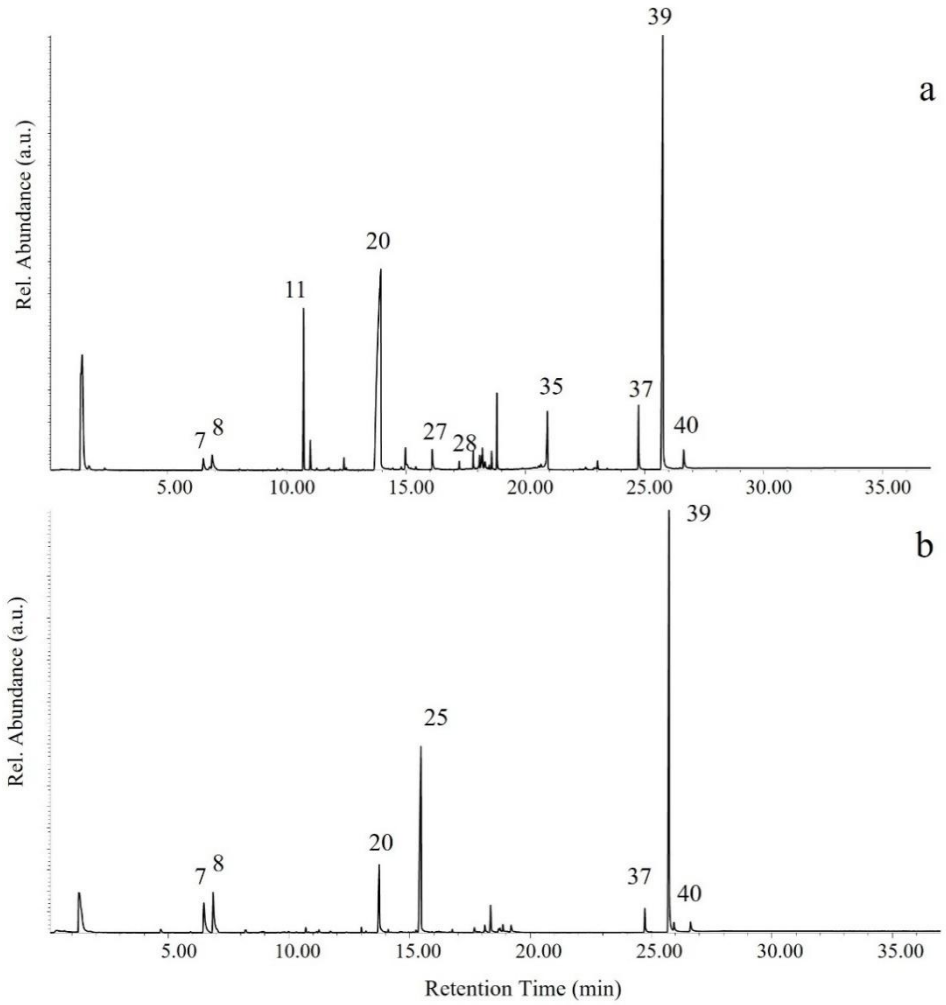

Figure 8. Desorption step of double-shot Py-GC/MS of Paraloid® B44 coatings with 5% w/w MPT and Tinuvin® 312 coatings, unaged (a) and after 1000h of ageing (b).

As for the pyrolysis step at 500 °C (Table 6), it caused the expected fragmentation of the acrylic resin. At lower retention times the two most intense peaks are referable to the two structural units of Paraloid® B44, i.e EA (ethyl acrylate) at 2.23 min and MMA (methyl methacrylate) at 2.52 min. Added to these, there are two pyrolysis by-products, MA (methyl acrylate) and EMA (ethyl methacrylate). At higher retention times, the main peaks are assigned to sesquimers, dimers and trimers of acrylic and methacrylic units. The chromatograms of the second shot of the Py-GC/MS analyses

do not show significant differences between the various types of coatings, nor between aged and unaged coatings. (Figure 6A-addendum)

To further study the permanence of corrosion inhibitors in the coating and to investigate a possible effect of the support, mock ups were prepared by applying coatings containing 5% w/w corrosion inhibitors and 3% w/w Tinuvin® 312 on the surface of polished bronze discs (Cu-Sn-Pb-Zn) (i.e bronze covered with the thin native oxide formed immediately after exposing the reduced metal to air). Micro-FTIR analyses highlighted that in coatings with MPT the corrosion inhibitor was still present and clearly detected even after 1000 hours of artificial ageing (Figure 3S, Supplementary Material), suggesting a higher affinity for the bronze surface rather than for glass. This confirms the preferential interaction of the corrosion inhibitor with bronze and suggests that adsorption of MPT on the metal surface can occur not only when the inhibitor is applied alone [32], but also when it is applied as an additive to an acrylic coating. The preferential interaction of MPT with the bronze surface slows the loss of inhibitor from the coating over time, compared to inert surfaces such as glass.

As regards the coatings containing AEDTA, surprisingly, the micro-FTIR spectra did not show, even in the unaged coating, the characteristic absorption peak of AEDTA at 1637 cm^{-1}. This is in contrast to what was observed in coatings applied on glass slides. The same, albeit with a different inhibitor, had already been observed by Giuliani *et al.* [33] who also demonstrated the formation of a layer of inhibitor concentrated at the bronze-coating interface. Accordingly, the coating was peeled off the bronze disc and spectra were collected all over the exposed surface of the bronze. The spectra thus obtained were characterized by all the significant peaks of AEDTA (Figure 9). This result indicates that most of AEDTA is located on the surface of the coating in contact with bronze, which makes it difficult to detect the inhibitor directly through FTIR reflection analyses. At the same time, the formation of an AEDTA layer at the coating-bronze interface is something positive as it ensures the presence of the anticorrosion additive right on the surface on which it is expected to act.

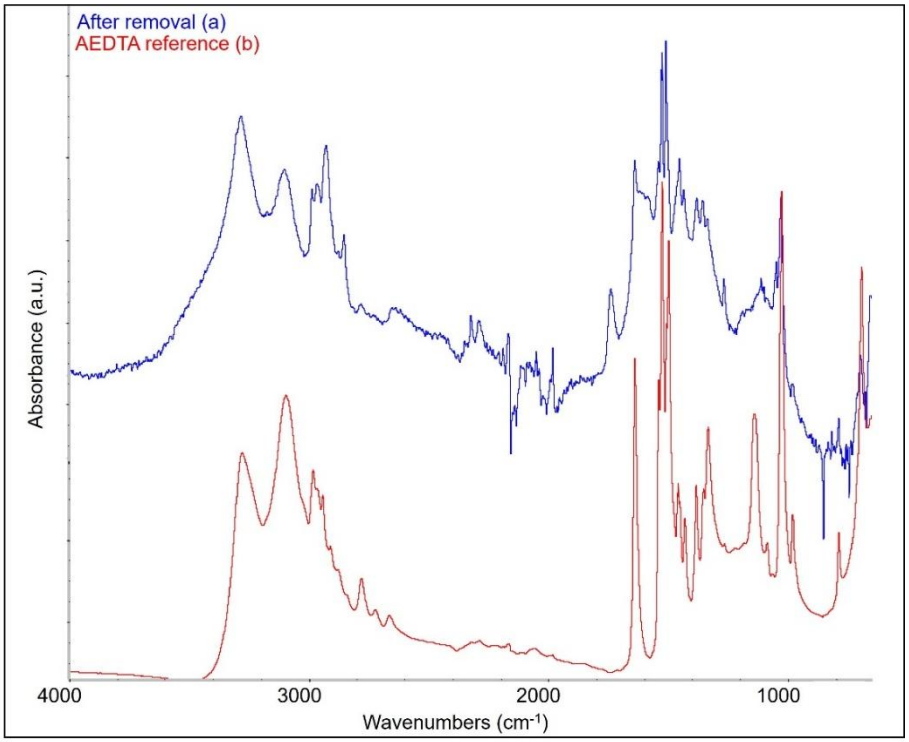

Figure 9. FTIR spectrum of the bronze mock up after peeling off the coating (a) and AEDTA reference spectrum (b).

5.5 Conclusions

The photo-oxidative stability of Paraloid® B44 coatings containing sustainable corrosion inhibitors and light stabilizers, as well as their ability to retain the inhibitors in the film longer than currently commercial products, were investigated. All the coatings modified with AEDTA showed negligible colour changes over time, a highly desirable feature as protective coatings for cultural heritage must not alter the visual aspect of the artwork. On the other hand, coatings containing MPT were homogeneous and transparent but with a clear tendency to turn yellow over time.

Both inhibitors make Paraloid more brittle and decrease its reversibility, however the presence of light stabilizers mitigates these problems by reducing both the glass transition temperature variation over time and the percentage of insoluble material. This is especially true for coatings with AEDTA and light stabilizers.

Overall, Paraloid® B44 is confirmed to be stable to aging as there is no evidence of oxidation in the FTIR analyses, however both inhibitors dispersed in it tend to leave the coating over time. Furthermore, MPT is not stable under solar light aging; in fact,

the Py-GC/MS marker peaks of this inhibitor after aging are not exactly the same as unaged samples or have very low intensities. The same can be said for BTA and Tinuvin® 5050 (Please refer to Supplementary Material). Conversely, AEDTA and Tinuvin® 312 are more stable over time.

Finally, the comparison between coatings applied on glass and on bronze demonstrates that inhibitors interact preferentially with bronze, probably through formation of Cu-inhibitor complexes, which attenuate the problem of the inhibitor release into the environment.

In particular, in the Paraloid coatings modified with AEDTA and applied on bronze discs, a layer of AEDTA adsorbed on the metal surface was detected at the bronze-coating interface, which appears to be an ideal stratigraphy to ensure effective anticorrosion activity to the acrylic coating.

In conclusion, Paraloid® B44 modified with AEDTA 5% w/w and Tinuvin® 312 is the coating with the best performance in terms of stability of chemical and physical properties. The study here reported shows that the corrosion inhibitor AEDTA is stable over time and, even when embedded in a polymer matrix, it tends to concentrate on the bronze surface and to remain in the coating longer than other inhibitors such as MPT and BTA. One of the aspects that deserves to be explored in the future is the influence of the application method since the protective performance of the coating can be influenced by the thickness, number of layers and drying time [34]. Further studies are now underway aimed at evaluating the effective applicability and anticorrosive efficacy of the coatings here described on patinated bronze surfaces such as those found in outdoor works of art.

Acknowledgments

This research contributed to setting up the coatings and analytical procedures for the PRIN 2022 Project InCARE - Innovative multi analytical Characterisation of the influence of pAtina-coating inteRaction on anti-corrosive propErties, funded by MUR. D. Scalarone and G. Pellis acknowledge support from the Project CH4.0 under the MUR program "Dipartimenti di Eccellenza 2023-2027" (CUP: D13C22003520001).

5.6 References

[1] Artesani A, Di Turo F, Zucchelli M, Traviglia A. Recent Advances in Protective Coatings for Cultural. Coatings 2010; 10 (217). doi:10.3390/coatings10030217

[2] Salvadori B, Cagnini A, Galeotti M, Porcinai S, Goidanich S, Vincenzo A, Celi C, Frediani P, Riosi L, Frediani M, Giuntoli G, Brambilla L, Beltrami R, Trassatti S. Traditional and innovative protective coatings for outdoor bronze: Application and performance comparison. J Appl Polym Sci. 2018; 135(12). doi: 10.1002/app.46011

[3] Baglioni M, Poggi G, Chelazzi D, Baglioni P. Advanced materials in cultural heritage conservation. Molecules 2021; 26 (13). doi: 10.3390/ molecules26133967

[4] Letardi P. Testing new coatings for outdoor bronze monuments: A methodological overview. Coatings 2021; 11 (2): 1–16. doi: 10.3390/coatings11020131

[5] Scott D A. Metallography and microstructure in ancient and historic metals. Marina del Rey, CA: Getty Conservation Institute in association with Archetype Books, 1991. http://hdl.handle.net/10020/gci_pubs/metallography_microstructure

[6] Strandberg H. Reactions of copper patina compounds - Influence of some air pollutants. Atmos Environ. 1998; 32 (20): 3511–3520.

[7] Giuntoli G, Rosi L, Frediani M, Sacchi B, Salvadori B, Porcinai S, Frediani P. Novel coatings from renewable resources for the protection of bronzes. Prog Org Coatings 2014; 77(4): 892–903. doi: 10.1016/j.porgcoat.2014.01.021

[8] Cano E, Lafuente D. 26 - Corrosion inhibitors for the preservation of metallic heritage artefacts, in: Dillmann P, Watkinson D, Angelini E, Adriaens A editors., vol 65: European Federation of Corrosion (EFC) Series. Eds. Woodhead Publishing in Materials, 2013. pp. 570–594. doi: 10.1533/9781782421573.5.570

[9] Fent K, Chew G, Li J, Gomez E. Benzotriazole UV-stabilizers and benzotriazole: Antiandrogenic activity in vitro and activation of aryl hydrocarbon receptor pathway

in zebrafish eleuthero-embryos. Sci Total Environ. 2014; 482–483 (1): 125–136. doi: 10.1016/j.scitotenv.2014.02.109

[10] Ellingson L A, Shedlosky T J, Bierwagen G P, de la Rie E R, Brostoff L B. The use of electrochemical impedance spectroscopy in the evaluation of coatings for outdoor bronze. Stud Conserv 2004; 49 (1): 53–62. doi: 10.1179/sic.2004.49.1.53

[11] Moffett D L, Wax Coatings on Ethnographic Metal Objects: Justifications for Allowing a Tradition to Wane. J Am Inst Conserv. 1996; 35(1): 1–7. doi: 10.1179/019713696806124557

[12] Kosec T, Novak Ž, Fabjan E Š, Škrlep L, Sever Škapin A, Ropret P. Corrosion protection of brown and green patinated bronze Prog Org Coatings 2021; 161. doi: 10.1016/j.porgcoat.2021.106510

[13] Kosec T, Škrlep L, Fabjan E Š, Sever Škapin A, Masi G, Bernardi E, Chiavari E, Josse C, Esvan J, Robbiola L. Development of multi-component fluoropolymer based coating on simulated outdoor patina on quaternary bronze. Prog Org Coatings 2019; 131: 27–35. doi: 10.1016/j.porgcoat.2019.01.040

[14] Mihelčič M, Slemenik Peršek L, Šest E, Jerman I, Giuliani C, Di Carlo G, Lavorga M, Surca A K. Development of solvent- and water-borne fluoropolymer protective coatings for patina-free bronze discs. Prog Org Coatings 2018; 125: 266–278. doi: 10.1016/j.porgcoat.2018.09.014

[15] Masi G, Josse C, Esvan J, Bernardi E, Martini C, Bignozzi M C, Skerlp L, Fabjan E S, Kosec T Aufray M, Robbiola L, Chiavari C. Micro-characterisation of innovative organic coatings applied for the protection of outdoor bronze monuments. EUROCORR 2017-The Annual Congress of the European Federation of Corrosion, 20th International Corrosion Congress and Process Safety Congress 2017.

[16] Monari G, Galeotti M, Matteini M, Salvadori B, Stifanese R, Traverso P, Vettori S, Letardi P. Protective treatments for copper alloy artworks: preliminary studies of sodium oxalate and limewater effectiveness against bronze disease. Environmental Science and Pollution Research 2023; 30: 27441–27457. doi: 10.1007/s11356-022-24107-0

[17] Molina M T, Cano E, Ramírez-Barat B. Protective coatings for metallic heritage conservation: A review. J Cult Herit. 2023; 62:99–113. doi: 10.1016/j.culher.2023.05.019

[18] Faraldi F, Angelini E, Riccucci C, Mezzi A, Caschera D, Grassini S. Innovative diamond-like carbon coatings for the conservation of bronzes. Surf Interface Anal. 2014; 46(10–11):764–770. doi: 10.1002/sia.5367

[19] Watkinson D, Preservation of Metallic Cultural Heritage. Elsevier: Oxford, 2010.

[20] De Luna M S, Buonocore G G, Giuliani C, Messina E, Di Carlo G, Lavorgna M, Ambroio L, Ingo G M. Long-Lasting Efficacy of Coatings for Bronze Artwork Conservation : The Key Role of Layered Double Hydroxide Nanocarriers in Protecting Corrosion Inhibitors from Photodegradation. Angew Chem Int Ed 2018; 7380–7384. doi: 10.1002/anie.201713234

[21] Pillard D A, Cornell J S, DuFresne D L, Hernandez M T. Toxicity of benzotriazole and benzotriazole derivatives to three aquatic species. Water Res. 2001; 35 (2):557–560. doi: 10.1016/s0043-1354(00)00268-2

[22] Wolfe J, Grayburn R, Khanjian H, Heginbotham A, Phenix A. Deconstructing Incralac: A formulation study of acrylic coatings for the protection of outdoor bronze sculpture. ICOM-CC 18th Triennial Conference Preprints, Copenhagen, 4–8 September 2017, ed. J. Bridgland, art. 0808. Paris: International Council of Museums.

[23] Witzel R F, Burnham R W, Onley J. W. Threshold and suprathreshold perceptual color differences. JOSA 1973; 63(5):615–625.

[24] Horie V. Materials for conservation: Organic consolidants, adhesives and coatings. Paperback edition of 2nd. London, New York: Routledge, 2011.

[25] Chiantore O, Lazzari M. Photo-oxidative stability of paraloid acrylic protective polymers. Polymer (Guildf) 2001; 42(1):17–27. doi: 10.1016/S0032-3861(00)00327-X

[26] Lazzari M, Scalarone D, Malucelli G, Chiantore O. Durability of acrylic films from commercial aqueous dispersion: Glass transition temperature and tensile behavior as indexes of photooxidative degradation. Prog. Org. Coatings

2011;70(2):116–121.
doi: 10.1016/j.porgcoat.2010.11.002

[27] Chiantore O, Lazzari M. Characterization of acrylic resins. Int. J. Polym. Anal. Charact.1996; 2(4):395–408.
doi: 10.1080/10236669608033358

[28] Chiantore O, Trossarelli L, Lazzari M. Photooxidative degradation of acrylic and methacrylic polymers. Polymer (Guildf) 2000; 41 (5):1657–1668.
doi: 10.1016/S0032-3861(99)00349-3

[29] Chiantore O, Scalarone D, Learner T. Characterization of artists' acrylic emulsion paints. Int. J. Polym. Anal. Charact. 2003; 8(1):67–82.
doi: 10.1080/10236660304884

[30] Scalarone D, Lazzari M, Chiantore O. Acrylic protective coatings modified with titanium dioxide nanoparticles: Comparative study of stability under irradiation. Polym Degrad Stab 2012; 97(11): 2136–2142.
doi: 10.1016/j.polymdegradstab.2012.08.014

[31] Monticelli C, Fantin G, Di Carmine G, Zanotto F, Balbo A. Inclusion of 5-mercapto-1-phenyl-tetrazole into β-cyclodextrin for entrapment in silane coatings: An improvement in bronze corrosion protection. Coatings 2019; 9 (8).
doi:10.3390/coatings9080508

[32] Mihit M, Salghi R, El Issami S, Bazzi L, Hammouti B, Ait Addi El, Kertit S. A study of tetrazoles derivatives as corrosion inhibitors of copper in nitric acid. Pigment Resin Technol. 2006; 35(3):151–157.
doi: 10.1108/03699420610665184

[33] Giuliani C, Pascucci M, Riccucci C, Messina E, Salzano de Luna M, Lavorgna M, Ingo G M, Di Carlo G. Chitosan-based coatings for corrosion protection of copper-based alloys: A promising more sustainable approach fo cultural heritage applications. Progress in Organic Coatings 2018; 122: 138-146.
doi: 10.1016/j.porgcoat.2018.05.002

[34] Molina M T, Cano E, Ramirez-Barat B. Testing protective coatings for metal conservation: the influence of the application method. Heritage Science. 2023; 11 (94).
doi: 10.1186/s40494-023-00937-0

[35] E.M. Sherif, S.M. Park, 2-Amino-5-ethyl-1,3,4-thiadiazole as a corrosion inhibitor for copper in 3.0% NaCl solutions, Corros Sci 48 (2006) 4065–4079. https://doi.org/10.1016/j.corsci.2006.03.011.

Supplementary material Article A

Table 1S. Average variation and standard deviation of the CIELab colour coordinates after 1000 hours under artificial solar light with respect to unaged coating (See Table 4 for coating labels).

Coating	ΔL*	Δa*	Δb*
BA9	-0.3 ± 0.3	-0.05 ± 0.05	0.2 ± 0.2
BA5	-0.2 ± 0.1	0.08 ± 0.02	0.08 ± 0.06
BA1	-0.2 ± 0.2	0.09 ± 0.02	0.07 ± 0.04
BA9T5	-0.2 ± 0.1	-0.09 ± 0.06	0.5 ± 0.2
BA5T5	-0.0 ± 0.1	0.03 ± 0.03	0.11 ± 0.05
BA1T5	0.09 ± 0.09	0.02 ± 0.02	0.02 ± 0.05
BA9T3	-0.4 ± 0.3	-0.17 ± 0.07	1.2 ± 0.5
BA5T3	0.1 ± 0.2	-0.10 ± 0.02	0.80 ± 0.06
BA1T3	-0.13 ± 0.09	-0.05 ± 0.03	0.58 ± 0.06

BM9	-2.4 ± 0.2	0.33 ± 0.04	0.9 ± 0.1
BM5	-1.1 ± 0.2	0.31 ± 0.04	0.57 ± 0.07
BM1	-1.7 ± 0.2	0.30 ± 0.03	0.5 ± 0.2
BM9T5	-0.9 ± 0.2	-0.02 ± 0.03	1.0 ± 0.2
BM5T5	-0.8 ± 0.2	0.04 ± 0.05	0.7 ± 0.1
BM1T5	-0.3 ± 0.3	0.06 ± 0.04	0.3 ± 0.2
BM9T3	-0.7 ± 0.2	-0.19 ± 0.03	1.6 ± 0.2
BM5T3	-0.6 ± 0.1	-0.07 ± 0.05	0.9 ± 0.2
BM1T3	-0.6 ± 0.1	-0.01 ± 0.05	0.6 ± 0.2
B	-1.0 ± 0.1	0.40 ± 0.05	0.2 ± 0.1
Incralac®	-1.3 ± 0.2	0.27 ± 0.02	0.71 ± 0.06

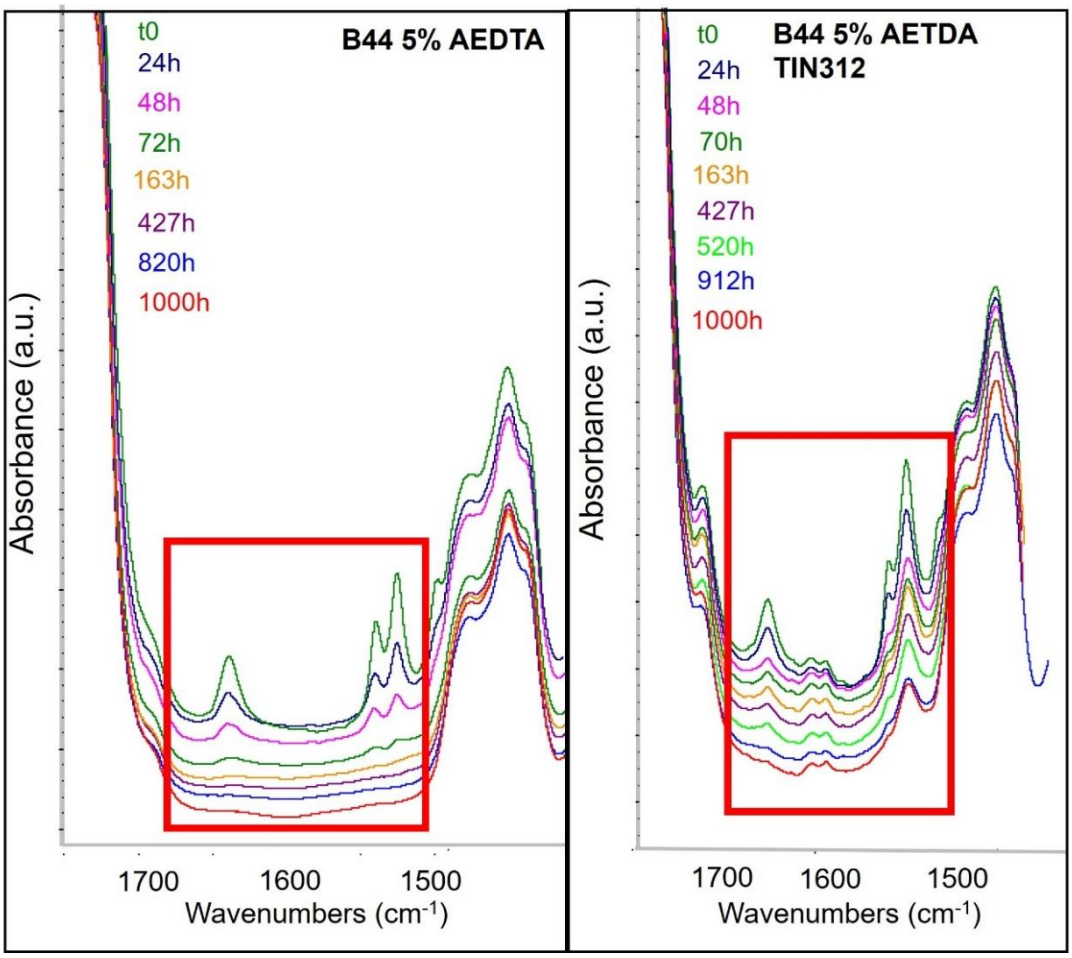

Figure 1S. Detail of the FTIR spectra of Paraloid® B44 coatings with 5% w/w AEDTA (left) and 5% w/w AEDTA and Tinuvin® 312 (right). In the left figure the characteristic peak of AEDTA at 1630 cm^{-1} disappears after 72 hours of aging. In the right figure, which refers to the coating containing AEDTA and Tinuvin® 312, the characteristic peak of AEDTA is still detectable after 1000 hours of artificial solar aging.

Table 2S. Assignment of the chromatographic peaks detected in the thermal desorption step of the double-shot Py-GC/MS analysis of Incralac ®, unaged and aged 1000 hours under artificial solar light.

DESORPTION STEP				
Peak number	**Rt (min)**	**Assignment**	**Unaged**	**Aged 1000h**
1	1.60	1-methoxypropan-2-ol	X	X
2	2.87	2-methylpropyl acetate	X	
3	3.1	ethyl prop-2-enoate (EA)		X
4	3.29	methyl 2-methylprop-2-enoate (MMA)		X
5	3.6	Butyl acetate	X	
6	4.21	ethyl 2-methylprop-2-enoate (EMA)		X
7	4.54	ethylbenzene	X	X
8	4.70	1,3-xylene	X	
9	5.12	1,2-xylene		X
10	5.22	1,4-xylene	X	X
11	5.49	ethyl (*E*)-2-methylbut-2-enoate		X
12	6.55	methyl 2,4-dimethylpent-4-enoate		X
13	6.85	(alpha-methylphenyl)methanol		X
14	6.98	2-methylbenzaldehyde		X
15	7.18	2-methylpropyl but-2-enoate		X
16	8.51	4-methylbenzaldehyde	X	
17	9.10	dimethyl 2-methylidenebutanedioate		X
18	10.56	2-methylbenzotriazole	X	X
19	10.26	dimethyl 2-methylpentanedioate		X
20	10.76	dimethyl 2,4-dimethylpentanedioate		X
21	11.28	sesquimer EA-MMA	X	X
22	11.78	m/z 168, 155, 140, 126,111, 95, 67		X
23	12.45	m/z 154, 141, 125, 109, 81		X
24	12.50	dimer EA	X	X
25	13.09	1-methylbenzotriazole	X	
26	14.38	benzotriazole (BTA)	X	X
27	17.82	trimer EA-MMA-MMA	X	X
28	18.07	m/z 269, 255, 222,194, 166, 148, 139, 120, 93	X	X
29	18.19	m/z 200, 167, 153, 135, 127, 107, 95	X	X
30	18.61	trimer EA	X	X
31	18.82	m/z 268, 255,200, 149, 121, 93	X	X

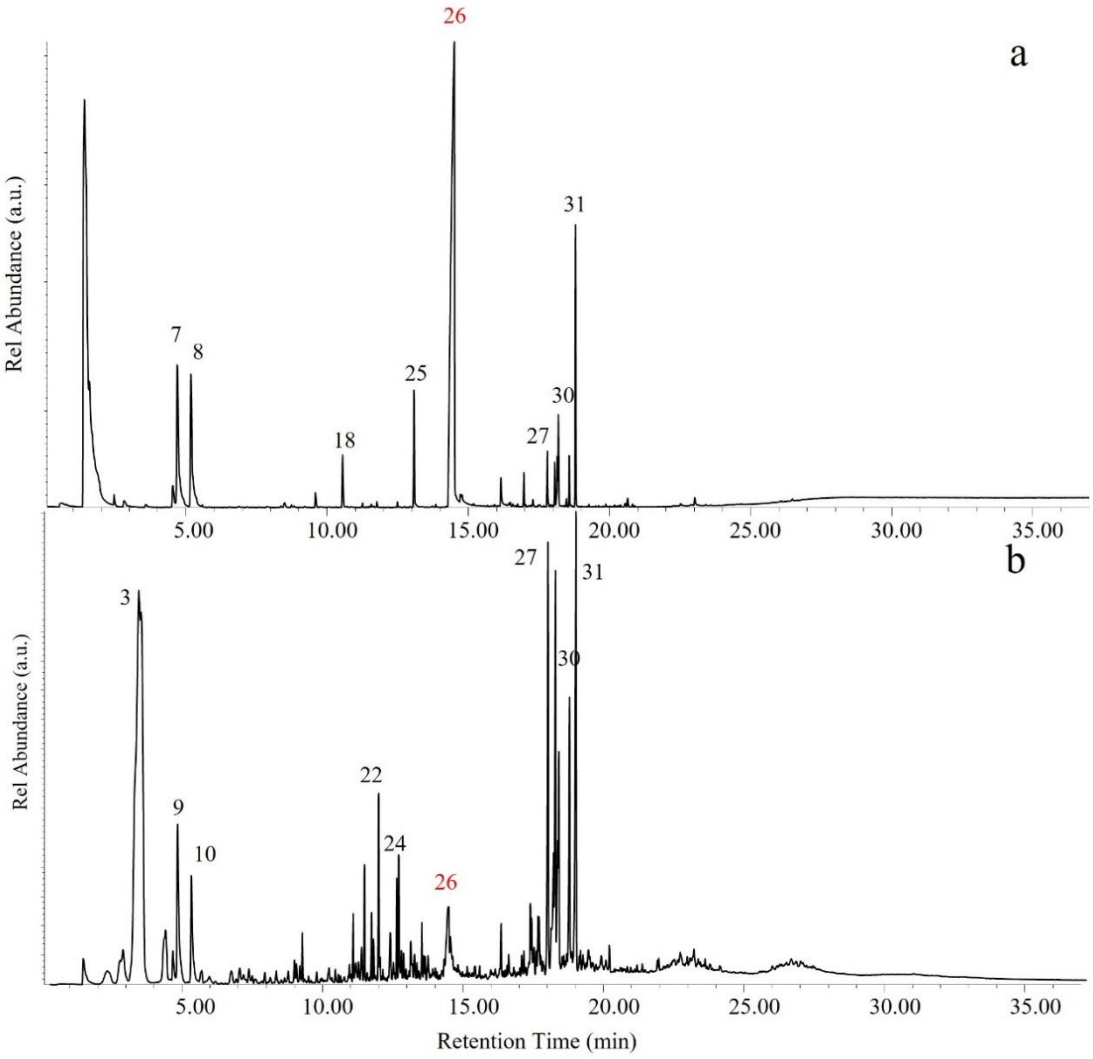

Figure 2S. Desorption step of double-shot Py-GC/MS of Incralac® coatings at time zero (a) and after 1000h of ageing (b). Benzotriazole (peak 26) is lost during ageing. In aged Incralac® the desorption of significant quantities of EA, MMA, dimers and trimers indicates that during accelerated photooxidative aging the coating undergoes polymer chain scission reactions with formation of such small volatile fragments.

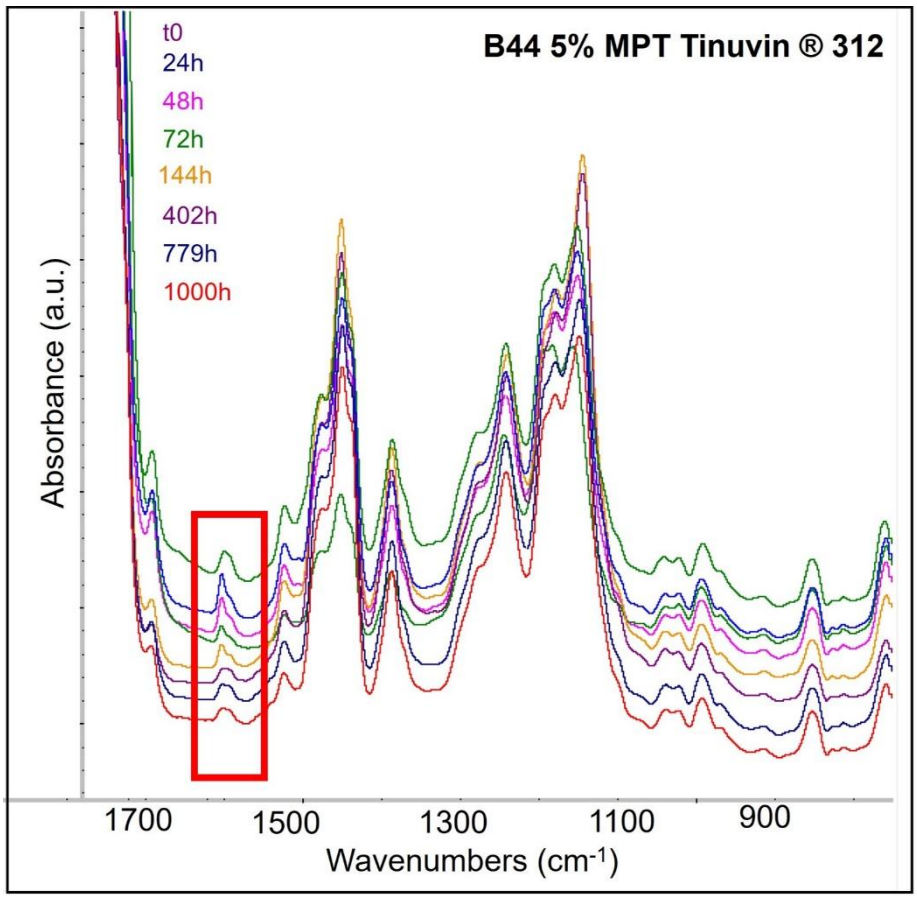

Figure 3S. Detail of the FTIR spectra of Paraloid® B44 coatings with 5% w/w MPT and Tinuvin® 312 applied on a bronze surface and aged up to 1000 hours of artificial solar light. The red box highlights MPT absorption peak.

Addendum

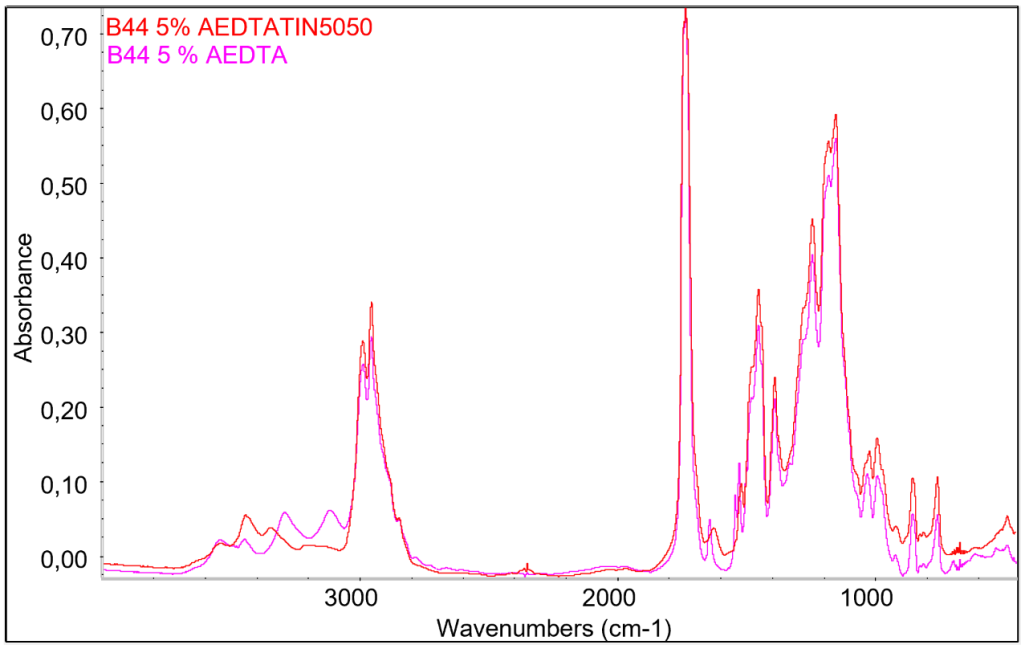

Figure 1A: Comparison of the FTIR spectra of coatings with only AEDTA (in pink) and with AEDTA and Tinuvin ® 5050 (in red)

No peaks belonging to Tinuvin® 5050 are seen.

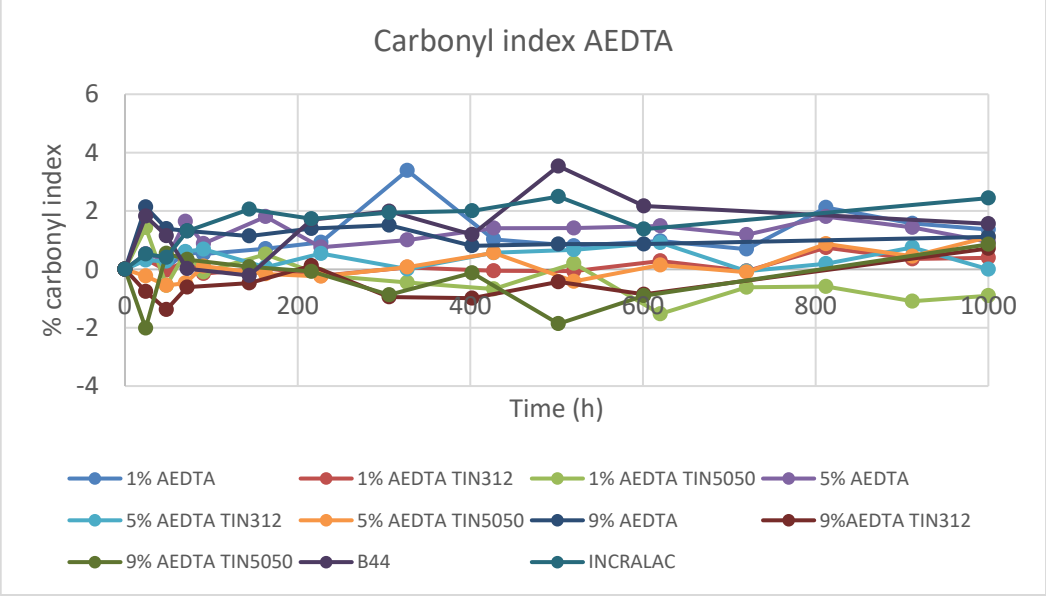

Figure 2A: Carbonyl index of AEDTA coatings and Incralac

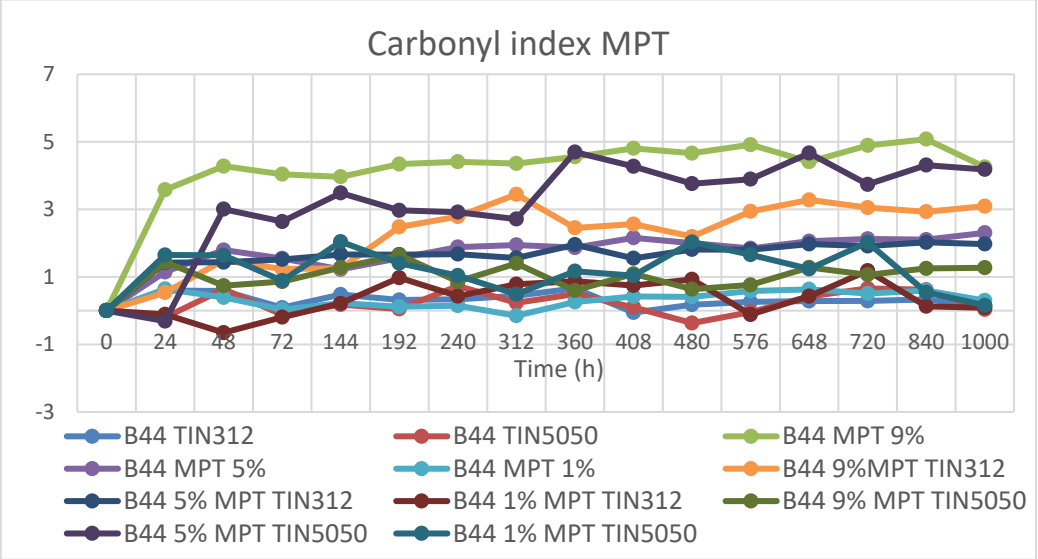

Figure 3A: Carbonyl index of MPT coatings

The Carbonyl Index (CI) helps to monitor the variation of the carbonyl groups through time. It is determined considering the ratio between the area of the C=O vibrational mode at 1735 cm^{-1} and the area of the CH_3 bending at 1385 cm^{-1}. All the ratios were normalized subtracting each value to the value of the unaged sample.

The graph shows the trend of the CI of the AEDTA and MPT coatings through time. All the samples have a low CI, meaning that it does not change through time, as seen before. The major changes are related to the samples without the UV stabilizers, meaning that probably the two types of Tinuvin are able to reduce the oxidation phenomena during time.

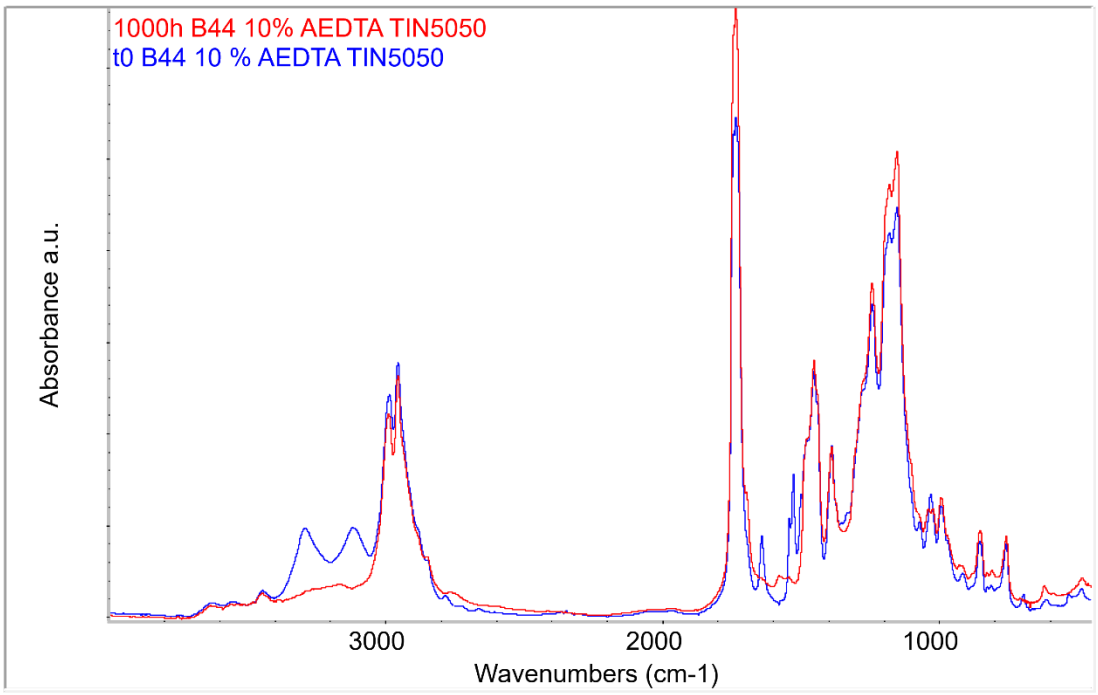

Figure 4A: Comparison of FTIR spectra of coatings with AEDTA 10% and Tinuvin ® 5050 at 1000 hours of ageing (in red) and time zero (in blue)

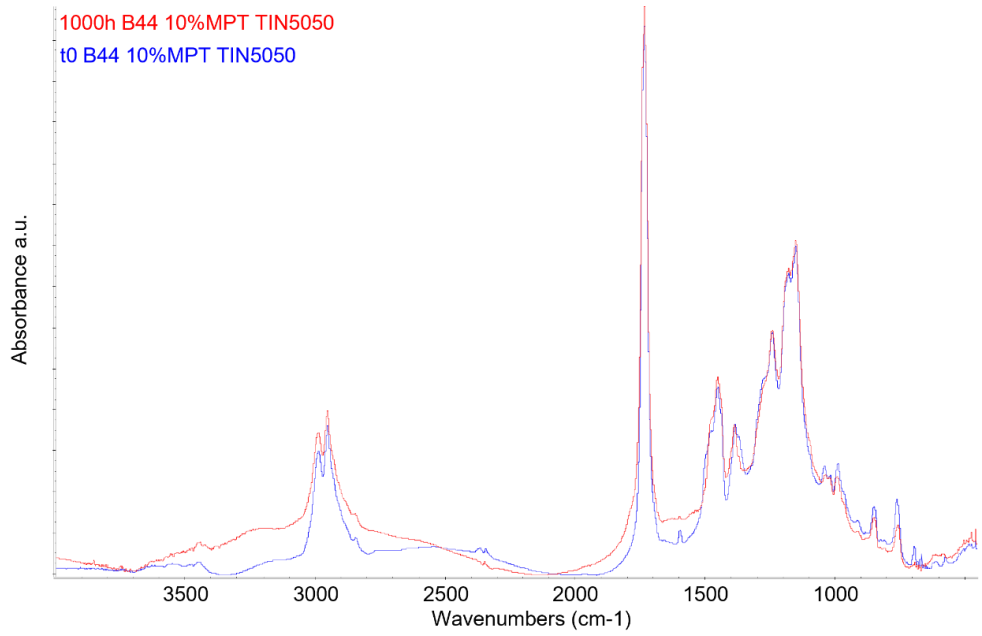

Figure 5A: Comparison of FTIR spectra of coatings with MPT 10% and Tinuvin ® 5050 at 1000 hours of ageing (in red) and time zero (in blue)

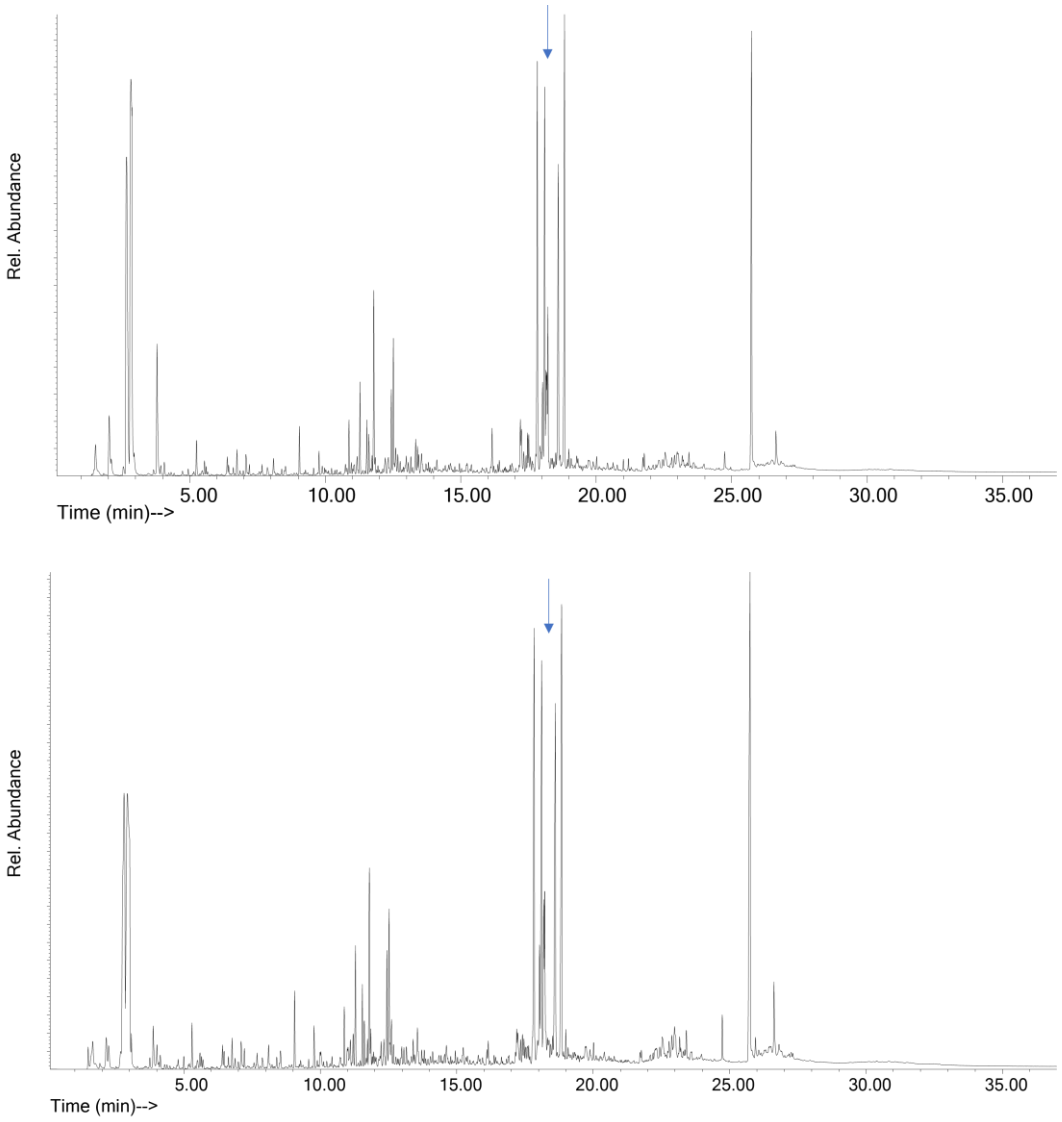

Figure 6A: Chromatograms of the pyrolysis step of 5% AEDTA and Tinuvin 312 coatings. In the upper part there is the chromatogram of the coating at time zero. In the lower part the chromatogram of 1000 hours of ageing. The arrows indicates the olygomers of the acrylic resin.

Figure 6A display a representative coating, all the pyrolysis steps are the same for all the samples. As can be seen from the arrow, the olygomers of the acrylic resin are the same. Please refer to Table 6 for the assignments.

Chapter 6

Advancing preservation: a chemometric approach for monitoring the degradation of protective coatings for bronze statues

Giulia Pellis[1], Maxim Tiburziano[2], Barbara Giussani[2*], Paola Letardi[3], Barbara Salvadori[4], Antonio Sansonetti[5] and Dominique Scalarone[1]

(1) Department of Chemistry, University of Torino, Via Pietro Giuria 7, Torino, Italy

(2) Science and High Technology Department, Università degli Studi dell'Insubria, Via Valleggio 9, Como, Italy

(3) Institute of Anthropic Impacts and Sustainability in the Marine Environment, CNR, Via De Marini 6, Genova, Italy

(4) Institute of Heritage Science, CNR, Via Madonna del Piano 10, Sesto Fiorentino, Italy

(5) Institute of Heritage Science, CNR, Via Roberto Cozzi 53, Milan, Italy

6.1 Abstract

Bronze outdoor statues are often covered by a corrosion patina that forms due to environmental exposure, providing both aesthetic value and, partly, a surface passivation. However, this patina does not prevent from decay by external factors such as pollution, UV radiation, and humidity. To mitigate these decay processes,

protective coatings are commonly used, but existing solutions often have drawbacks related to health, durability, and the need for frequent reapplication. The development of reliable, long-term conservation methods is essential. This work focuses on evaluating coatings formulated with Paraloid® B44, incorporating non-toxic corrosion inhibitors and light stabilizers. A total of twenty-one coatings were subjected to accelerated aging with artificial sunlight, and their decay was monitored using a multi-analytical approach involving Fourier Transform Infrared Spectroscopy (FT-IR) and UV-Vis spectroscopy, both with benchtop and portable spectrometers. The aim is to propose a method that combines spectroscopic data with chemometrics, specifically Principal Component Analysis (PCA), to objectively assess coating decay over time. The results demonstrate that PCA provides a simple yet powerful tool to distinguish between different formulations, track their aging, and rationalize decay processes. This approach not only facilitates the comparative analysis of coatings but also holds potential for field applications using portable instruments. By integrating spectroscopy with chemometrics, this method aligns with the principles of green analytical chemistry, offering a non-invasive, efficient means to monitor the effectiveness of protective coatings for cultural heritage preservation.

6.2 Introduction

Bronze outdoor statues are usually perceived as being covered by a corrosion patina resulting from their exposure to the environment. This patina plays an important aesthetic and passivation role on the surface; however, it does not hamper decay processes promoted by light, oxygen, pollution and humidity [1]. To slow down these disfiguring processes protective. coatings are applied. However, the most commonly used ones have several drawbacks related to health and durability and need to be replaced [2]. The development of safe and reliable long-term methods and strategies for the conservation of these artworks is nowadays a mandatory prerequisite [3,4].

A wide variety of materials have been developed so far, including organic coatings based on organosilanes [5–7], fluoropolymers [8,9], acrylic resins [10–12], cellulose nitrate [13], natural or synthetic waxes (with or without corrosion inhibitors)[14,15]. Moreover, different techniques and aging methods have been proposed in the literature, with many attempts to make a complex comparison between them. The typical approach involves aging the coatings either through accelerated or natural methods, and monitoring their decay using a multi-analytical approach [4]. This is necessary because treatments aimed at the preservation of

cultural heritage must meet specific requirements which make the simultaneous observation of various parameters necessary [16].

Many of these studies rely on discussions of spectroscopic data through visual and qualitative comparisons, leading to partial and scattered results without a systematic organisation [4]. The aim of this work is to propose a method that facilitates the study of ageing processes by leveraging chemometrics. Chemometrics serves as a valuable tool for highlighting differences in coatings over time and for discerning the individual contributions of the formulation components throughout the ageing process. It has demonstrated its effectiveness in various areas of cultural heritage, where inherently multivariate techniques are frequently employed for analysis. [17]

The data were collected during the accelerated light ageing of Paraloid® B44-based coatings prepared by casting solutions also containing a non-toxic corrosion inhibitor and a light stabilizer. Two types of corrosion inhibitors and two types of light stabilizers were selected. While the concentration of the corrosion inhibitors varied among the formulations, the concentration of Paraloid® B44 and the stabilizer remained constant, resulting in a total of twenty-one formulations (Table 1). Their stability over time was assessed by accelerated light ageing and monitored at specific intervals to observe decay phenomena .

Fourier Transformed-Infrared Spectroscopy and UV-Vis spectroscopy were used to monitor the aging process, both using benchtop and portable spectrometers.

In this article, we present a method for laboratory studies that allows for an objective comparison of different coating formulations while remaining simple and easy to interpret. This approach also facilitates the application of the same methodology to real samples in real working conditions, enabling the use of techniques—preferably portable and in line with the principles of green analytical chemistry—to develop models for monitoring the effectiveness of protective treatments over time. The proposed method is based on the well-established technique of Principal Component Analysis (PCA) [18–20]. PCA has the powerful ability to extract relevant information from data while providing easily interpretable visual results. Here, we will leverage the strengths of spectroscopic techniques, including the ability to analyse samples non-invasively, combined with PCA.

6.3 Materials and methods

6.3.1 Samples

For this research, a set of 21 samples were prepared, following the scheme reported in Table 1. The coating formulation consists of an acrylic resin, Paraloid ® B44 (ethyl acrylate/methyl methacrylate copolymer, with methyl methacrylate>50%) purchased from Sinopia s.a.s., in solution with a combination of a corrosion inhibitor and a light stabiliser. Two types of corrosion inhibitors have been investigated: 5-mercapto-1-pheniltetrazole (MPT), purchased from Alfa Aesar and 2-amino-5-ethyl-1,3,4-thiadiazole (AEDTA) purchased from Sigma Aldrich. Two stabilizers were chosen based on their different mechanisms of action: Tinuvin® 312 (TIN312 in the text), ethanediamide N-(2-ethoxyphenil)-N'-(2-ethylphenil), and Tinuvin® 5050 (TIN5050 in the text), a mixture of 2-(2-hydroxyphenyl) benzotriazole and a HALS-Hindered Amine Light Stabilizer (the structure is unknown) obtained from BASF. The solvent used to solubilize the various components and prepare the coatings is 1-methoxy-2-propanol purchased from Sigma Aldrich.

Table 1: Different formulations of the coatings involved in the study.

Composition (wt%)	Sample number																				
	B44	**B44 TIN312**	**B44 TIN5050**	**B44 1% MPT**	**B44 0.5% MPT**	**B44 0.1% MPT**	**B44 1% MPT TIN312**	**B44 0.5% MPT TIN312**	**B44 0.1% MPT TIN312**	**B44 1% MPT TIN5050**	**B44 0.5% MPT TIN5050**	**B44 0.1% MPT TIN5050**	**B44 1% AEDTA**	**B44 0.5% AEDTA**	**B44 0.1% AEDTA**	**B44 1% AEDTA TIN312**	**B44 0.5% AEDTA TIN312**	**B44 0.1% AEDTA TIN312**	**B44 1% AEDTA TIN5050**	**B44 0.5% AEDTA TIN5050**	**B44 0.1% AEDTA TIN5050**
B44	10	10	10	10	10	10	10	10	10	10	10	10	10	10	10	10	10	10	10	10	10
AEDTA	/	/	/	/	/	/	/	/	/	/	/	/	1.0	0.5	0.1	1.0	0.5	0.1	1.0	0.5	0.1
MPT	/	/	/	1.0	0.5	0.1	1.0	0.5	0.1	1.0	0.5	0.1	/	/	/	/	/	/	/	/	/
TIN312	/	0.3	/	/	/	/	0.3	0.3	0.3	/	/	/	/	/	/	0.3	0.3	0.3	/	/	/
TIN5050	/	/	0.3	/	/	/	/	/	/	0.3	0.3	0.3	/	/	/	/	/	/	0.3	0.3	0.3
1-methoxy-2-propanol	90.0	89.7	89.7	89	89.5	89.9	88.7	89.2	89.6	88.7	89.2	89.6	89	89.5	89.9	88.7	89.2	89.6	88.7	89.2	89.6

The coatings were aged for 1000 hours in a Q-Sun Xe-1 Xenon Test Chamber (Q-Lab Corporation, UK) at a constant temperature of 50 °C, irradiance set at 0.68 W/m^2 at 340 nm and Daylight Q filter (cut-on at 295 nm), simulating exposure to direct sunlight. During ageing, the coatings were regularly monitored by a multi-

analytical approach, whose outcomes have been the starting point for this work [10]. Indeed, the results of portable spectrophotometer measurements, UV-Vis and FTIR spectroscopy have been analysed using chemometrics.

For each analysis, a different type of support and coating application method was used. For UV-Vis the coatings were applied on quartz slides using a pipette, ensuring that the thickness was consistent across all samples. For FTIR analyses, silicon wafers were used, with the coatings applied in a controlled manner to ensure maximum reproducibility and consistency in the results. In particular, the thickness of the coatings was monitored to ensure that the absorbance of the most intense peak was between 0.7 and 1. For portable spectrophotometer measurements, a white tile was used, and the coatings were applied with a brush using two strokes in the same direction. This application protocol serves as a reasonable model for actual in situ application conditions.

6.3.2 Experimental plan

The samples were monitored through the three spectroscopic techniques mentioned above and divided into four groups due to spatial constraints inside the ageing chamber. Here, in Table 2, all the measurements made during ageing are reported.

Table 2: Experimental plan

	Group 1	Group 2	Group 3	Group 4
	B44 0.5% AEDTA		**B44**	**B44 1% MPT TIN312**
	B44 0.1% AEDTA		**B44 TIN312**	**B44 0.5% MPT TIN312**
	B44 0.5% AEDTA TIN312		**B44 TIN5050**	**B44 0.1% MPT TIN312**
	B44 0.1% AEDTA TIN312	**B44 1% AEDTA**	**B44 0.5% MPT**	**B44 1% MPT TIN5050**
	B44 0.5% AEDTA TIN5050	**B44 1% AEDTA TIN312**	**B44 1% MPT**	**B44 0.5% MPT TIN5050**
	B44 0.1% AEDTA TIN5050	**B44 1% AEDTA TIN5050**	**B44 0.1% MPT**	**B44 0.1% MPT TIN5050**
t[h]	0	0	0	0
	24	24	24	48
	48	48	48	96
	70	72	72	168
	91	144	144	216
	163	216	192	264
	227	307	240	336
	327	402	312	384
	427	502	360	432
	520	661	408	528
	620	1000	480	600
	720		576	696
	812		648	768
	912		720	864
	1000		840	932
			1000	1000

6.3.3 Characterization

6.3.3.1 Fourier Transform Infrared Spectroscopy (FTIR)

All coatings were applied on silicon supports and analysed in transmission mode with a Perkin Elmer Spectrum 100 spectrometer equipped with a DTS detector. Each analysis was performed by carrying out 16 scans in a range from 450 cm^{-1} to 4500 cm^{-1}, with a resolution of 4 cm^{-1}. A single analysis was performed for each sample.

6.3.3.2 Portable UV Spectroscopy

UV spectra were recorded from 360 nm to 700 nm. Thin coatings were applied by brush on a white tile and analysed by a Portable Spectrophotometer CM-700d KONICA Minolta in SCI (Specular Component Included) mode. For each mock-up, a total of 15 measurements (5 measurement points, 3 measurements for each point) were acquired.

6.3.3.3 Benchtop UV-VIS spectroscopy

The UV-Vis spectra were acquired using a PerkinElmer Lambda 25 UV/vis spectrometer (Waltham, MA, USA) from 200 nm to 400 nm. Coatings were applied on quartz slide so that the extinction values did not exceed A=1. A single analysis was performed for each sample.

6.3.3.4 Principal Component Analysis (PCA)

Data treatment has been carried out using Matlab2012b PCA toolbox.

Spectra of coatings were organized in matrices, with wavelengths as columns and samples analysed at different times as rows. Each sample was represented as the average of the spectra obtained from each technique. The rows represent samples characterized by the concentration of the corrosion inhibitor (0.1%, 0.5%, and 1% of AEDTA or MPT) and the type of light stabilizer used (TIN312 or TIN5050). They were monitored ranging from 0 to 1000 hours of the aging process as reported in Table 2.

Prior to PCA, spectra were pretreated to correct unwanted variations caused by noise, atmospheric interferences like CO_2, baseline shifts and scattering effect [21,22].

The FTIR spectra comprised 1869 variables covering the 399-3992 cm^{-1} range, but better results were obtained for FTIR spectra considering the range 460-3750 cm^{-1} and removing regions ascribable to CO_2 (2300-2400 cm^{-1}) and matrix interferences (615, 746, 856, 1150, 1150-1190 and 1739 cm^{-1}) - as reported in [23]. Savitsky-Golay first derivative (21 pt window, second order polynomial for the AEDTA formulations; 11 pt window, second order polynomial for the MPT formulations and for the multiple-class models), SNV and mean centring were applied to this dataset.

UV-Vis spectra recorded with the portable instrument included 39 variables spanning from 360 to 740 nm. Savitsky-Golay first derivative (7 pt window, second order polynomial), and mean centring were applied before PCA modelling.

Concerning the benchtop UV-Vis data, the relevant information was found in the spectral region between 200 and 400 nm, therefore the rest of the spectrum was excluded from the calculations. Smoothing (31 pt window), first derivative (second order polynomial, 9 pt window) SNV and mean centring were applied before PCA calculation.

6.4 Results and Discussion

In the following sections of the article, the results of the chemometric reprocessing of the spectroscopic data collected during the aging of the samples are presented. PCA provides two main plots: the scores plot, which describes the samples, and the loadings plot, which, in the case of spectroscopic techniques, highlights the spectral regions most significant for distinguishing differences between the samples. The score plots are usually displayed in a two-dimensional form. Additionally, when useful, the scores of individual principal components are plotted over time to emphasise how the samples change throughout the ageing process. Clear and straightforward graphs have been thus used to illustrate how the samples change over time, based on the information captured by each analytical technique.

6.4.1 Fourier Transform Infrared Spectroscopy (FTIR)

The very first model constructed with the FTIR data included the entire spectra. However, the resulting PCA model (data not shown) did not reveal a clear time evolution trend. The loadings analysis indicated that this outcome was probably due to the stability of the polymer, which remained nearly unchanged during the accelerated aging in all the samples, while other compounds underwent changes [10]. To enhance the information concerning changes during aging, specific spectral regions (polymer signal) were excluded [22] and a new model was recalculated.

The PC1 vs. PC2 score plot (Figure 1a) clearly shows that the samples are distributed in the space according to their formulation. The possibility of distinguishing formulations containing TIN5050 is significant as the absorption peaks of this light stabiliser are masked by those of other components, making the FTIR spectra of these coatings visually indistinguishable from each other. Using multivariate analysis, they are clearly identifiable in the graph.

A clear distinction emerges between two subgroups: the coatings with AEDTA at positive PC1 values (represented with triangles in the figure) and the coatings with MPT at more negative values of the same component (square icon). PC1 also differentiates the samples based on the concentration of AEDTA. Increasing concentrations of the corrosion inhibitor (0.1%, 0.5%, and 1%) are represented by red, green, and blue triangles, respectively. This trend is particularly noticeable in samples containing TIN5050: as the concentration of the corrosion inhibitor increases, the PC1 values shift toward the higher positive part of the axis.

Information concerning the evolution in time can be found in PC2 vs PC3 score plot (Figure 1c), with blue representing 0 hours and red corresponding to 1000 hours of aging. PC3 captures the information regarding the time evolution of most samples, except for the coatings with 1% AEDTA, which display a distinct behaviour. The changes over time could be attributed to the fact that both types of corrosion inhibitors volatilize, which is a known drawback of this category of inhibitors [24].

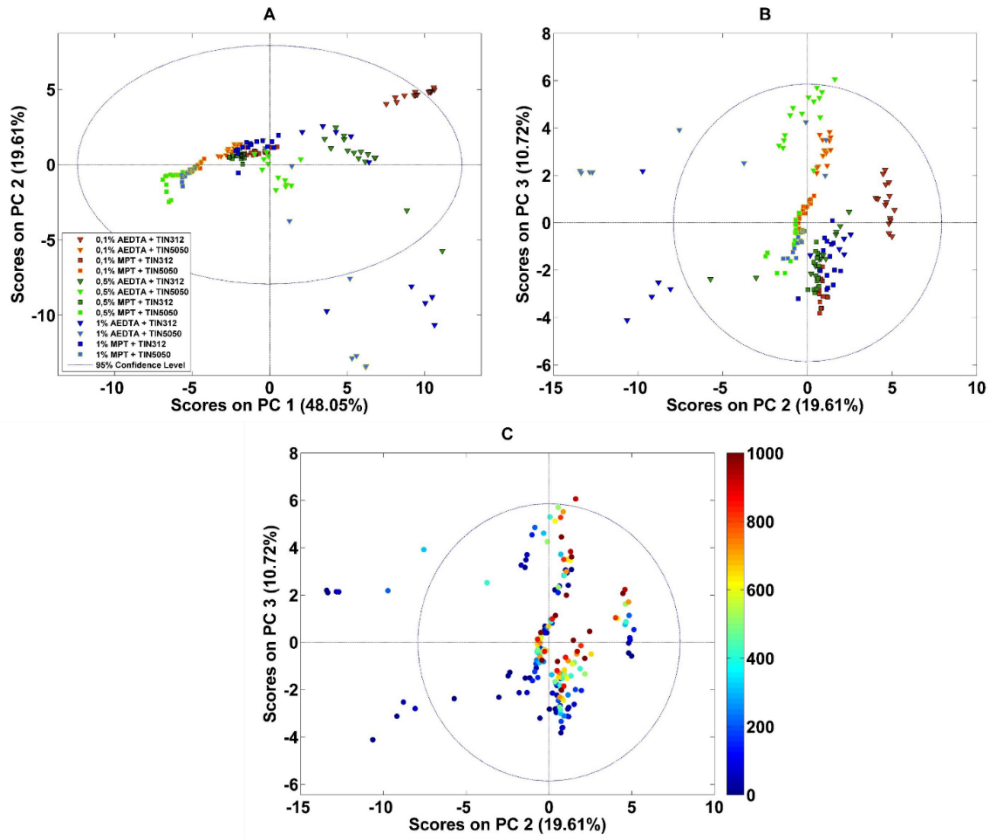

Figure 1: Score plot PC1 vs PC2 (a) and PC2 vs PC3 (b-c) of the model built with all the studied formulations. Coatings with AEDTA are indicated by a triangular icon, while those with MPT are marked with a square icon. Formulations with a concentration of 0.1% w/w of corrosion inhibitor and Tinuvin 312 are colored dark red with black border, while those with the same concentration of inhibitor but with Tinuvin 5050 are orange with yellow border. The ones with a concentration of 0.5% w/w of corrosion inhibitor and Tinuvin 312 are colored dark green with black border, while those with Tinuvin 5050 are light green with yellow border. Formulations with a concentration of 1% w/w of corrosion inhibitor and Tinuvin 312 are colored dark blue with black border, while those with Tinuvin 5050 are light blue with yellow border. Graph C describes the same samples over time: red colour represents 1000 hours of ageing; blue colour represents time zero.

The above presented model encompasses all the information contained within the dataset. To facilitate a more structured analysis, a viable approach is to develop models restricted to specific categories of samples, thereby enabling the model to process one set of information at a time more effectively. The initial step involves

creating two separate models based on the type of corrosion inhibitor: one model for samples containing AEDTA and another for those with MPT.

As an example, the score plot for the model with AEDTA-containing samples is presented (Figure 2a). This model again distinctly differentiates the samples according to the type of light stabiliser, placing samples with TIN5050 at more positive PC1 values compared to those with TIN312. As shown in the plot (Figure 2b), the samples are also arranged according to their aging process, but the evolution follows distinct directions. For example, the sample containing 0.1% AEDTA + TIN312 (represented by a dark red triangle) shifts from the upper left of the plot towards a lower right position as it ages, while samples with 0.5% AEDTA + TIN312 (dark green triangle) evolve from a lower-left position to a higher-right one. These differing evolutionary directions indicate that these samples change differently over time depending on the concentrations of the corrosion inhibitors. PC3 (shown in Figure 2c and 2d) again accounts for information concerning evolution over time (Figure 2d).

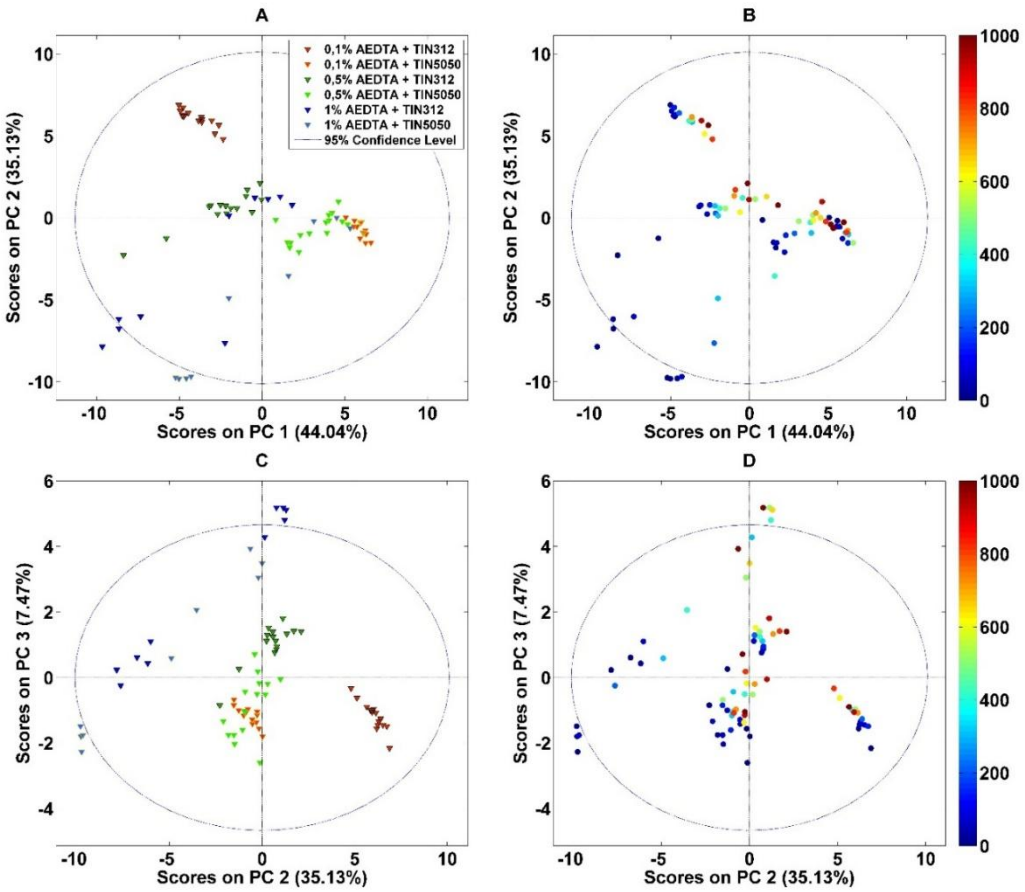

Figure 2: Score plot PC1 vs PC2 (a-b) and PC2 vs PC3 (c-d) of the model built with AEDTA formulations. Formulations with a concentration of 0.1% w/w of corrosion inhibitor and Tinuvin 312 are colored dark red with black border, while those with the same concentration of inhibitor but with Tinuvin 5050 are orange with yellow border. The ones with a concentration of 0.5% w/w of corrosion inhibitor and Tinuvin 312 are colored dark green with black border, while those with Tinuvin 5050 are light green with yellow border. Formulations with a concentration of 1% w/w of corrosion inhibitor and Tinuvin 312 are colored dark blue with black border, while those with Tinuvin 5050 are light blue with yellow border. Graphs B and D describe the same samples over time: red colour represents 1000 hours of ageing; blue colour represents time zero.

It is worth noting that in a score plot, samples that are similar with respect to the variables used to describe them are positioned close together, while samples that are farther apart are more different. This means that the greater the distance between samples at time 0 and those at time 1000, the larger the differences observed in their Mid-Infrared (MIR) spectra. In other words, the more distant they are, the greater the changes that occurred during the artificial aging process. This is a significant result, as it enables a visual comparison of the outcomes of a controlled aging experiment, thereby facilitating the identification of the formulations most prone to aging and thus the selection of the more stable ones, for further development.

By delving into the analysis, it becomes feasible to model the evolution of individual samples to gain a deeper understanding of their trends. In this context, PCA should be conducted exclusively on samples belonging to a specific category, thereby allowing for the observation of differences at various stages of the controlled aging experiment. As an example, the results obtained from the models developed for the samples containing 0.5% AEDTA and MPT are presented, utilizing the light stabilizer TIN5050 in one instance and TIN312 in another.

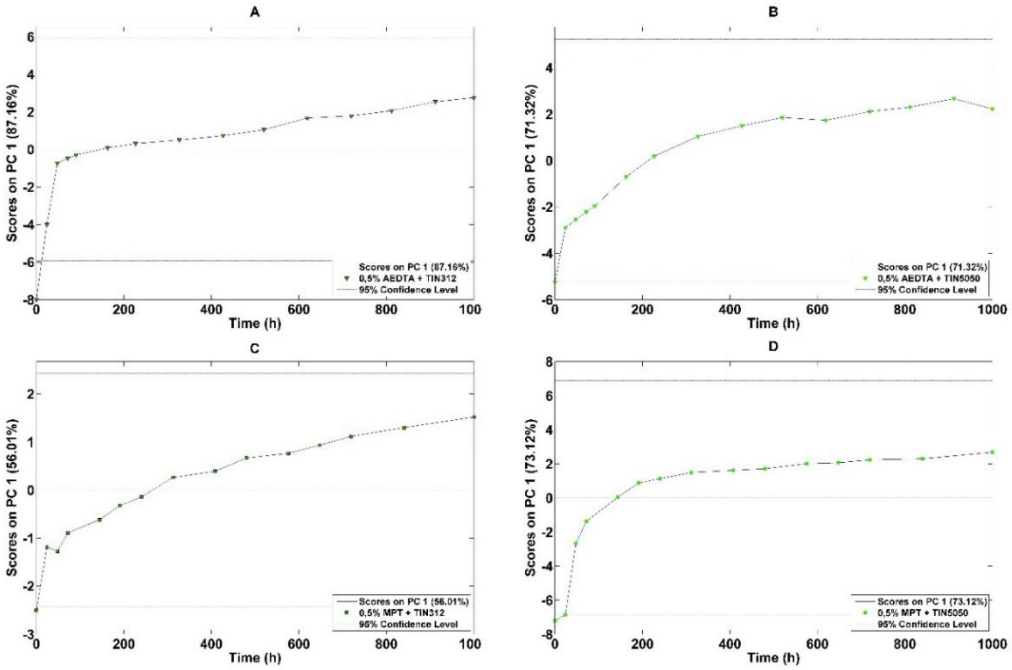

Figure 3: Plot of the scores on PC1 versus time (hours) of 0.5% w/w AEDTA, Tinuvin 312 (Graph A), 0.5% AEDTA Tinuvin 5050 (Graph B), 0.5% w/w MPT and Tinuvin 312 (graph C), 0.5% w/w MPT and Tinuvin 5050 (Graph D).

In this case, in Figure 3 only the score values of PC1 for both models are presented. It is clearly demonstrated that the sample containing 0.5% AEDTA + TIN312 undergoes a significant change during the initial phase of the accelerated aging, followed by minimal alterations after 100 hours, exhibiting a slow yet continuous evolution. Conversely, the sample with TIN5050 experiences a more gradual change at the beginning, reaching a state of stability approximately around 500 hours of artificial aging. In the case of samples containing 0.5% MPT, a similar behaviour is observed. When TIN312 is present, there is a noticeable change at the beginning (though not as significant as that observed for AEDTA), followed by a gradual continuous change. Conversely, with TIN5050, a near plateau is reached after approximately 300 hours. This approach allows for the rationalization and comparison of the evolutions of individual samples under investigation in a visual and intuitive manner.

Monitoring evolution in time with PCA is advantageous for several reasons. First, models proved to be capable of distinguishing between different formulations based on the type of inhibitor and light stabilizer, which is not a trivial task, given

that some of these compounds exhibit overlapping signals in the MIR spectrum. Second, this approach enables a straightforward and intuitive comparison of the behaviours of these various protective coatings, identifying common or differing evolutionary directions over time, thereby facilitating informed decisions regarding the optimal formulation. Third, it allows for the monitoring of individual samples over time, providing insights into their evolution.

6.4.2 Portable UV spectroscopy

The analysis with portable UV spectrophotometer produced intriguing results regarding the decay of light stabilisers and corrosion inhibitors.

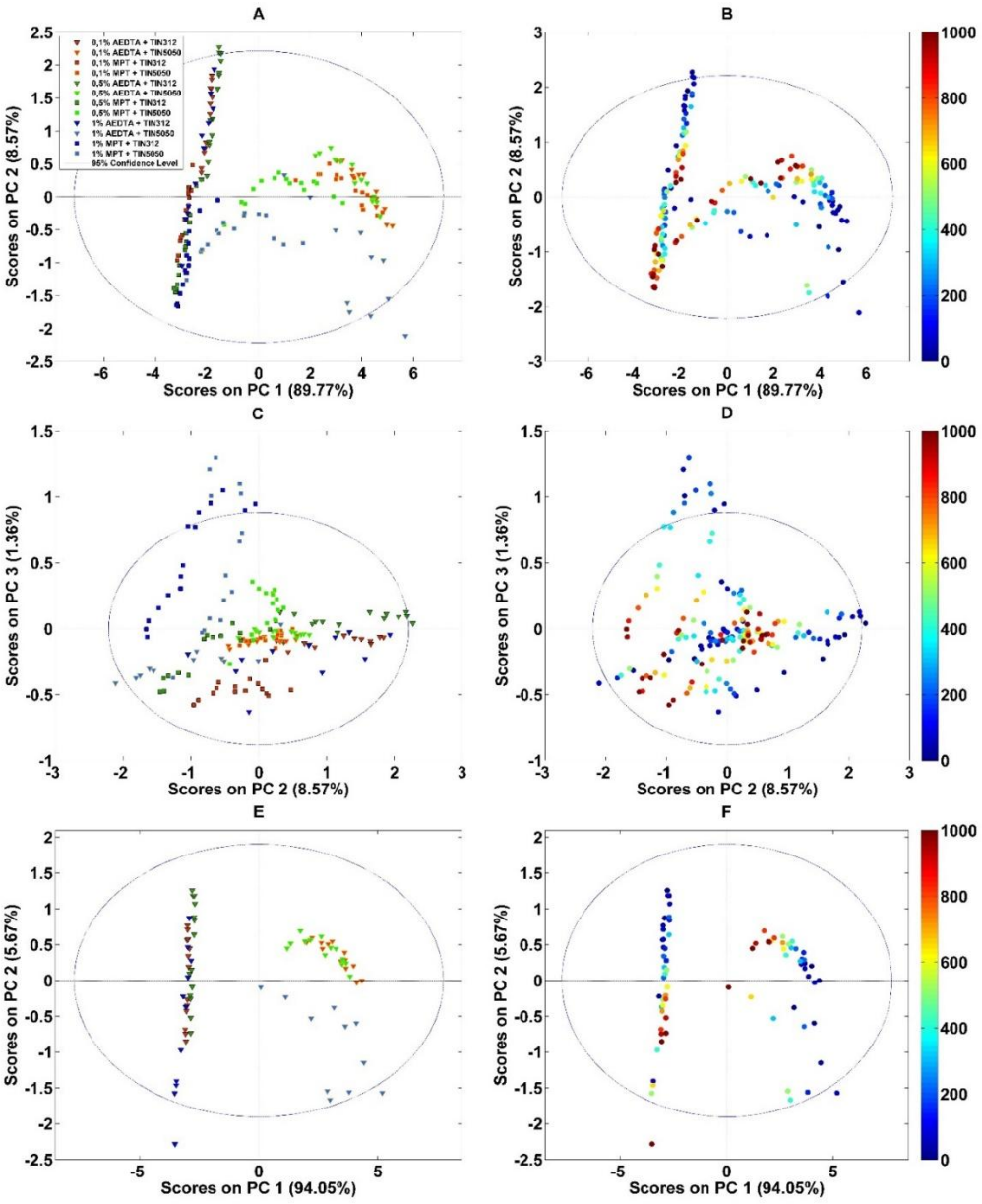

Figure 4: Score plot PC1 vs PC2 (a-b), PC2 vs PC3 (c-d) of the model built with all formulations. Graph E and graph F are referred only to score plots PC1 vs PC2 of AEDTA coatings. Formulations with a concentration of 0.1% w/w of corrosion inhibitor and Tinuvin 312 are colored dark red with black border, while those with the same concentration of inhibitor but with Tinuvin 5050 are orange with yellow border. The ones with a concentration of 0.5% w/w of corrosion inhibitor and Tinuvin 312 are colored dark green with black border, while those with Tinuvin 5050 are light green with yellow border. Formulations with a concentration of 1% w/w of corrosion inhibitor and Tinuvin 312 are colored dark

blue with black border, while those with Tinuvin 5050 are light blue with yellow border. Graphs B, D and F describe the same samples over time: red colour represents 1000 hours of ageing; blue colour represents time zero.

As highlighted in Figure 4, the difference between the two Tinuvin is clear: the symbols with the yellow border- namely the coatings with Tinuvin 5050- stay on the right while the ones with the black border are on the left. On PC1, the evolution with time of Tinuvin 5050-based formulations emerges, while on PC2, the temporal evolution of Tinuvin 312-based formulations and the difference between coatings with MPT or AEDTA can be seen. The evolutions, being almost orthogonal to each other, suggest independent mechanisms of decay involving the light stabilizers, that are specific for the chemical classes they are in.

On PC2, an evolutionary direction can be identified, which, for almost all samples, moves from more positive PC2 values toward more negative ones. Samples that show greater distances between the starting point of the accelerated aging (0h) and the final point (1000h) are more different, indicating that accelerated aging has caused a more significant change in their composition. The PC2 versus PC3 plot highlights the time evolution of 1% MPT-containing formulations on PC3. This could indicate that the direction of evolution over time, i.e., the decay of MPT, strongly depends on its concentration, as samples with the three MPT concentrations follow different evolutionary paths. In contrast, formulations containing AEDTA follow a single evolutionary direction. It is interesting to note also that the direction of evolution of 1% MPT samples moves from more positive PC3 values toward values similar to those of the other samples. This could indicate that, after the aging process, the samples with 1% MPT exhibit a chemical composition—detectable by the sensor used in this experiment—more akin to that of the samples with lower concentrations of the same chemical substance. In other words, it is as if the MPT concentration shifts from 1% to values closer to those of the other samples, which contain 0.5% and 0.1%. This suggests that the coating decay is more pronounced at higher MPT concentrations, confirming what already been demonstrated by Pellis and co-authors [10].

As before, to better rationalize the information contained in this graph, it is useful to create submodels by dividing the different categories of samples.

Figures 4e and 4d present the score plot for the PCA model developed using samples containing AEDTA. The first principal component (PC1) accounts for the

majority of the variance and effectively separates the samples based on the type of Tinuvin used. However, when the samples are color-coded according to the aging time, it becomes evident that those containing TIN5050 are arranged along PC1 in line with their evolution, progressing from time 0, located at more positive PC1 values, toward the centre of the model. In contrast, samples with TIN312 are organized according to their aging along PC2, which explains less than 6% of the total information. This observation reinforces the notion that each light stabilizer follows its unique direction of change over time, with TIN5050 demonstrating more significant variations compared to TIN312, whose signal remains relatively stable [10]. It is crucial to recall that the results of a PCA depend on the chemical signals (the variables) used in its construction.

6.4.3 Benchtop UV spectroscopy

The benchtop UV spectrometer was thus used to confirm the results already obtained for the samples containing AEDTA, whose behaviour during accelerated aging proved to be more homogeneous across different AEDTA concentrations, and therefore more stable and easier to rationalize. The Principal Component Analysis performed on the data collected from the UV range measured by this instrument yields interesting insights.

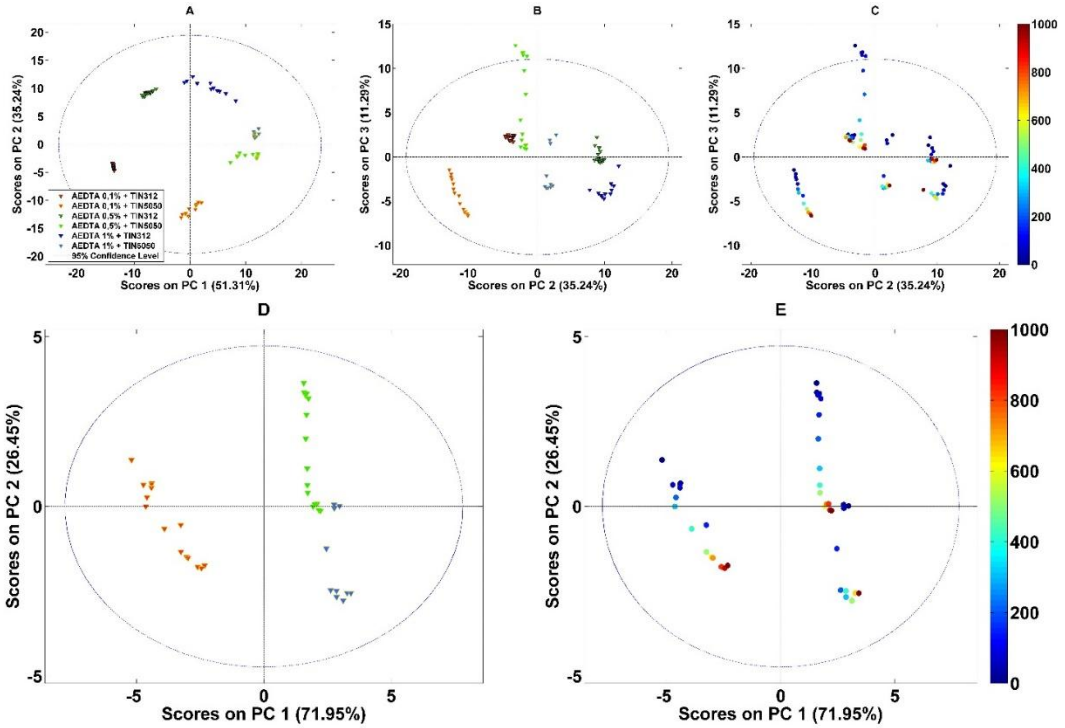

Figure 5: Score plot PC1 vs PC2 (a) and PC2 vs PC3 (b-c) of the model built

with AEDTA formulations. Graphs D and E refer only to AEDTA and Tinuvin 5050 coatings. Formulations with a concentration of 0.1% w/w of corrosion inhibitor and Tinuvin 312 are colored dark red with black border, while those with the same concentration of inhibitor but with Tinuvin 5050 are orange. The ones with a concentration of 0.5% w/w of corrosion inhibitor and Tinuvin 312 are colored dark green with black border, while those with Tinuvin 5050 are light green with yellow border. Formulations with a concentration of 1% w/w of corrosion inhibitor and Tinuvin 312 are colored dark blue with black border, while those with Tinuvin 5050 are light blue with yellow border. Graphs C and E describe the same samples over time: red colour represents 1000 hours of ageing; blue colour represents time zero.

As we expected, the model is able to group the samples based on their chemical composition. Moreover, the model can also arrange the samples containing AEDTA according to its concentration: samples with lower concentrations of AEDTA are positioned in the low left quadrant, while those with higher concentrations are located in the high positive one. The model distinguishes also the presence of the light stabilizer: samples with TIN5050 are located in the lower right part of the graph, while samples containing TIN312 lie in the upper left part. Looking at PC3, it is possible to see that the samples are arranged based on time variability. What stands out most from this model is that the samples containing TIN5050 undergo greater changes over time compared to those containing TIN312, especially for samples containing low concentration levels of corrosion inhibitor. This agrees with results observed in the chemometric analysis of MIR data and also with those by py-GC/MS determination [10].

Further narrowing down the dataset, the model obtained for the samples with AEDTA and TIN5050 is presented. The information contained in the first axis, which represents the greatest variability, is the difference in the concentration of the corrosion inhibitor, while the second axis shows the evolution over time. It is clearly visible that samples with a low concentration of AEDTA evolve more significantly over time compared to samples with a high concentration of the same corrosion inhibitor, according to the information that this instrument operating between 200 and 400 nm is capable of capturing. The models are therefore capable on the one hand to recognize the different formulations and on the other to visually represent their evolution over time, allowing for easy comparison.

6.5 Conclusions

Monitoring the evolution of coatings designed to protect metal artworks from corrosion presents a significant challenge for researchers. This article proposes a methodology based on spectroscopic techniques paired with chemometric data analysis. The techniques used proved to be effective for this purpose, and the article emphasizes the complementary and similar insights they offer. A monitoring system based on principal component analysis is introduced, which not only distinguishes between various types of coatings—both in terms of the corrosion inhibitor and light stabilizer—but also simplifies the interpretation of decay differences as these formulations age. This method facilitates an easy and intuitive selection of optimal formulations using simple, interpretable two-dimensional graphs, allowing users to understand without any expertise in spectra interpretation. The portable UV-Vis data indicated that MPT coatings are more prone to degradation, whereas benchtop UV-Vis analysis revealed that Tinuvin 5050 experiences more substantial changes over time. This complementary information, easily interpreted through the chemometric approach proposed, led to the selection of AEDTA and Tinuvin 312 as the optimal solution. The results obtained in this study confirm those of previous work, demonstrating that this approach is effective and robust for decay studies.

6.6 Bibliography

1. Letardi, P. Testing New Coatings for Outdoor Bronze Monuments: A Methodological Overview. Coatings 11 (2021) doi:10.3390/coatings.

2. Salvadori, B.; Cagnini, A.; Galeotti, M.; Porcinai, S.; Goidanich, S.; Vicenzo, A.; Celi, C.; Frediani, P.; Rosi, L.; Frediani, M.; et al. Traditional and Innovative Protective Coatings for Outdoor Bronze: Application and Performance Comparison. J. Appl. Polym. Sci. 135 (2018) doi:10.1002/app.46011.

3. Molina, M.T.; Cano, E.; Ramírez-Barat, B. Testing Protective Coatings for Metal Conservation: The Influence of the Application Method. Herit. Sci. 11 (2023) doi:10.1186/s40494-023-00937-0.

4. Molina, M.T.; Cano, E.; Ramírez-Barat, B. Protective Coatings for Metallic Heritage Conservation: A Review. J. Cult. Herit. 62 (2023) 99–113.

5. Masi, G.; Josse, C.; Esvan, J.; Chiavari, C.; Bernardi, E.; Martini, C.; Bignozzi, M.C.; Monticelli, C.; Zanotto, F.; Balbo, A.; et al. Evaluation of the Protectiveness of an Organosilane Coating on Patinated Cu-Si-Mn Bronze for Contemporary Art. Prog. Org. Coat. 127 (2019) 286–299, doi:10.1016/j.porgcoat.2018.11.027.

6. Bescher, E.; Mackenzie, J.D. Sol-Gel Coatings for the Protection of Brass and Bronze. J. Solgel. Sci. Technol. 26 (2003) 1223–1226, doi:10.1023/A:1020724605851.

7. Chiavari, C.; Balbo, A.; Bernardi, E.; Martini, C.; Zanotto, F.; Vassura, I.; Bignozzi, M.C.; Monticelli, C. Organosilane Coatings Applied on Bronze: Influence of UV Radiation and Thermal Cycles on the Protectiveness. Prog. Org. Coat. 82 (2015) 91–100, doi:https://doi.org/10.1016/j.porgcoat.2015.01.017.

8. Kosec, T.; Škrlep, L.; Švara Fabjan, E.; Sever Škapin, A.; Masi, G.; Bernardi, E.; Chiavari, C.; Josse, C.; Esvan, J.; Robbiola, L. Development of Multi-Component Fluoropolymer Based Coating on Simulated Outdoor Patina on Quaternary Bronze. Prog. Org. Coat. 131 (2019) 27–35, doi:10.1016/j.porgcoat.2019.01.040.

9. Bierwagen, G.; Shedlosky, T.J.; Stanek, K. Developing and Testing a New Generation of Protective Coatings for Outdoor Bronze Sculpture. In Proceedings of the Progress in Organic Coatings; December 2003; Vol. 48, pp. 289–296.

10. Pellis, G.; Giussani, B.; Letardi, P.; Poli, T.; Rizzi, P.; Salvadori, B.; Sansonetti, A.; Scalarone, D. Improvement in the Sustainability and Stability of Acrylic Protective Coatings for Outdoor Bronze Artworks. Polym. Degrad. Stab. 218 (2023) doi:10.1016/j.polymdegradstab.2023.110575.

11. Kosec, T.; Ćurković, H.O.; Legat, A. Investigation of the Corrosion Protection of Chemically and Electrochemically Formed Patinas on Recent Bronze. Electrochim. Acta 56 (2010) 722–731. doi:10.1016/j.electacta.2010.09.093.

12. Kosec, T.; Legat, A.; Stupnišek-Lisac, E. Improvement of Corrosion Stability of Patinated Bronze. In Corrosion of Archaeological and Heritage Artefacts EFC 45; Routledge, 2017; pp. 327–333.

13. Bostan, R.; Varvara, S.; Găină, L.; Petrisor, T.; Mureşan, L.M. Protective Effect of Inhibitor-Containing Nitrocellulose Lacquer on Artificially Patinated Bronze. Prog. Org. Coat. 111 (2017) 416–427, doi:https://doi.org/10.1016/j.porgcoat.2016.08.004.

14. Jáuregui-Gónzalez, D.A.; Rodríguez-Gómez, F.J.; Contreras-Vargas, J.; Roncagliolo-Barrera, P.; López-Arriaga, M. Influence of the Application and Preparation of Wax Coatings on Artificially Patinated Bronze Surfaces. METAL 2016, 170–177.

15. Swartz, N.; Clare, T.L. On the Protective Nature of Wax Coatings for Culturally Significant Outdoor Metalworks: Microstructural Flaws, Oxidative Changes, and Barrier Properties. J. of the Am. Inst. for Conserv. 54 (2015) 181–201, doi:10.1179/1945233015Y.0000000012.

16. Cano, E.; Lafuente, D.; Bastidas, D.M. Use of EIS for the Evaluation of the Protective Properties of Coatings for Metallic Cultural Heritage: A Review. J. of Solid State Electrochem. 14 (2010) 381–391. https://doi.org/10.1007/s10008-009-0902-6

17. Riu, J.; Giussani, B. Analytical Chemistry Meets Art: The Transformative Role of Chemometrics in Cultural Heritage Preservation. Chemom. and Intell. Lab. Syst. 247 (2024) doi:10.1016/j.chemolab.2024.105095.

18. Esbensen, K.H.; Geladi, P. Principal Component Analysis: Concept, Geometrical Interpretation, Mathematical Background, Algorithms, History, Practice. In: S. Brown, R. Tauler, B. Walczak (Eds), Comprehensive chemometrics: Chemical and biochemical data analysis, Elsevier, 2020; Vol. 2 ISBN 0444641653.

19. Mardia K. V.; Kent J.T.; Bibby J.M. *Multivariate Analysis*; Academic Press, London, 1989; ISBN 0323-3847.

20. Jackson, J.E. *A User's Guide to Principal Components*; John Wiley & Sons, 2005; ISBN 0471725323.

21. Rinnan, Å.; Van Den Berg, F.; Engelsen, S.B. Review of the Most Common Pre-Processing Techniques for near-Infrared Spectra. Trends in Anal. Chem. 28 (2009) 1201–1222. https://doi.org/10.1016/j.trac.2009.07.007

22. Rinnan, Å.; Norgaard, L.; van den Berg, F.; Thygesen, J.; Bro, R.; Engelsen, S.B. Data Pre-Processing. In: Da-Wen Sun, (Eds), Infrared Spectroscopy for Food Quality Analysis and Control; Elsevier, Amsterdam, 2008, pp. 29–50.

23. Haris, M.; Kathiresan, S.; Mohan, S. FT-IR and FT-Raman Spectra and Normal Coordinate Analysis of Poly Methyl Methacrylate. Der Pharma Chemica 2 (2010) 316–323.

24. Nawaz, M.; Ahmad, S.; Taryba, M.G.; Montemor, M.F.; Kahraman, R.; Shakoor, R.A. Improvement in Inhibition Performance of Anti-Corrosion Coatings Using Polyolefin Matrix Embedded with Modified TiO2 Nanoparticles. Prog. Org. Coat. 195 (2024) doi:10.1016/j.porgcoat.2024.108659.

Acknowledgements

This research was funded by Progetto di Ricerca di Interesse Nazionale PRIN 2022 “Innovative multi analytical Characterisation of the influence of pAtina-coating inteRaction on anti-corrosive propErties – InCARE” (Project code: 2022895PTX), funded by MUR and the European Union – Next Generation EU, M4.C2.1.1, CUP B53D23001230006.

G.P and D.S. acknowledge support from the Project CH4.0 under the MUR program "Dipartimenti di Eccellenza 2023-2027" (CUP: D53D23009030006).

Chapter 7

Enhancing Permanence of Corrosion Inhibitors Within Acrylic Protective Coatings for Outdoor Bronze Using Green Nanocontainers

Giulia Pellis, Fabrizio Caldera , Francesco Trotta, Thais Biazioli de Oliveira, Paola Rizzi, Tommaso Poli and Dominique Scalarone

Department of Chemistry, University of Torino, Via Pietro Giuria 7, 10125 Torino, Italy

7.1 Abstract

Outdoor bronze statues are constantly exposed to weather conditions and reactive compounds in the atmosphere that can interact with their surfaces. To avoid these interactions, a commonly used method is the application of coatings with corrosion inhibitors. However, a significant limitation of these inhibitors is their gradual loss over time. In this study, we aimed to improve the durability of 2-amino-5-ethyl-1,3,4-thiadiazol- (AEDTA), the inhibitor chosen to formulate new acrylic coatings for outdoor bronzes. Methyl-β-cyclodextrin (Me-β-CD) was selected to host the inhibitor due to the capability of cyclodextrins to form complexes incorporating small organic molecules. The complexes of Me-β-CD and AEDTA were prepared and the inclusion of AEDTA was proved by Fourier-transform infrared spectroscopy, X-ray diffraction and nuclear magnetic resonance spectroscopy. Then, acrylic coatings were prepared at different concentrations of the Me-β-CD/AEDTA system. They were thermally aged and monitored every 24 h. To evaluate the volatilization of the corrosion inhibitor, solid phase

microextraction-gas chromatography/mass spectrometry (SPMEGC/MS) and thermal desorption-GC/MS (TD-GC/MS) analyses were performed during the first 72 h. The results were compared to those of pure AEDTA films and Incralac®. The outcomes showed that Me-β-CD/AEDTA complexes are promising candidates for developing coatings with improved stability and longer retention of AEDTA.

7.2 Introduction

Bronze statues are among the most widespread forms of outdoor public art in urban environments. However, their conservation poses significant challenges due to the lack of funding and the limited effectiveness of conservation treatments over time. These artworks are often coated with either natural or artificial patinas, but in the long term this does not fully prevent degradation processes driven by external factors, including pollution, UV rays, and humidity. One of the most common approaches to mitigate these effects involves the application of protective coatings. However, the most widely used acrylic coating for bronze restoration, Incralac®, contains benzotriazole (BTA), a compound that is both toxic and suspected of being carcinogenic [1]. Therefore, there is a need for the development of safer, more effective, and long-lasting conservation strategies, which require the replacement of hazardous materials currently in use [2,3]. Among the non-toxic, cost-effective alternatives to BTA, 5-ethyl-1,3,4-thiadiazol-2- amine (AEDTA) has been proposed since it has been shown to reduce the corrosion of copper in 3.0% NaCl solutions [3]. A more recent study has identified AEDTA as a promising substitute of BTA, being safer, more stable, and with a lower tendency to leave the coating over time [5]. In this study, we propose to improve the permanence of AEDTA in acrylic coatings using methyl-β-cyclodextrin (Me-β-CD) as a green nanocontainer for the corrosion inhibitor.

Cyclodextrins (CDs) have gathered significant attention across various scientific disciplines due to their versatility. These water-soluble, macrocyclic oligosaccharides are composed of at least six α-D-glucopyranose units linked via α-(1→4)-glycosidic bonds and are produced through the enzymatic degradation of starch by cyclodextrin glucanotransferase (CGTase) [6]. The outer surface of the molecule is hydrophilic, rendering it water-soluble, while the inner cavity is less hydrophilic, creating a favourable environment for non-polar compounds. Various CD derivatives, such as hydroxypropyl-β-CD and methyl-β-CD, have been developed to improve their performance, including enhanced complexation efficiency and controlled release properties [7]. CDs are extensively used in the pharmaceutical, biomedical, and food industries, and their unique ability to form

inclusion complexes with guest molecules has expanded their applications by improving the solubility, stability, and bioavailability of these molecules [8]. Several studies have demonstrated the potential of CDs to host corrosion inhibitors, which are typically small organic molecules [9]. The use of CDs as complexing agents aims to increase the retention of corrosion inhibitors within protective coatings, as these inhibitors often separate and leach out of the film, losing their effectiveness [10]. By incorporating corrosion inhibitors into carriers, such issues can be mitigated [11]. Research has shown that CDs are reliable carriers for this purpose: β-CD has successfully encapsulated 5-mercapto-1-phenyl-tetrazole to improve bronze corrosion resistance [12]; α- and β-CD complexes with dibenzylthiourea (DBT) enhanced carbon steel corrosion protection by improving DBT's solubility [13]; and β- and γ-CDs complexes with various organic inhibitors have demonstrated improved corrosion resistance for aluminium alloys and zinc [14–17]. Additionally, β-CD complexes with 2-phosphonobutane-1,2,4-tricarboxylic acid have shown enhanced corrosion protection for carbon steel [18], while hydroxypropyl-β-CD complexes with octadecylamine (ODA) have improved anticorrosion properties for steel due to the increased solubility of the guest [19].

Based on these studies, we sought to investigate the potential of methyl-β-cyclodextrin (Me-β-CD) as a green nanocontainer for the AEDTA corrosion inhibitor (Figure1), with the aim of improving its retention within Paraloid® B44 acrylic coatings.

Methyl-β-cyclodextrin, due to its methoxy groups in place of primary hydroxyls, offers better compatibility with acrylic resins than β-CD. The complexes of methyl-β-cyclodextrin and AEDTA were successfully synthesized, and the inclusion of AEDTA was confirmed by Fourier-transform infrared spectroscopy (FTIR), X-ray diffraction (XRD), and nuclear magnetic resonance (NMR) spectroscopy. The stoichiometry of the complex was determined using the continuous variation method [19]. Furthermore, three types of acrylic coatings containing varying concentrations of the methyl-β-cyclodextrin/AEDTA complex were prepared and applied to both inert substrates and polished bronze discs. These samples underwent accelerated aging at 80 °C, monitoring chemical changes every 24 h by FTIR in both transmission and reflection modes, depending on the substrate. Solid phase microextraction-gas chromatography/mass spectrometry (SPME-GC/MS) and thermal desorption-GC/MS (TD-GC/MS) were used to assess the volatilization of the corrosion inhibitor from the acrylic matrix, comparing the Me-β-CD/AEDTA complex to AEDTA alone. Both systems were then compared with Incralac®.

7.3. Materials and Methods

7.3.1 Materials

Paraloid® B44 (ethyl acrylate/methyl methacrylate copolymer) was purchased from Sinopia s.a.s., 2-amino-5-ethyl-1,3,4-thiadiazol- (AEDTA) (MW 129.18 g/mol) from Sigma Aldrich, and methyl-β-cyclodextrin with 0.5% of methylation was kindly provided by Roquette Freres (MW 1190 g/mol) (Figure 1). The solvent used to prepare the coatings was 1-methoxypropan-2-ol, purchased from Sigma Aldrich.

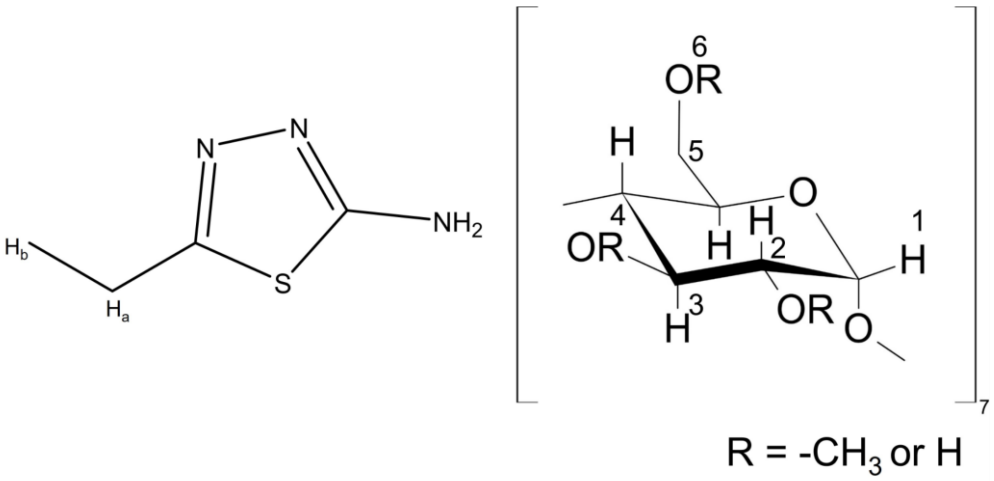

Figure 1. 2-amino-5-ethyl-1,3,4-thiadiazol- (AEDTA) and methyl-β-cyclodextrin.

7.3.2. Synthesis of Methyl-β-Cyclodextrin/AEDTA Complexes

The complexes were synthetized at different molar concentrations (Table 2). At first, the calculated amount of AEDTA was mixed with deionized water and then methyl-β-cyclodextrin was added. For example, Solution No. 1 in Table 2 was prepared by mixing 0.64 mg of AEDTA in 20 mL of deionized water and then adding 65.45 mg of methyl-β-cyclodextrin. The obtained solutions were stirred overnight at room temperature with a stirring rate of 200 rpm. After that, they were

lyophilized for two days and then pounded in a mortar, obtaining a homogeneous white powder.

Table 1: Molar concentrations of the complex solutions

Solution No.	AEDTA (mM)	Methyl-β-Cyclodextrin (mM)
1	0.25	2.75
2	0.50	2.50
3	0.75	2.25
4	1	2
5	1.25	1.75
6	1.50	1.50
7	1.75	1.25
8	2	1
9	2.25	0.75
10	2.50	0.50
11	2.75	0.25
12	0	3
13	3	0

7.3.3. Preparation of the Physical Mixture

The physical mixture was prepared by adding AEDTA and methyl-β-cyclodextrin in a mortar in a weight ratio of 1:10. The two powders were mixed until a homogeneous mixture was obtained.

7.3.4. Formulation of the Coatings

The solutions were prepared by adding the various ingredients in a vial in the following order: acrylic resin, additives, and finally the solvent. They were stirred for 24 h until complete solubilization.

Four types of solutions were prepared containing 0.5%, 1.5%, and 2% w/w of the methyl-β-cyclodextrin /AEDTA complex (1:1 molar ratio) in a 10% w/w Paraloid® B44 solution in 1-methoxypropan-2-ol, and, for the fourth solution, 0.5% w/w of uncomplexed AEDTA in a 10% w/w Paraloid® B44 solution.

The solutions were applied by brush on polished bronze discs (Cu-Sn-Pb-Zn) or poured with the aid of a pipette on glass slides or silicon supports and left to dry until complete solvent evaporation and formation of a thin solid film.

7.3.5. Instrumentation

7.3.5.1. Fourier-Transform Infrared Spectroscopy (FTIR)

FTIR was used for chemical characterization and to monitor chemical changes over time. All coatings were applied on silicon supports and analyzed in transmission mode with a Perkin Elmer Spectrum 100 spectrometer equipped with a DTS detector (Waltham, MA, USA). The thickness of the coatings was controlled by assuring that the absorbance of the most intense peak was between 0.7 and 1. Each analysis was performed carrying out 16 scans in a range from 450 cm^{-1} to 4500 cm^{-1}, with a resolution of 4 cm^{-1}. For the ATR-FTIR analyses of the powders, the range was from 650 cm^{-1} to 4500 cm^{-1}, with a resolution of 4 cm^{-1}. For analyses on polished bronze discs, a Bruker Alpha II spectrometer (Bruker Optics, Entrigen, Germany; Billerica, MA, USA) operating in external reflection mode was used, collecting 32 scans with a resolution of 4 cm^{-1} in a range from 400 cm^{-1} to 4000 cm^{-1}.

7.3.5.2. X-Ray Diffraction (XRD)

XRD analyses were performed in capillary mode using a Malvern Panalytical X'Pert diffractometer (Malvern, UK) with Cu Kα1 radiation as the source. Measurements were taken across an angular range of 5° to 50° 2θ, with a step size of 0.017° 2θ, and a duration of 79.95 s per step. Baseline correction was applied to each diffractogram using X'Pert HighScore 2.2.1 software.

7.3.5.3. Nuclear Magnetic Resonance (NMR) Spectroscopy

NMR Spectroscopy was used to investigate the nature of the interaction between the host and the guest and to study the stoichiometry of the complex. The 13 solutions listed in Table 1 were analyzed.

Solution 1H NMR spectra were acquired on a Bruker 400 instrument operating at 400 MHz (Bruker Corporation, Billerica, MA, USA) and processed with MestReNova v1.19 software (Santiago de Campostela, Spain). A total of 10 mg of complex was dissolved in 0.6 mL of D_2O. For pure compounds, the concentration of the solution in D2O was kept constant at 3 mM.

7.3.5.4. Thermal Desorption-Gas Chromatography/Mass Spectrometry (TD-GC/MS)

TD-GC/MS analyses were used to ascertain the presence of the corrosion inhibitor in coatings over time. Sampling for TD-GC/MS analyses was carried out on unaged coatings and after 72 h of thermal aging at 80 °C. Samples were taken with a scalpel by scratching the coatings applied on bronze discs.

The analyses were performed with a micro-furnace Multi-Shot Pyrolyzer EGA/Py-3030D (Frontier Lab, Koriyama, Japan) coupled to a GC/MS system. Samples were placed into a stainless-steel cup and inserted into the micro-furnace. The desorption temperature was set at 250 °C and kept constant for 1 min. The interface temperature of the pyrolizer was 280 °C and the temperature of the GC injector was kept at 280 °C. The GC was equipped with a methylphenyl-polysiloxane cross-linked 5% phenyl methyl silicone (30 m, 0.25 mm i.d., 0.25 µm film thickness) capillary column. The carrier gas was helium (1.0 mL/min) and the split ratio was one-twentieth of the total flow. The following temperature program was used for the gas chromatographic separation: isotherm of 2 min at 50 °C, ramp of 10 °C/min up to 300 °C, and isotherm at 300 °C for 10 min. An Agilent 8860 Gas Chromatograph and a 5977B Mass Selective Detector (Agilent Technologies,

Sta. Clara, CA, USA) were used. Mass spectra were recorded under electron impact at 70 eV, with a scan range of 45–800 m/z. All instruments were controlled by Agilent Mass Hunter Workstation (ver. 10.1.49) software. The mass spectra assignment was done by mass library searches (NIST2008), by comparison with the literature data and the interpretation of fragmentation paths of mass spectra.

7.3.5.5. SPME-Gas Chromatography/Mass Spectrometry (SPME-GC/MS)

SPME-GC/MS analyses were used to assess the volatilization of corrosion inhibitors over time. Small amounts of coatings were placed in hermetic vials. The vials were placed in an oven at 80 °C and the head space was monitored every 24 h. The sampling of the head space was performed by exposing a SPME fiber for three minutes out of the oven.

The analyses were performed with a 6890 Series Gas Chromatographer system coupled with a 5973 Network Mass Detector (Agilent Technologies, Sta. Clara, CA, USA). The capillary column used was the Agilent HP 5MSUI (30 m, 0.25 mm i.d., 0.25 µm film thickness). Supelco SPME fibers in PDMS/DVB (polydimethylsiloxane/divynilbenzene), with a diameter of the fiber 65 µm, were used.

The exposure time of the fiber inside the injector was 30 s. The column temperature was maintained at 50 °C for 4 min and then increased from 50 °C to 250 °C at a rate of 10 °C per minute and maintained at 250 °C for 5 min. All instruments were controlled by Enhanced Chem Station (ver. 9.00.00.38) software.

7.4 Results and Discussion

The research plan envisaged three main phases: (1) the investigation of the interaction between methyl-β-cyclodextrin and AEDTA, (2) the determination of the stoichiometry of the methyl-β-cyclodextrin/AEDTA complex, and (3) the evaluation of the prolonged permanence within the coating of the corrosion inhibitor hosted in the methyl-β-cyclodextrin cavity.

7.4.1. Methyl-β-Cyclodextrin/AEDTA Complex Characterization

The interaction between methyl-β-cyclodextrin and AEDTA was investigated by FTIR, XRD, and NMR spectroscopy, well-established techniques for studying cyclodextrin inclusion complexes [12]. The methyl-β-cyclodextrin/AEDTA complex with a 1:1 molar ratio was extensively analyzed. To further confirm the

interaction between the host and guest molecules, a physical mixture with the same molar ratio was also prepared.

It has been vastly reported that the variation of the shape, shift, and intensity of the FTIR absorption bands of the guest or host molecule can provide information concerning the formation of complexes [20,21]. Figure 2 illustrates the infrared spectra of methyl-β-cyclodextrin, AEDTA, and of the binary systems (complex and physical mixture). The characteristic AEDTA absorption peak at 1636 cm^{-1}, attributed to the scissoring vibration of the amino group [20,22], shifted and changed in shape in the spectrum of the complex. The broadening of the same peak suggested an amorphization of AEDTA, a reasonable consequence of its complexation, while the shift toward lower wavenumbers reflected a change in the vibration energy of the amino group. These changes in the characteristic absorption band of the corrosion inhibitor highlighted the occurring of an interaction and opened two potential scenarios: the formation of an inclusion or non-inclusion complex. Conversely, the spectrum of the physical mixture perfectly overlapped with the spectra of the individual components, and the peak at 1636 cm^{-1} remained sharp and centred at the same wavenumber of the AEDTA reference, indicating no significant interaction between the two components.

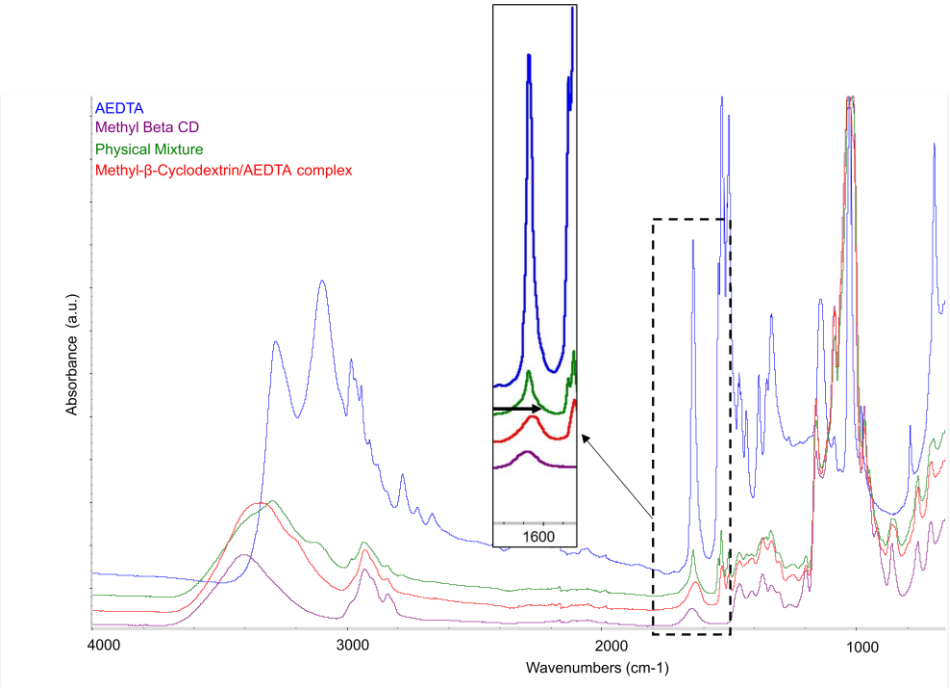

Figure 2. ATR-FTIR spectra of AEDTA, Me-β-CD, their complex, and physical mixture. The box shows the spectral region with the characteristic absorption band of AEDTA and its shift due to complexation.

The successful complexation of AEDTA and methyl-β-cyclodextrin was confirmed by XRD, a useful technique for the detection of cyclodextrin complexation in a powder or microcrystalline state [23,24]. The XRD diffractograms are reported in Figure 3: the diffraction pattern of AEDTA exhibited several sharp peaks, indicating its crystalline structure, while the diffractogram of cyclodextrin was characteristic of an amorphous material. As expected, the XRD pattern of the physical mixture was a direct superimposition of those of the individual components, whereas the methyl-β-cyclodextrin/AEDTA complex showed two broad halos in the diffraction similar to those of methyl-β-cyclodextrin, indicating its amorphous state. This loss of crystallinity suggested that AEDTA and methyl-β-cyclodextrin were mixed at a molecular level, providing further evidence of complexation [25].

The nature of the interaction between AEDTA and methyl-β-cyclodextrin was also explored using 1H NMR spectroscopy, a powerful method for analyzing supramolecular assemblies in solution. Significant chemical shift changes in

specific host or guest nuclei between the free and bound states can confirm the formation of inclusion complexes in solution [7]. Figure 4 presents the NMR spectra of AEDTA, methyl-β-cyclodextrin, and the methyl-β-cyclodextrin/AEDTA complex (1:1 molar ratio), with the chemical shifts (δ) and displacements (Δδ) detailed in Table 2 [26].

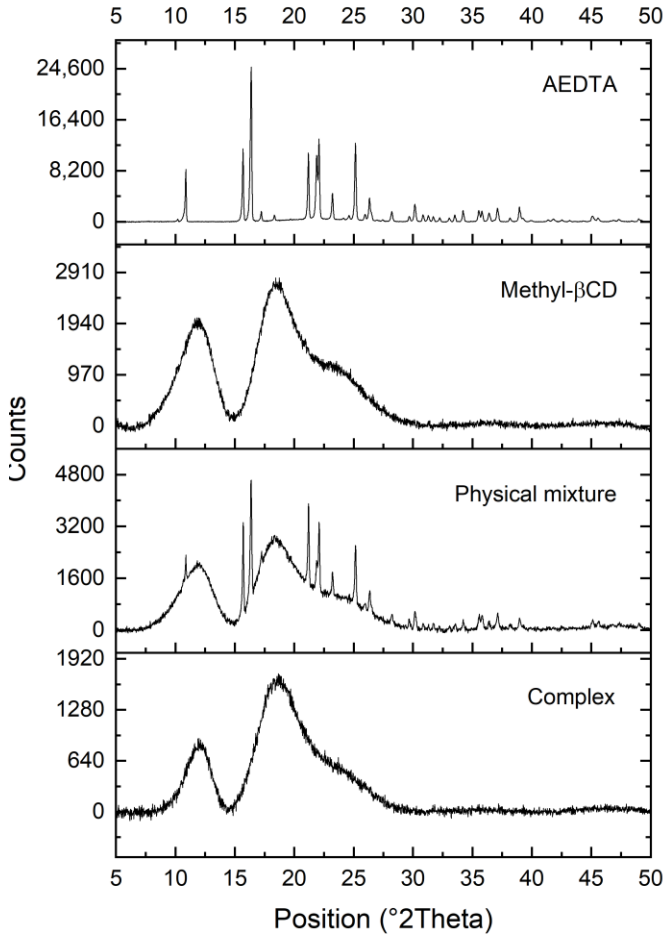

Figure 3. XRD diffractograms of AEDTA, methyl-β-cyclodextrin, their complex, and their physical mixture.

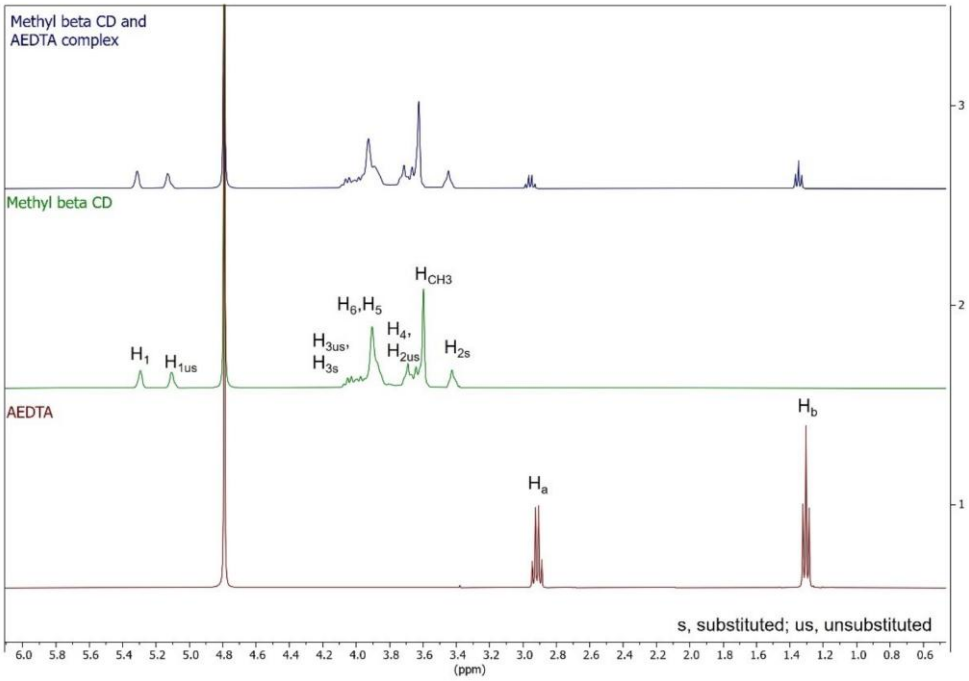

Figure 4. 1H-NMR spectra (600 MHz, D2O) of AEDTA, methyl-β-cyclodextrin, and their complex.

The inclusion of AEDTA in the methyl-β-cyclodextrin cavity was indicated by the chemical shift variations in the host protons H3 and H5, compared to their positions in free CD molecules (Figure 5). Both cyclodextrin protons were shielded, signifying the inclusion of an electron-rich group, likely the -NH_2 group of AEDTA. The signals due to the more external protons, H1 and the protons of the methoxy groups (Figure 5), underwent a minor shift, further indicating that the guest interacted with the internal cavity. The NH2 signal of AEDTA could not be seen in the NMR spectra because the amino group had exchangeable protons that broadened the signals. Thus, no direct interaction between these protons and the host was detectable by NMR. Nonetheless, the change in the amino group scissoring vibration, observed in the FTIR spectra, supported the hypothesis of an interaction between AEDTA and methyl-β-cyclodextrin involving the NH_2 group and the cyclodextrin internal protons, while the thiadiazole ring and ethyl group of AEDTA remained external to the cavity.

It is worthy of note that no new peaks were observed in the NMR spectrum of the complex, suggesting that the inclusion of AEDTA in methyl-β-cyclodextrin occurred with an exchange process in the NMR timescale [12].

Table 2. Chemical shifts (δ) of methyl-β-cyclodextrin and chemical shifts displacements (Δδ) in the complex (1:1 molar ratio).

Methyl-β-Cyclodextrin	H_1	H_{1us}	H_{3s}	H_{3us}	H_5, H_6	H_4	H_{2us}	H_{CH3}	H_{2s}
δ (ppm)	5.313	5.131	4.636	4.401	3.926	3.712	3.664	3.624	3.445
$\Delta\delta_{\text{free-complex}}$ (ppm)	−0.007	−0.002	0.558	0.346	0.006	0.006	−0.006	0	−0.007

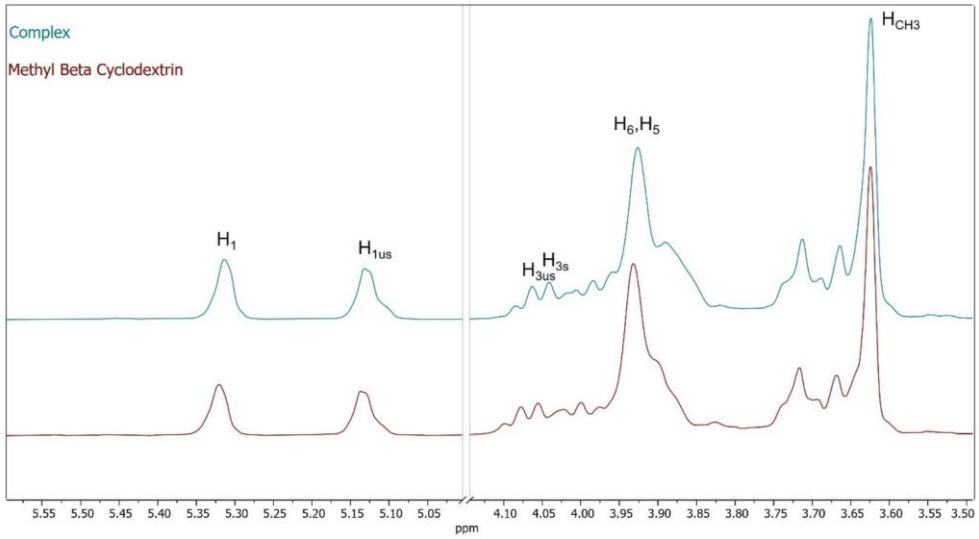

Figure 5. Zoom in on NMR spectra of methyl-β-cyclodextrin and the complex.

7.4.2. Study of the Methyl-β-Cyclodextrin/AEDTA Complex

To gather information on the stoichiometry of the complex, thirteen complexes were synthetized employing different host/guest molar ratios (Table 1, paragraph 3.2).

^{1}H NMR spectra of pure components and methyl-β-cyclodextrin/AEDTA complexes are reported in Figure 6.

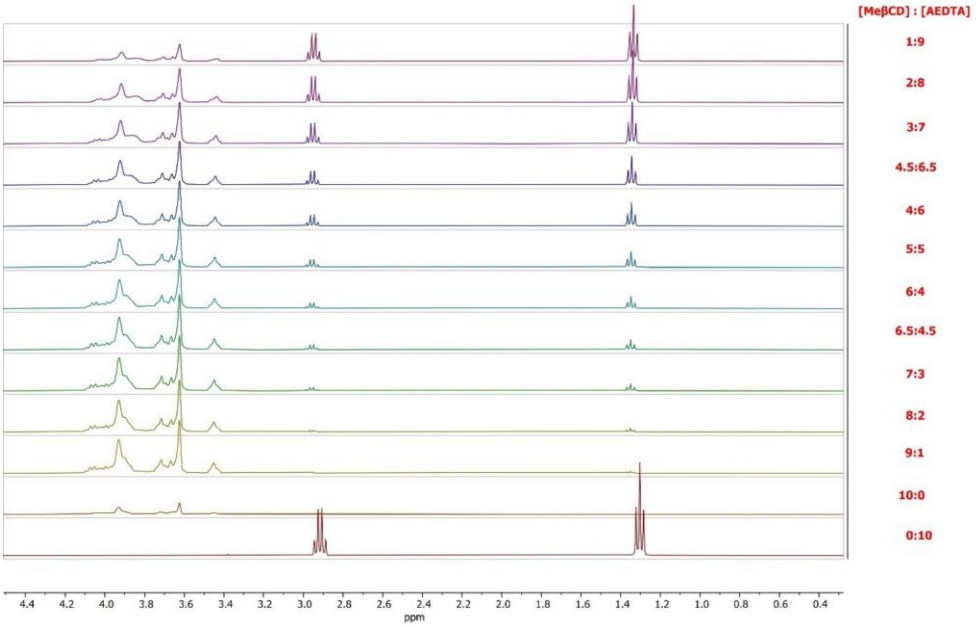

Figure 6. NMR spectra of AEDTA, methyl-β-cyclodextrin, and their complex at different molar ratio.

The stoichiometry of the complex was determined using the continuous variation method, originally proposed by Paul Job (1928) [27]: this method is based on induced chemical shift variation, Δδ, that is experimentally determined, and it is directly related to the concentration of the complex. Δδ is defined as the difference between the chemical shifts of the free molecule and the bounded one.

NMR spectra were recorded for a series of solutions in which the total concentration of the two species was kept constant at 3 mM and the concentration ratio of the single components (r = [AEDTA]/([AEDTA] + [Me-β-CD]) or r = [Me-β-CD]/([AEDTA] + [Me-β-CD]) was varied between 0 and 1.

Under these conditions, if a physical quantity directly related to the concentration of the complex can be measured and plotted as a function of r, its maximum value will be reached at r = m/m + n, where m and n are AEDTA and methyl-β-cyclodextrin proportions in the complex, respectively. When signals are rapidly averaged by the exchange between free and bound states, the quantity $\Delta\delta_{obs}$[AEDTA] or $\Delta\delta_{obs}$[Me-β-CD] (where $\Delta\delta_{obs}$ is the chemical shift difference between free AEDTA or Methyl-β-Cyclodextrin and the observed value for a given ratio r) will be proportional to the complex concentration. Therefore, $\Delta\delta_{obs}$[AEDTA] or $\Delta\delta_{obs}$[Me-β-CD] can be plotted against r [28,29]. Figure 7

highlights the most significantly affected chemical shifts. The continuous variation plot of $\Delta\delta_{obs}$[Me-β-CD] against r of the internal protons H3 and H5 showed a maximum at r = 0.5, indicating a 1:1 complex stoichiometry.

A corresponding Job's plot for the NH_2 protons could not be drawn, as no visible signal was observed in the spectra. However, it is reasonable to assume that the complex followed an equimolar host–guest ratio.

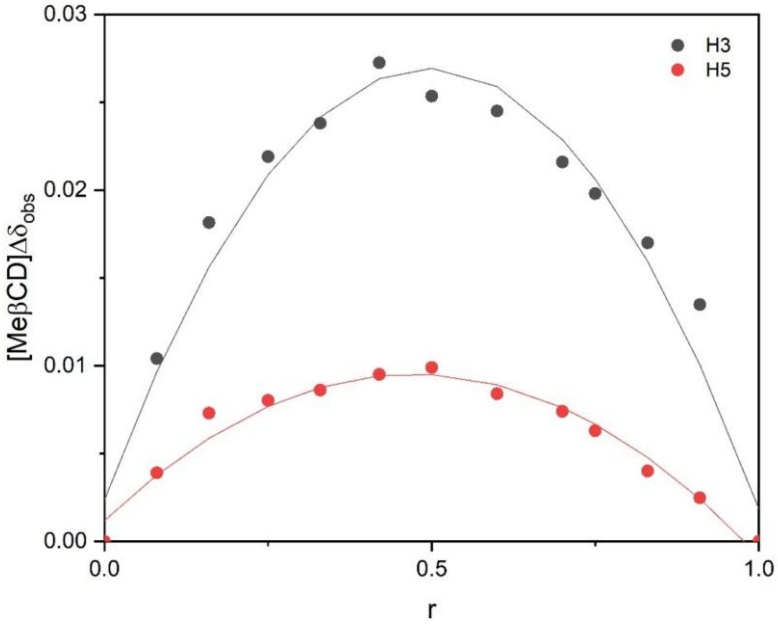

Figure 7. Job's plot of H_3 and H_5 of Me-β-CD.

7.4.3. Characterization of Acrylic Coatings Containing Methyl-β-Cyclodextrin/AEDTA Complex

To ascertain whether the complexation of the corrosion inhibitor enhances its permanence within acrylic coatings, coatings made of Paraloid® B44 and containing 5%, 15%, and 20% *w*/*w* of the methyl-β-cyclodextrin /AEDTA complex were prepared from the solutions previously described. These coatings were then thermally aged at 80 °C, and AEDTA volatilization was monitored using FTIR, SPME-GC/MS, and TD-GC/MS.

In Figure 8, the FTIR spectra recorded during the first 250 h of aging of the coatings containing 20% *w*/*w* of the complex, which corresponded to 2% *w*/*w* of AEDTA, were compared to the spectra of coatings containing 5% *w*/*w* of uncomplexed AEDTA and to the spectra of Incralac®. For clarity, only part of the FTIR spectra is shown.

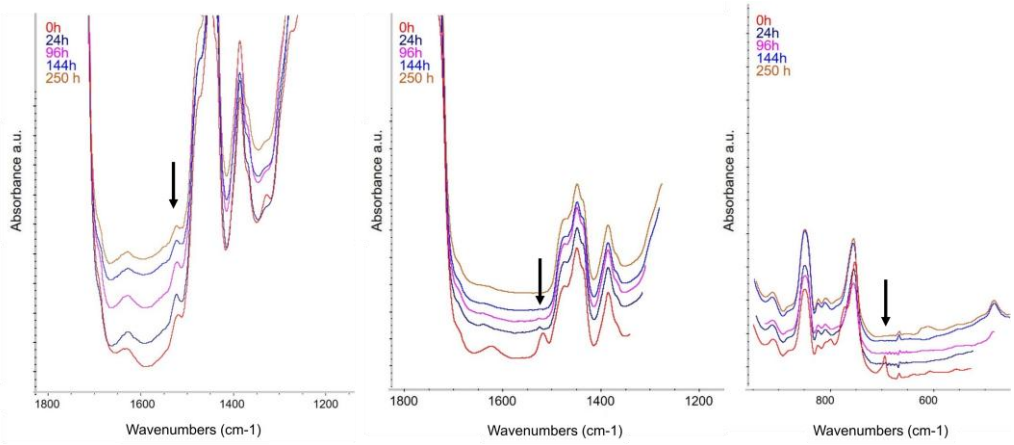

Figure 8. FTIR monitoring during aging at 80 °C: acrylic coating with 2% w/w of complexed AEDTA (left); acrylic coating with 5% w/w of uncomplexed AEDTA (centre), and Incralac® (right).

In the coating with the complex, the characteristic peak of AEDTA at 1636 cm−1 remained visible throughout the monitoring period, whereas in the coating with uncomplexed AEDTA, the same peak diminished rapidly and disappeared entirely after 100 h of aging. Similarly, in Incralac®, the characteristic BTA peak at 740 cm^{-1}, attributed to the CH stretching vibration of the aromatic ring [30], decreased in intensity shortly after aging began. This demonstrates that including AEDTA in methyl-β-cyclodextrin significantly extends the inhibitor retention within the coating. Further confirmation of the improved coating performance was provided by TD-GC/MS and SPME-GC/MS analyses.

SPME-GC/MS results are shown in Figure 9. Acrylic coatings treated with AEDTA released the inhibitor over time: in the headspace analysis of the unaged coating, AEDTA was clearly detected (Figure 9a), while the analysis of the coating thermally aged for 72 h did not show any AEDTA peak, which means that the inhibitor had left the coating (Figure 9b). In contrast, the chromatogram of the coating containing the methyl-β-cyclodextrin/AEDTA complex (Figure 1A and 2A- addendum) revealed no AEDTA peaks at either time zero or after 72 h of

thermal aging. This result suggests that complexation prolongs the retention of AEDTA within the coating.

The presence or absence of the inhibitor in the coatings was double-checked by TD-GC/MS analysis at 250 °C (Figure 10). In coatings with uncomplexed AEDTA aged for 72 h, no AEDTA peak was observed, confirming that the corrosion inhibitor went away. On the contrary, the coating containing the methyl-β-cyclodextrin/AEDTA complex showed the peak of the corrosion inhibitor, providing clear evidence that complexation improves the permanence of the corrosion inhibitor in the coating. Based on these results, the use of cyclodextrins as nanocontainers for corrosion inhibitors offers a highly effective and promising approach for developing long-lasting anti-corrosion coatings suitable for protecting outdoor bronze artworks.

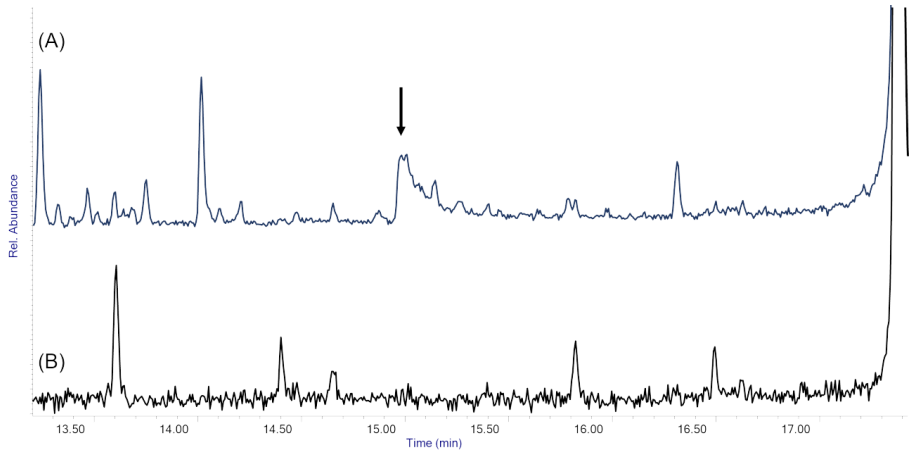

Figure 9. Detail of SPME-GC/MS curves obtained from acrylic coatings treated with uncomplexed AEDTA: (a) unaged coating, (b) coating aged 72 h at 80 °C. The arrow highlights the AEDTA peak.

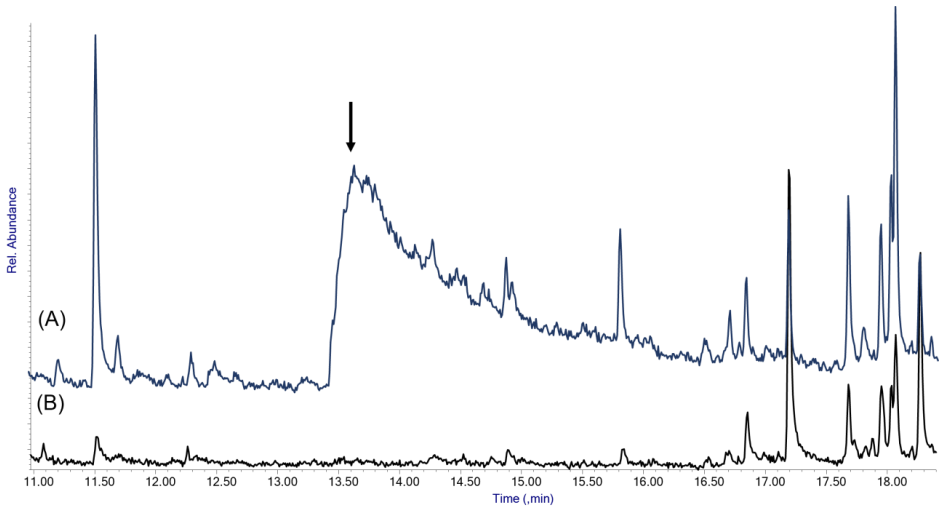

Figure 10. Detail of the TD-GC/MS analysis of acrylic coatings aged 72 h at 80 °C and treated with the methyl-β-cyclodextrin/AEDTA complex (a) and with uncomplexed AEDTA (b). The arrow highlights the AEDTA peak in the coating containing the inclusion complex.

7.5 Conclusions

A comprehensive study of the methyl-β-cyclodextrin /AEDTA complex was carried out to evaluate its potential as a corrosion inhibitor for bronze. The results demonstrated the formation of an inclusion complex with a 1:1 stoichiometry, in which AEDTA interacted with the internal cavity of the cyclodextrin through the NH_2 side group. The toroidal structure of the cyclodextrin and its size compatibility with AEDTA facilitated this process. Reasonably, the primary driving force in the formation of the complex was the displacement of high-enthalpy water molecules from the cyclodextrin cavity as the less polar guest molecule entered.

The efficacy of the complex in extending the retention of the corrosion inhibitor within the protective acrylic coatings was evaluated by thermally aging the coatings at 80 °C and monitoring the release of AEDTA in both uncomplexed and complexed forms. These results were also compared to the commercial product Incralac®, which contains BTA as a corrosion inhibitor.

The research herein reported demonstrates that methyl-β-cyclodextrin/AEDTA complexes might be promising candidates for the development of novel coatings with enhanced stability, prolonged retention of AEDTA, and other valuable properties such as cost-effectiveness, environmental compatibility, and ease of

handling. Further investigation into the anticorrosive properties of these protective coatings is currently underway.

7.6 References

1. Salvadori, B.; Cagnini, A.; Galeotti, M.; Porcinai, S.; Goidanich, S.; Vicenzo, A.; Celi, C.; Frediani, P.; Rosi, L.; Frediani, M. Traditional and Innovative Protective Coatings for Outdoor Bronze: Application and Performance Comparison. J. Appl. Polym. Sci. 2018, 135, 46011. DOI: https://doi.org/10.1002/app.46011

2. Letardi, P. Testing New Coatings for Outdoor Bronze Monuments: A Methodological Overview. Coatings 2021, 11, 131. DOI: https://doi.org/10.3390/coatings11020131

3. Sherif, E.M.; Park, S.-M. 2-Amino-5-ethyl-1,3,4-thiadiazole as a corrosion inhibitor for copper in 3.0% NaCl solutions. Corros. Sci. 2006, 48, 4065–4079. DOI: https://doi.org/10.1016/j.corsci.2006.03.011

4. Casaletto, M.P.; Cirrincione, C.; Privitera, A.; Basilissi, V. A Sustainable Approach to the Conservation of Bronze Artworks by Smart Nanostructured Coatings. In Proceeding of the Interim Meeting of the ICOM.CC Metal Working Group, New Delhi, India, 26–30 September 2016.

5. Pellis, G.; Giussani, B.; Letardi, P.; Poli, T.; Rizzi, P.; Salvadori, B.; Sansonetti, A.; Scalarone, D. Improvement in the Sustainability and Stability of Acrylic Protective Coatings for Outdoor Bronze Artworks. Polym. Degrad. Stab. 2023, 218, 110575. DOI: https://doi.org/10.1016/j.polymdegradstab.2023.110575

6. Del Valle, E.M.M. Cyclodextrins and Their Uses: A Review. Process Biochem. 2004, 39, 1033–1046. DOI: https://doi.org/10.1016/S0032-9592(03)00258-9

7. Figueiras, A.; Sarraguça, J.M.G.; Carvalho, R.A.; Pais, A.A.C.C.; Veiga, F.J.B. Interaction of Omeprazole with a Methylated Derivative of β-Cyclodextrin: Phase Solubility, NMR Spectroscopy and Molecular Simulation. Pharm. Res. 2007, 24, 377–389. DOI: https://doi.org/10.1007/s11095-006-9161-8

8. Matencio, A.; Hoti, G.; Monfared, Y.K.; Rezayat, A.; Pedrazzo, A.R.; Caldera, F.; Trotta, F. Cyclodextrin Monomers and Polymers for Drug Activity Enhancement. Polymers 2021, 13, 1684. DOI: https://doi.org/10.3390/polym13111684

9. Berdimurodov, E.; Eliboyev, I.; Berdimuradov, K.; Kholikov, A.; Akbarov, K.; Dagdag, O.; Rbaa, M.; El Ibrahimi, B.; Verma, D.K.; Haldhar, R.; et al. Green β-Cyclodextrin-Based Corrosion Inhibitors: Recent Developments, Innovations and Future Opportunities. Carbohydr. Polym. 2022, 292, 119719. DOI: https://doi.org/10.1016/j.carbpol.2022.119719

10. Nawaz, M.; Ahmad, S.; Taryba, M.G.; Montemor, M.F.; Kahraman, R.; Shakoor, R.A. Improvement in Inhibition Performance of Anti-Corrosion Coatings Using Polyolefin Matrix Embedded with Modified TiO2 Nanoparticles. Prog. Org. Coat. 2024, 195, 108659. DOI: https://doi.org/10.1016/j.carbpol.2022.119719

11. Montemor, M.F. Functional and Smart Coatings for Corrosion Protection: A Review of Recent Advances. Surf. Coat. Technol. 2014, 258, 17–37. DOI: https://doi.org/10.1016/j.surfcoat.2014.06.031

12. Monticelli, C.; Fantin, G.; Di Carmine, G.; Zanotto, F.; Balbo, A. Inclusion of 5-Mercapto-1-Phenyl-Tetrazole into β-Cyclodextrin for Entrapment in Silane Coatings: An Improvement in Bronze Corrosion Protection. Coatings 2019, 9, 508. DOI: https://doi.org/10.3390/coatings9080508

13. de Souza, T.M.; Cordeiro, R.F.B.; Viana, G.M.; Aguiar, L.C.S.; de Senna, L.F.; Malta, L.F.B.; D'Elia, E. Inclusion Compounds of Dibenzylthiourea with Hydroxypropylated-Cyclodextrins for Corrosion Protection of Carbon Steel in Acidic Medium. J. Mol. Struct. 2016, 1125, 331–339. DOI:https://doi.org/10.1016/j.molstruc.2016.06.072

14. Khramov, A.N.; Voevodin, N.N.; Balbyshev, V.N.; Donley, M.S. Hybrid Organo-Ceramic Corrosion Protection Coatings with Encapsulated Organic Corrosion Inhibitors. Thin Solid. Film. 2004, 447–448, 549–557. DOI: https://doi.org/10.1016/j.tsf.2003.07.016

15. Khramov, A.N.; Voevodin, N.N.; Balbyshev, V.N.; Mantz, R.A. Sol-Gel-Derived Corrosion-Protective Coatings with Controllable Release of Incorporated Organic Corrosion Inhibitors. Thin Solid. Film. 2005, 483, 191–196. DOI: https://doi.org/10.1016/j.tsf.2004.12.021

16. Amiri, S.; Rahimi, A. Anticorrosion Behavior of Cyclodextrins/Inhibitor Nanocapsule-Based Self-Healing Coatings. J. Coat. Technol. Res. 2016, 13, 1095–1102. DOI: https://doi.org/10.1007/s11998-016-9824-2

17. Altin, A.; Rohwerder, M.; Erbe, A. Cyclodextrins as Carriers for Organic Corrosion Inhibitors in Organic Coatings. J. Electrochem. Soc. 2017, 164, C128–C134. DOI: 10.1149/2.0481704jes

18. Zou, C.J.; Tang, Q.W.; Zhao, P.W.; Guan, E.D.; Wu, X.; Ye, H. Further Study on the Inclusion Complex of 2-Phosphonobutane-1,2,4-Tricarboxylic Acid with B-Cyclodextrin: A New Insight of High Inhibition Efficiency for Protecting Steel Corrosion. J. Pet. Sci. Eng. 2013, 103, 29–35. DOI: https://doi.org/10.1016/j.petrol.2013.02.013

19. Fan, B.; Hao, H.; Yang, B.; Li, Y. Insights into the Inhibition Mechanism of a Novel Supramolecular Complex towards the Corrosion of Mild Steel in the Condensate Water: Experimental and Theoretical Studies. Res. Chem. Intermed. 2018, 44, 5711–5736. DOI: https://doi.org/10.1007/s11164-018-3451-8

20. Zoppi, A.; Delrivo, A.; Aiassa, V.; Longhi, M.R. Binding of Sulfamethazine to β-Cyclodextrin and Methyl-β-Cyclodextrin. AAPS PharmSciTech 2013, 14, 727–735. DOI: https://doi.org/10.1208/s12249-013-9958-9

21. Wang, X.; Luo, Z.; Xiao, Z. Preparation, Characterization, and Thermal Stability of β-Cyclodextrin/Soybean Lecithin Inclusion Complex. Carbohydr. Polym. 2014, 101, 1027–1032. DOI: https://doi.org/10.1016/j.carbpol.2013.10.042

22. Shaaban, I.A.; Hassan, A.E.; Abuelela, A.M.; Zoghaieb, W.M.; Mohamed, T.A. Infrared, Raman and NMR Spectral Analysis, Vibrational Assignments, Normal Coordinate Analysis, and Quantum Mechanical Calculations of 2-Amino-5-Ethyl-1,3,4-Thiadiazole. J. Mol. Struct. 2016, 1103, 70–81. DOI: https://doi.org/10.1016/j.molstruc.2015.09.007

23. Ribeiro, A.; Figueiras, A.; Santos, D.; Veiga, F. Preparation and Solid-State Characterization of Inclusion Complexes Formed between Miconazole and Methyl-β-Cyclodextrin. AAPS PharmSciTech 2008, 9, 1102–1109. DOI: https://doi.org/10.1208/s12249-008-9143-8

24. Naidu, N.B.; Chowdary, K.P.R.; Murthy, K.V.R.; Satyanarayana, V.; Hayman, A.R.; Becket, G. Physicochemical Characterization and Dissolution Properties of Meloxicam–Cyclodextrin Binary Systems. J. Pharm. Biomed. Anal. 2004, 35, 75–86. DOI: https://doi.org/10.1016/j.jpba.2004.01.003

25. Eid, E.E.M.; Abdul, A.B.; Suliman, F.E.O.; Sukari, M.A.; Rasedee, A.; Fatah, S.S. Characterization of the Inclusion Complex of Zerumbone with Hydroxypropyl-β-Cyclodextrin. Carbohydr. Polym. 2011, 83, 1707–1714. DOI: https://doi.org/10.1016/j.carbpol.2010.10.033

26. Delrivo, A.; Zoppi, A.; Longhi, M.R. Interaction of Sulfadiazine with Cyclodextrins in Aqueous Solution and Solid State. Carbohydr. Polym. 2012, 87, 1980–1988. DOI: https://doi.org/10.1016/j.carbpol.2011.10.025

27. Job, P. Formation and Stability of Inorganic Complexes in Solution. Ann. Chim 1928, 9, 113–134.

28. Ganza-Gonzalez, A.; Vila-Jato, J.L.; Anguiano-Igea, S.; Otero-Espinar, F.J.; Blanco-Mkndez, J. A Proton Nuclear Magnetic Resonance Study of the Inclusion Complex of Naproxen with P-Cyclodextrin. Int. J. Pharm. 1994, 106, 179–185. DOI: https://doi.org/10.1016/0378-5173(94)90001-9

29. Floare, C.G.; Bogdan, M.; Tomoaia-Cotişel, M.; Mocanu, A. 1H NMR Spectroscopic Characterization of Inclusion Complex of Desferrioxamine B Chelator and β-Cyclodextrin. J. Mol. Struct. 2022, 1248, 131477. DOI https://doi.org/10.1016/j.molstruc.2021.131477

30. Zou, C.; Liu, Y.; Yan, X.; Qin, Y.; Wang, M.; Zhou, L. Synthesis of Bridged β-Cyclodextrin–Polyethylene Glycol and Evaluation of Its Inhibition Performance in Oilfield Wastewater. Mater. Chem. Phys. 2014, 147, 521–527. DOI: https://doi.org/10.1016/j.matchemphys.2014.05.025

Addendum

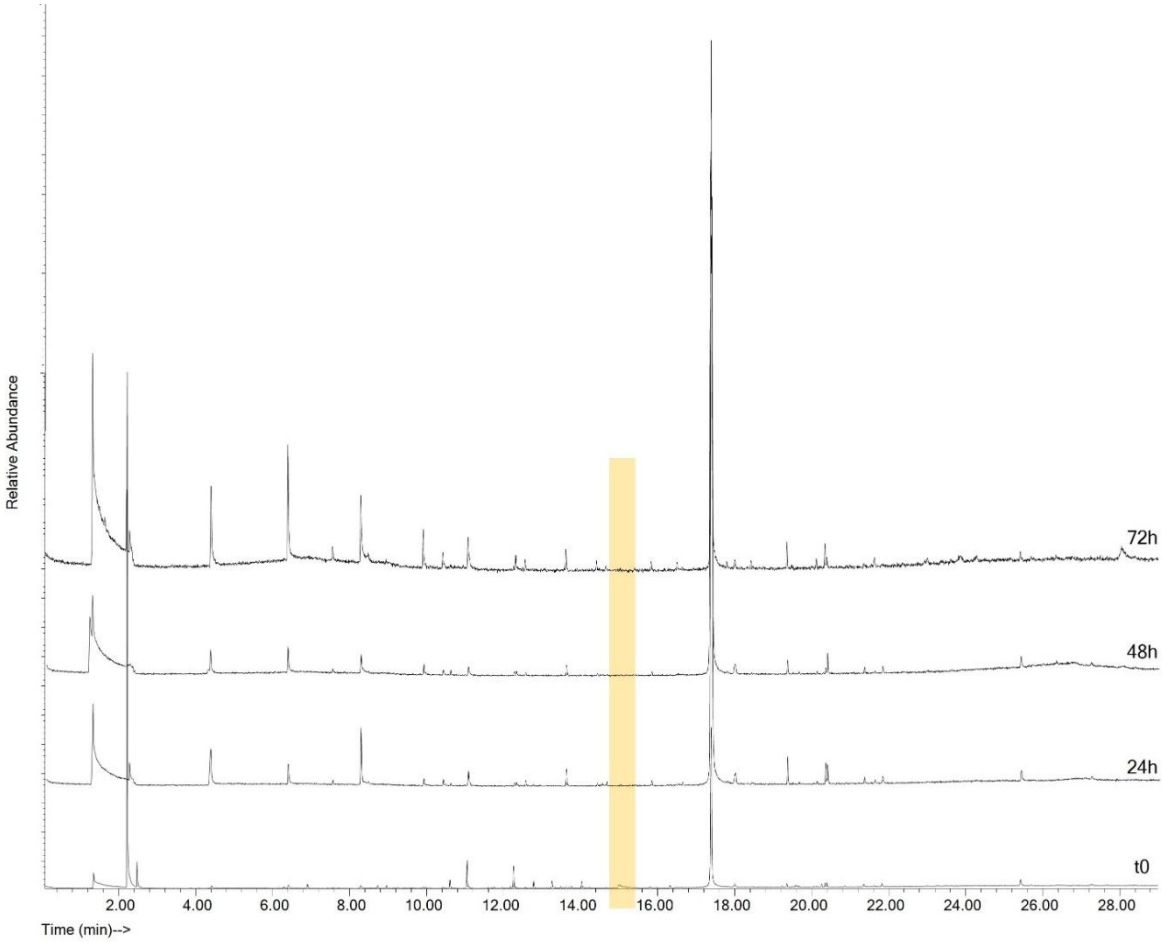

Figure 1A: SPME-GC/MS curves obtained from acrylic coatings treated with uncomplexed AEDTA from 0 hours of ageing until 72 hours of ageing

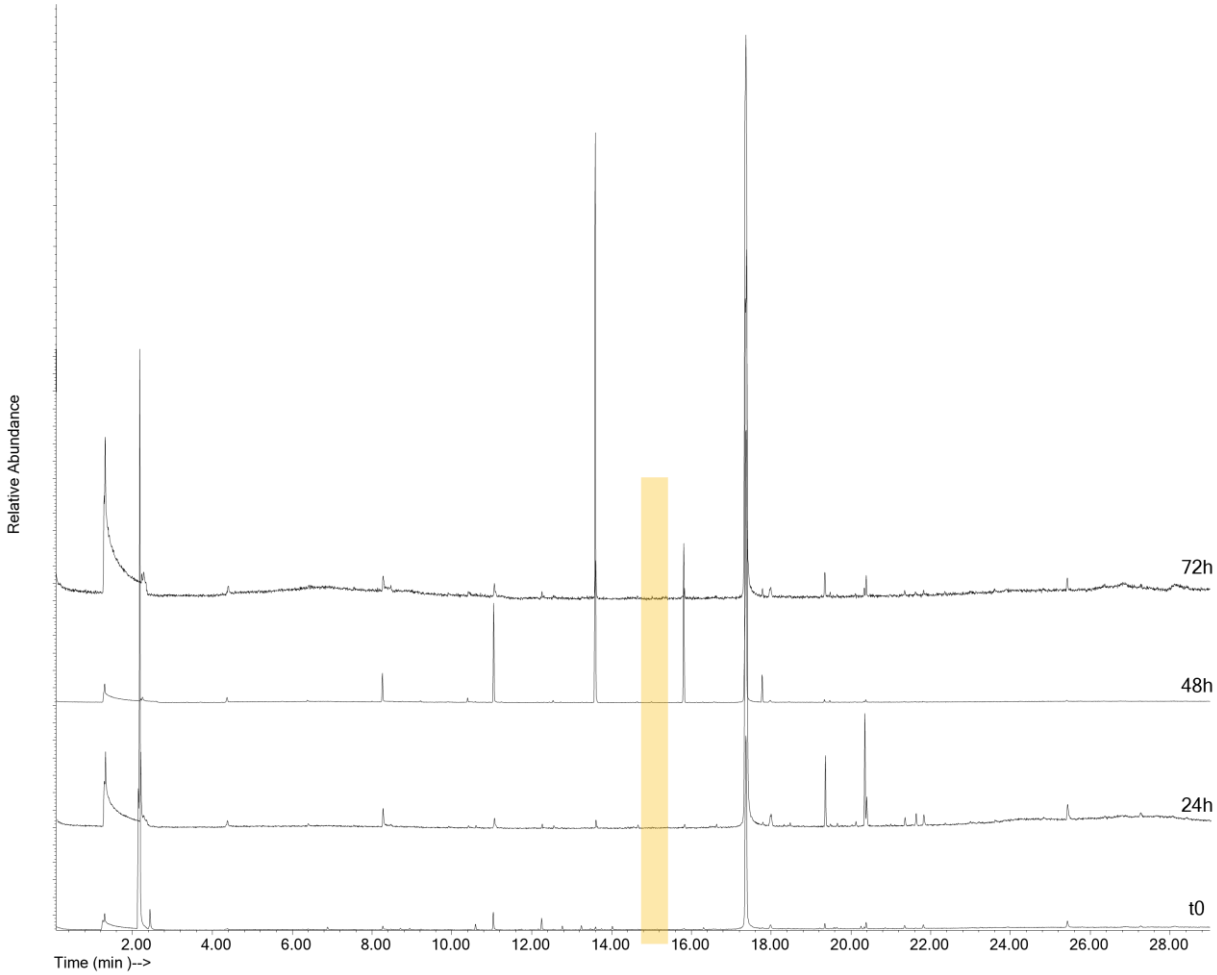

Figure 2A: SPME-GC/MS curves obtained from acrylic coatings treated with complexed AEDTA from 0 hours of ageing until 72 hours of ageing

Figure 2A clearly shows that no peaks corresponding to AEDTA are detected in the coatings with the methyl-β-cyclodextrin/AEDTA complex in any chromatogram, indicating that the methyl-β-cyclodextrin effectively retains AEDTA. In contrast, Figure 1A illustrates that for the uncomplexed AEDTA coatings, the peak of the corrosion inhibitor appears at both time zero and after 24 hours, indicating the leaching of AEDTA from the coating.

Chapter 8

Optimizing application methods of sustainable acrylic protective coatings of outdoor patinated bronze artworks-draft

8.1 Abstract

The research of more effective and sustainable coatings for the conservation of metallic heritage turned out to be a complex topic, where standardised practice to address the specific requirements to fulfil conservation and restoration criteria along with the complex corrosion issue represented by the bronze/patina/outdoor environment are still an open problem.

Recently, more sustainable coatings based on Paraloid® B44 with a light stabilizer and a corrosion inhibitor with a low toxicity profile have been optimised. Their physical-chemical properties were determined through a multi-analytical characterization and by monitoring changes occurring during light ageing. This resulted in acrylic coatings containing 5% w/w of corrosion inhibitor, namely 5-mercapto-1-pheniltetrazole (MPT) or 2-amino-5-ethyl-1,3,4-thiadiazol- (AEDTA), and Tinuvin® 312 as light stabilizer. The effectiveness of a coating is then affected by the application method in connection to the underlying surface properties. In this work the role of Paraloid® concentration in a two layer brush application method is addressed on quaternary bronze with *Verde Messina* foundry patina. The brush application method was chosen because it is widely adopted in conservation practices and the protective efficacy of two-layer coatings obtained by applying a 10% w/w Paraloid® solution twice was compared to the one of a first layer with Paraloid® at 5% w/w and the second at 10% w/w. Patinated bronze mock-ups were non-destructively characterized before and after treatment by Electrochemical Impedance Spectroscopy (EIS) to assess the corrosion resistance, colourimetry to

evaluate visual appearance, Eddy Current to measure the patina and coating thickness, and Fourier Transform Infrared Spectroscopy in external reflectance mode (ER-FTIR) to analyse molecular composition. After the artificial wet-dry ageing of treated mock-ups, ER-FTIR and colorimetry were used to assess treatment stability. Principal Component Analysis (PCA) on ER-FTIR spectra was used better to highlight differences in coatings over the ageing process. Results showed that all the tested treatments increased the corrosion resistance of *Verde Messina* patinated bronze and remained stable after 360h of artificial ageing; double-layer coatings with a more diluted first layer resulted in the preferable treatment as they provide comparable performance while using a smaller amount of Paraloid®.

8.2 Introduction

Outdoor metallic objects are continuously exposed to natural and anthropogenic degradation agents, which can damage their appearance and stability. These objects develop a layer of corrosion products that is referred to as patina. Its composition depends on the morphology of the surfaces, their roughness, the bronze composition and exposure conditions [1,2]. Patina holds aesthetic and historical value; however, it can contribute to further deterioration in polluted environments, necessitating protective treatments that preserve the underlying metal and the patina itself. Conservation practices prioritise minimally invasive methods to keep the original appearance of such artefacts [3]. The most commonly used conservation methods are coatings, which prevent the metal-patina layer from coming into contact with the active corrosion agents in the environment [4]. Nowadays, the most widely exploited protective treatments are polymer coatings and waxes, which may include corrosion inhibitors like benzotriazole (BTA). Despite its effectiveness, BTA poses concerns due to its suspect toxicity and limited permanence on treated surfaces, raising potential health risks for operators and visitors while impacting environmental safety [5,6].

To overcome this, the actual conservation perspective in recent decades focuses on eco-friendly and low-toxicity alternatives, such as organosilanes, carboxylates, or fluoropolymers [7]. Alternative solutions to reduce the toxicity of BTA have been suggested, including encapsulating it in nanocarriers made from halloysite or β-cyclodextrins. Both materials are naturally sourced, biocompatible, low-cost, and environmentally friendly, and they have shown promising results [8,9].

When designing new protective coatings, researchers must consider that, when dealing with heritage objects, they must meet stringent criteria, including transparency, long-term effectiveness, reversibility, and compatibility with existing patinas [4,10]. The development and evaluation of these protective coatings face significant challenges, primarily due to the lack of standardized testing methods for heritage surfaces. It is essential to consider that coatings behave differently depending on whether they are applied to bare metals, patinated surfaces, or corroded layers [11]. Therefore, reliable testing requires coupons that accurately replicate the surface characteristics of heritage objects. Traditional polished copper coupons are increasingly being replaced by those featuring alloys, natural patinas, or artificially patinated surfaces to better mimic real-world conditions [12]. Parameters such as coating thickness, number of coating layers, solvent properties, and drying time significantly influence the performance of protective systems and the reproducibility of results [10]. Proper coupon preparation and controlled application methodologies ensure meaningful comparisons across studies. Moreover, laboratory investigations must include multi-analytical methods to comprehensively characterise coatings, considering the surface composition, application techniques, and ageing tests [12].

This paper examines four application methods of newly formulated Paraloid® B44 coatings that are combined with non-toxic corrosion inhibitors and a light stabilizer [13]. The study evaluates the protective effectiveness and visual impact of various coatings on patinated bronze mock-ups. It considers factors such as the number of layers and the concentration of Paraloid® B44, as well as the effects of artificial aging. The goal is to identify the best option for protecting the bronze patinated mock-ups during natural ageing.

The coatings were composed of 5% w/w of corrosion inhibitor, namely 5-mercapto-1-pheniltetrazole (MPT) and 2-amino-5-ethyl-1,3,4-thiadiazol-(AEDTA), and Tinuvin® 312 as light stabilizer. To investigate the possible role of Paraloid® B44 concentration in the solution, a test was performed to compare the covering capability of two layers of coating with 10% w/w Paraloid each with that of a layer at 5% w/w followed by one at 10% w/w. Whatever the concentration of Paraloid® B44 in solution, the concentration of corrosion inhibitors was kept constant. The brush application method was chosen because it is widely adopted in conservation practices. The formulations were applied in two crisscrossed layers one week apart. Analytical techniques, including electrochemical impedance spectroscopy (EIS), colourimetry, and Eddy Current measurements, assessed the coating protective properties, visual appearance, and layer thickness. Before

exposing the coatings to weathering, a thermohygrometric artificial ageing was conducted to verify the results obtained right after the application.

8.3 Materials and Methods

8.3.1 Substrate

Mock-ups were prepared by an artistic foundry in Milan (*Fonderia Artistica Battaglia*). The specimens consist of quaternary bronze with a composition of 88.3% Cu, 5.7% Sn, 1.6% Pb, and 3.9% Zn, and have approximate dimensions of 5 cm x 5 cm. The artistic patina *Verde Messina* (Table 1) was selected based on conservators' recommendations. The patina process involves the use of ammonium sulphide as a base layer, followed by copper nitrate, and effectively replicates a highly reactive surface [14].

Table 1: Procedure for the realisation of Verde Messina patina [2]

Chemicals	Temperature	Procedure
Copper Nitrate in water	70-130°C	The metallic substrate was heated, and the solution was applied with a brush until the desired green shade was achieved. The surface was dried without letting it cool down.
Ammonium Sulphide 5% in water	30-60°C	Some drops of solutions were applied on the substrate by brush, maintaining it slightly hot. This procedure was repeated a few times to achieve a pale shade. Then, it was dried at room temperature.

8.3.2 Coatings

The coatings prepared and analysed in this research were based on Paraloid® B44 (ethyl acrylate/methyl methacrylate copolymer), purchased from Sinopia s.a.s. The corrosion inhibitor 5-mercapto-1-pheniltetrazole (MPT) was purchased from Alfa Aesar and 2-amino-5-ethyl-1,3,4-thiadiazol- (AEDTA) from Sigma Aldrich. Tinuvin® 312 (ethandiamide N'-(2-ethoxyphenyl)-N-(2-ethylphenyl)oxamide) was obtained from BASF. The solvent used to solubilize the various components and prepare the coatings was 1-methoxypropan-2-ol purchased from Sigma Aldrich.

The coatings were formulated according to the recipe reported in previous work[13] :

- 0.5% w/w AEDTA (2-amino-5-ethyl-1,3,4-thiadiazole), 0.3% w/w Tinuvin 312, 10% w/w Paraloid® B44 in 1-methoxypropan-2-ol;
- 0.5% w/w AEDTA, 0.3% w/w Tinuvin® 312, 5% w/w Paraloid® B44 in 1-methoxypropan-2-ol;
- 0.5% w/w MPT (5-mercapto-1-phnyltetrazole), 0.3% w/w Tinuvin® 312, 10% w/w Paraloid® B44 in 1-methoxypropan-2-ol;
- 0.5% w/w MPT, 0.3% w/w Tinuvin 312, 10% w/w Paraloid ® B44 in 1-methoxypropan-2-ol.

The solutions were prepared by adding the various components in a vial in the following order: acrylic resin, additives, and finally, the solvent. They were stirred for 24 hours until complete solubilisation and were applied by brush in crisscrossed layers on bronze patinated coupons. Table 2 illustrates the four types of application methods. Depending on the coating application method, 4 groups of coupons were prepared, each comprising 4 replicates, for a total of 16 coated coupons.

Table 2: Coating application methods

Coating	**Application**
5% w/w AEDTA, 0,3% w/w Tinuvin® 312 and 10% w/w Paraloid ®B44	TA10 = by brush, two crisscrossed layers one week apart
5% w/w AEDTA, 0,3% w/w Tinuvin® 312 and 5% w/w Paraloid® B44 AND 5% w/w AEDTA, 0,3% w/w Tinuvin® 312 and 10% w/w Paraloid® B44	TA5 = by brush, two crisscrossed layers one week apart (first the 5% w/w Paraloid® solution, then the 10% w/w one)
5% w/w MPT, 0,3% w/w Tinuvin® 312 and 10% w/w Paraloid® B44	MPT10 = by brush, two crisscrossed layers one week apart
5% w/w MPT, 0,3% w/w Tinuvin® 312 and 5% w/w Paraloid® B44 AND 5% w/w MPT, 0,3% w/w Tinuvin® 312 and 10% w/w Paraloid® B44	MPT5 = by brush, two crisscrossed layers one week apart (first the 5% w/w Paraloid® solution, then the 10% w/w one)

Each layer was left to dry in a ventilated environment (24.6 ± 3 °C and 38.2 ± 5% RH) for 1 week before applying the next layer.

8.3.3 Characterisation techniques

8.3.3.1 Electrochemical Impedance Spectroscopy (EIS)

The corrosion behaviour of both patinated and coated coupons were evaluated by electrochemical impedance spectroscopy (EIS) using the G-PE cell developed for electrochemical analysis in metallic heritage[4]. An AISI 316 stainless steel wire (1.5 mm thick) and AISI 316 stainless steel mesh were used as pseudo reference and counter electrode, respectively. The gel inside the cell is composed of 2% of agarose in an electrolyte solution that simulates rain according to the study of Timoncini et al. [5]

The measurement was performed with a Gamry Reference 600 potentiostat in five steps: 1) OCP (open Circuit Potential) measurement for 30 min, to let the system to stabilise 2) linear polarization resistance (LPR)measurement from -10 mV to 10 mV around E_{oc} with a scan rate of 0.1667 mV/sec; 3) OCP measurement for 16 min; 4) EIS measurement from 100 kHz to 10 mHz with V_{rms}=10 mV and 10 points/decade; 5) OCP measurement for 5 min. The mock up area exposed to the electrolyte was 3.14 cm^2. The experimental data were represented as Bode plots (i.e. the impedance modulus $|Z|$, phase shift Φ vs. frequency) and Nyquist plots (the real part of impedance Z_{re} (Ω cm^2) vs the imaginary part Z_i (Ω cm^2) were used to quickly assess similarities and differences among the spectra measured on different coupons.

8.3.3.2 Eddy Current measurements

Thickness measurements of the bare and coated patina were carried out with an Elcometer 456, using a probe for nonferrous materials based on electromagnetic induction. The manufacturer reports a ± 2.5 μm precision in measurement for this probe. A 12.3-micron gauge (Ser. N. KC8913) was used for calibration. Measurements of the coated patinas were taken one week after the application of both the first and second coating layers.

8.3.3.3 Colorimetric measurements

Colorimetric data were acquired using the portable spectrophotometer CM-700d Konica Minolta, in reflectance mode, with the specular component included (SCI) and excluded (SCE), using a measurement area (MAV) of 8 mm diameter, a measurement range of 360–700 nm, under D65 illuminant and a 10° observer. After calibrating the instrument on both white and black standards, colorimetric parameters L*, a*, and b* were measured for each sample at three points arranged on the diagonal of the coupon and identified by a specific mask.

8.3.3.4 Fourier-Transformed Infrared Spectroscopy

The Bruker Alpha II spectrometer operating in external reflection mode was used, collecting 128 scans with a resolution of 4 cm^{-1} in the range from 7500 cm^{-1} to 375 cm^{-1}. Spot size was 5 mm in diameter.

8.3.4 Artificial ageing

The coupons were placed in an Angelantoni Challenge 500 climate chamber to simulate an accelerated thermo-hygrometric aging process using wet/dry cycles, with temperature and relative humidity settings configured as indicated in Table 3.

Table 3: Conditions applied for each thermo-hygrometric cycle. Heating/cooling rate: 1 °C/min.

Temperature (C°)	**Relative Humidity (%)**	**Time (min)**
15	85	60
30	60	60
60	30	60
30	60	60

Each thermo-hygrometric cycle lasts approximately 6 hours, allowing for 4 cycles to be completed per day. After 60 cycles (15 days), the coupons were removed from the climate chamber and subjected to a series of inspections to assess

the presence of any chromatic, morphological, and/or compositional variations in the patinas and coatings.

8.3.5 Principal Component Analysis (PCA)

Data treatment was carried out using Matlab2012b PCA toolbox.

PCA was used to choose the best application method, employing FTIR data. The studied range was 1450-5500 cm^{-1}. Baseline (WLS), Smoothing (0 order, 19 pt window, tails weighted), SNV and Mean Center pretreatments were applied to this dataset. The explained variance was PC1 = 60.58% PC2 = 15.73% and PC3 = 10.44%.

8.4 Results and discussion

First of all, the surface properties of the 24 patinated mock-ups available for treatment application testing were characterised. Figure 2a shows Bode and Nyquist plots for the EIS measurements on each coupon. Without going into the detail of each curve, the pretty large variability on EIS spectra reflects the wide distribution of patina thickness and the uneven presence of pores, which characterise this foundry patinated mock-ups. These curves offer insights into the various patina behaviours; shape similarities can be associated with comparable patina morphologies. EIS spectra were thus used to identify and exclude the mock-ups with too much peculiar behaviour, as they would be unsuitable for application method effectiveness comparison (Figure 2 red plots). The remaining ones were roughly grouped according to shape and range (Figure 2b, green plots)

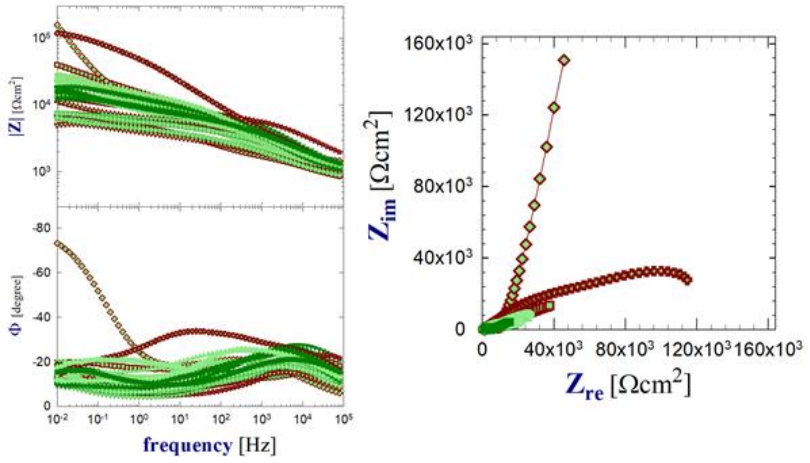

a)

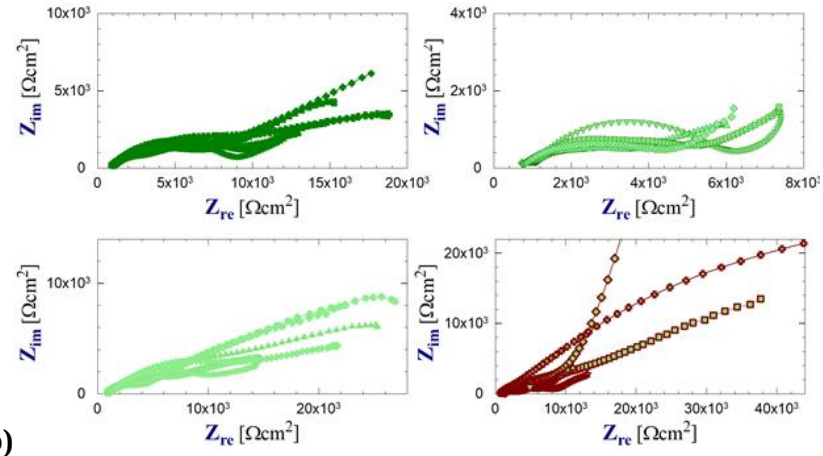

Figure 2: EIS spectra on the 24 mock-ups with verde messina patina a) Bode and Nyquist plots; b) details of Nyquist plot for groups of similar spectra; the last one (red lines) groups the more peculiar spectra

They were evenly distributed into four equivalent sets in a way that they were all characterised by almost the same average thickness, colour and polarisation resistance values of the measured parameters (Table 4). Although triplicate coupons are typically used in Corrosion Science, we assigned four coupons to each set to better cope with the large surface properties variability of these patinated mock-ups.

Table 4 - Average values measured on the four sets of mock-ups at S0 (bare patina) and after the first layer (S1_I) and the second layer (S1) of the selected treatment. Average values obtained at S0 for all 16 mock-ups considered are also reported.

S0 - Patina						S1_I - Coating first layer					S1 - Coating (double layer)				
thickness	colour				EIS	thickness	colour			EIS	thickness	colour			EIS
59 ± 12	**67 ± 2**		**-19 ± 3**	**1 ± 2**	**18 ± 8**										
S [μm]	L*	a*	b*	<Rp> [KΩ cm^2]	treatment	S [μm]	L*	a*	b*	<Rp> [MΩ cm^2]	S [μm]	L*	a*	b*	<Rp> [MΩ cm^2]
59 ± 13	68 ± 1	-18 ± 2	2 ± 1	21 ± 10	TA10	56 ± 18	62 ± 1	-19 ± 2	3 ± 1	0,8 ± 0,7	60 ± 20	60 ± 1	-20 ± 2	5 ± 1	4 ± 3
59 ± 16	67 ± 2	-20 ± 4	2 ± 3	19 ± 11	TA5	65 ± 15	63 ± 3	-21 ± 5	4 ± 3	0,25 ± 0,09	74 ± 9	60 ± 4	-21 ± 5	6 ± 2	3 ± 2
59 ± 14	67 ± 2	-20 ± 3	0 ± 2	15 ± 6	TM10	57 ± 13	64 ± 2	-21 ± 3	1 ± 2	0,5 ± 0,4	66 ± 17	62 ± 3	-21 ± 3	2 ± 2	2 ± 2
59 ± 6	66 ± 2	-19 ± 1	2 ± 1	17 ± 6	TM5	55 ± 6	63 ± 2	-20 ± 1	3 ± 1	0,4 ± 0,3	64 ± 13	60 ± 2	-19,9 ± 0,5	3 ± 1	0,7 ± 0,2

Each set was then randomly assigned to one of the treatment methods described in Table 2. Colorimetric measurements were used to characterise the visual appearance, which is one of the most important prerequisites for coatings applied

to Cultural Heritage items. The colour changes ΔE* after the application of the first coating layer and after the second one are shown in Figure 3.

All coatings exhibit a colour change after the application of the first layer; however, it is essential to consider that protective treatments inevitably alter the appearance of bronze-patinated surfaces [8]. Additionally, no gloss effect was observed here. Treatments containing AEDTA exhibit a more significant colour change after the application of both the first and second layers compared to those containing MPT. It is worth noting that when using the same corrosion inhibitor, the colour changes are essentially the same, indicating that the concentration of Paraloid® in the formulation does not affect the colour change.

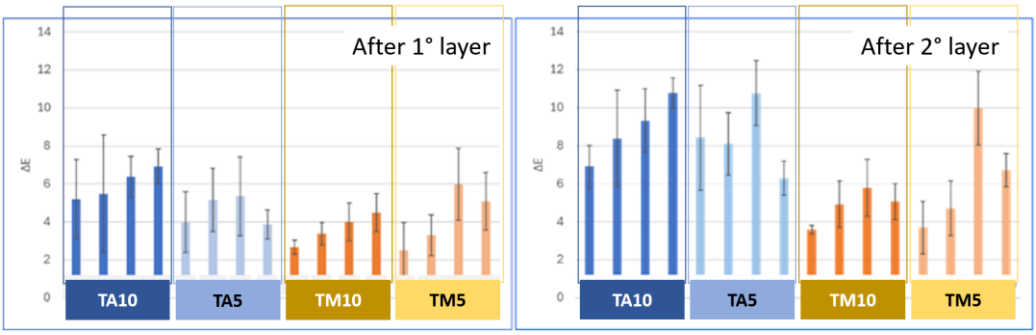

Figure 3: Colour changes after the application of the first coating layer (left) and the second layer (right) on each of the four mock-ups coated with the treatments listed in Table 2.

Table 4 shows the evolution of average colour coordinates from bare patina (S0) to the double layer coating (S1) to further explore which colour coordinate has the most significant impact on the overall colour change. Both after the first and the second layers, AEDTA treatments produce a more noticeable changes in the L* and b* colour coordinates than the MPT ones. This indicates a darkening (reduction of L* coordinate) and a yellowing of the surface (increase of the b* coordinate). This was also visible to the naked eye, with a darkening of the surface. Despite this, colour changes of this magnitude on patinated bronze surfaces are still considered acceptable.

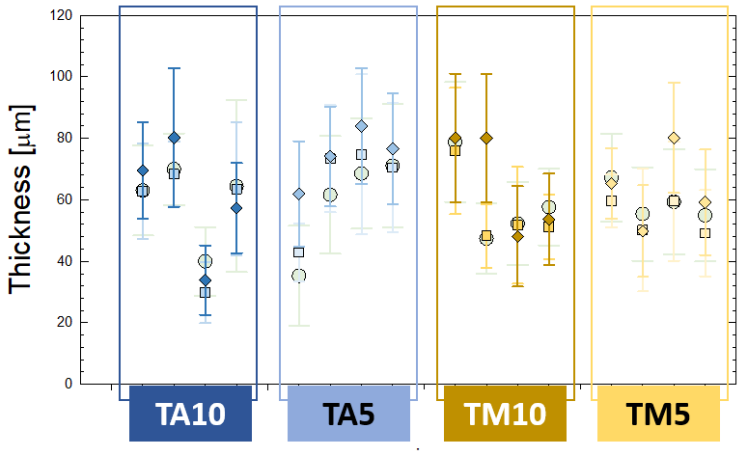

Figure 4: Thickness values measured on bare patina (circle), after the application of the first coating layer (square) and the second layer (diamond) on each of the four mock-ups coated with the treatments listed in Table 2.

The thickness measurements (Figure 4 and Table 4) were used to determine if the Paraloid® concentration of the different formulations could affect the overall thickness. The results show that after the application of the first coating layer (S1_I) the measured thickness is unchanged, or even becomes thinner. The instrument probe might not be suitable for this type of uneven and porous surface, as it led to significant variability in the data due to the high roughness of the surface in relation to the probe area. Nevertheless, this technique could still provide a rough estimate of the patina thickness [9]. As a matter of fact, the average thickness of the second layer (S1) is higher than that of the bare patina, which suggests that the first layer was probably filling the pores. Thickness differences between S0 and S1 ranging from 1 to 6 µm were measured, which is near the detection limit of the instrument. However, the obtained results indicate that all four application methods give coatings with similar thickness, which allows comparison of their corrosion protection by electrochemical analyses.

Table 4 and Figure 5 summarizes Rp average values obtained from LPR and EIS measurements for each coupon on bare patina and after the first and the second coating layer. The mock-ups with bare patina are characterised by a Rp around 18KΩcm^2, which suggests that it does not provide protection to the bronze substrate and highlights the need to develop optimal procedures for the preservation of this kind of surface finish [2]. The coupons treated with AEDTA coatings show two orders of magnitude higher corrosion resistance than bare patina after the second layer is applied, without relevant differences between TA10 and TA5, while the

coupons treated with MPT coatings show a bit lower Rp values thus demonstrating lower protective effectiveness.

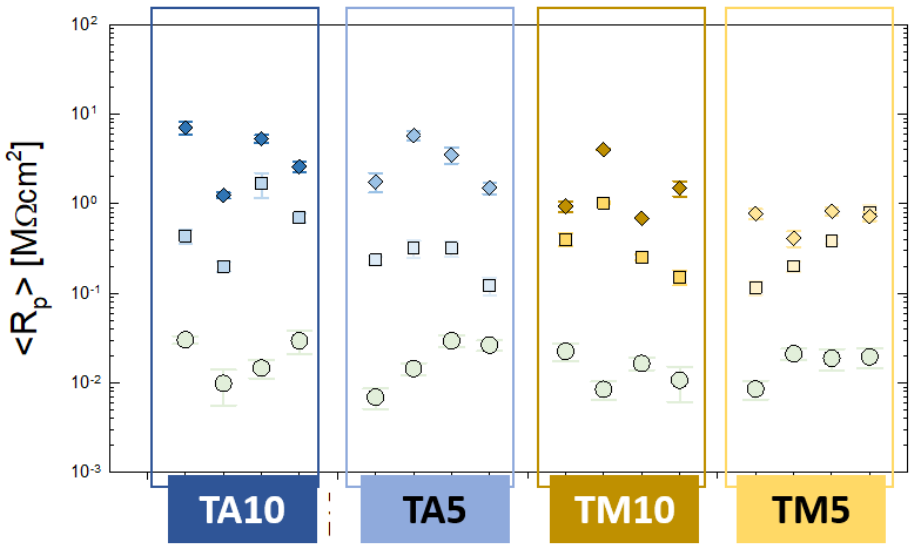

Figure 5: Average polarisation resistance values on bare patina (circle), after the application of the first coating layer (square) and the second layer (diamond) on each of the four mock-ups coated with the treatments listed in Table 2.

Based on these results, AEDTA appears to be a more effective corrosion inhibitor than MPT. It provides superior corrosion protection and, as observed in previous studies [3], it is more stable over time. TA5 seems to be the application method to be preferred, since it gives almost the same corrosion protection using less acrylic resin.

Finally, we decided to examine how the treated coupons respond to changes in temperature and humidity to complement data of light stability of the coatings obtained in previous research [13].

After the thermo-hygrometric ageing, no visible changes were observed. The colour change (ΔE*) before and after the artificial ageing of all coatings is below the threshold of perceptibility for the human eye (ΔE*=3) [11]. Coatings containing AEDTA showed higher ΔE values, mainly due to variations in the b* coordinate. The average ΔE is approximately 2 for TA10 and TA5, while it is about 1 for TM10 and TM5.

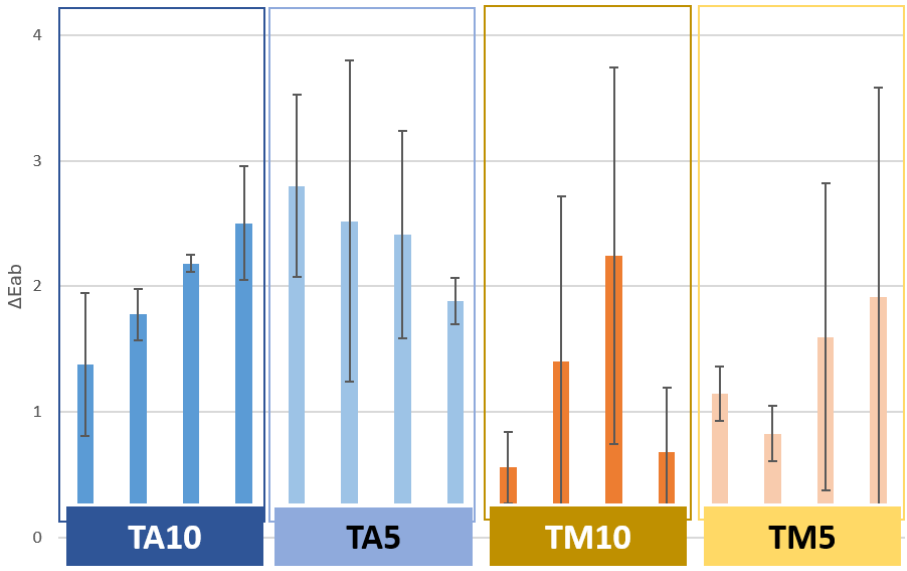

Figure 6: Colour difference after artificial ageing for each coupon

A comparison of the FTIR spectra of all the coated coupons before and after ageing showed no significant differences. This indicates that there are no detectable molecular changes, confirming the stability of all these treatments during the initial hours of wet-dry ageing and proving once again that they could be promising candidates for the protection of outdoor bronze statues. Figure 8 compares the spectra of the unaged coatings (S1) with those after ageing (S2) for each type of coating and application method.

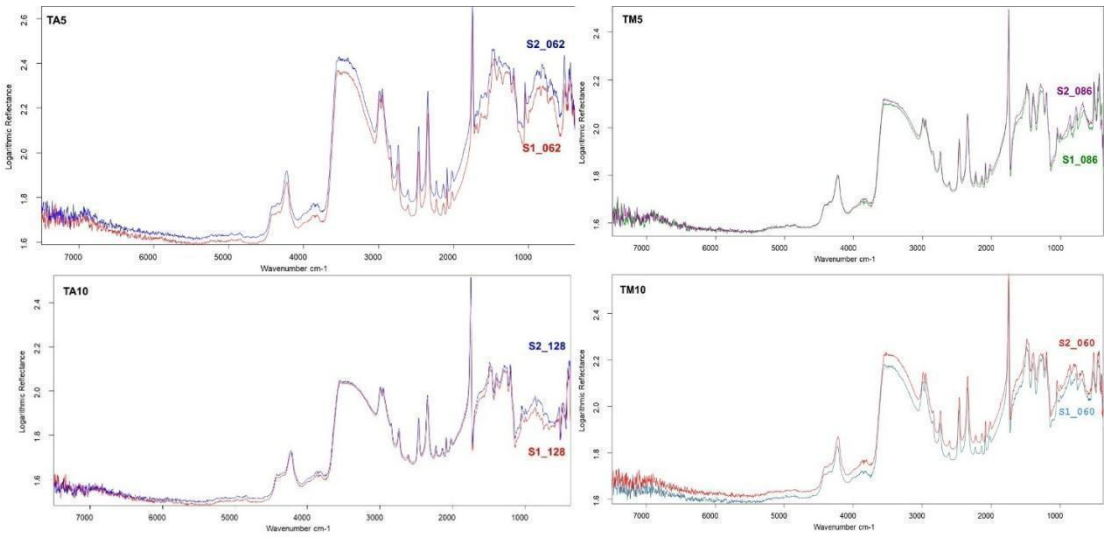

Figure 7: FTIR spectra of unaged (S1) and aged (S2) coated coupons

No significant differences were observed in the qualitative comparison of the FTIR spectra; therefore, Principal Component Analysis (PCA) was applied to identify any potential differences between the two treatments (see Figure 8). Chemometrics is a valuable tool for highlighting differences in coatings over time and for discerning the individual contributions of components within the formulation during the aging process. This method has previously been used to study the degradation of the same coatings on inert supports. The results were consistent with traditional visual comparisons, enabling us to examine the decay and differentiate among the various formulations [22].

Figure 7 displays the score plot of the first principal component versus the second principal component for the tested specimens, with colours representing the different treatments. In this case, the various formulations, including the aged samples, remain distinguishable even when applied to patinated coupons, which demonstrates the effectiveness of the method.

PCA reveals that treatments with 5% w/w Paraloid® solutions (TA5 and TM5), both before (S1_x) and after wet-dry aging (S2_x), are positioned close to each other. This proximity indicates a high degree of similarity among the samples, suggesting that the treatments studied are stable over time. The stability over time of the treatments containing 5% w/w Paraloid® may be attributed to the more diluted solution, which allows the corrosion inhibitor to permeate the patina better, thereby providing enhanced protection. The TA5 treatment is particularly stable, further confirming that AEDTA is the most effective corrosion inhibitor of the two.

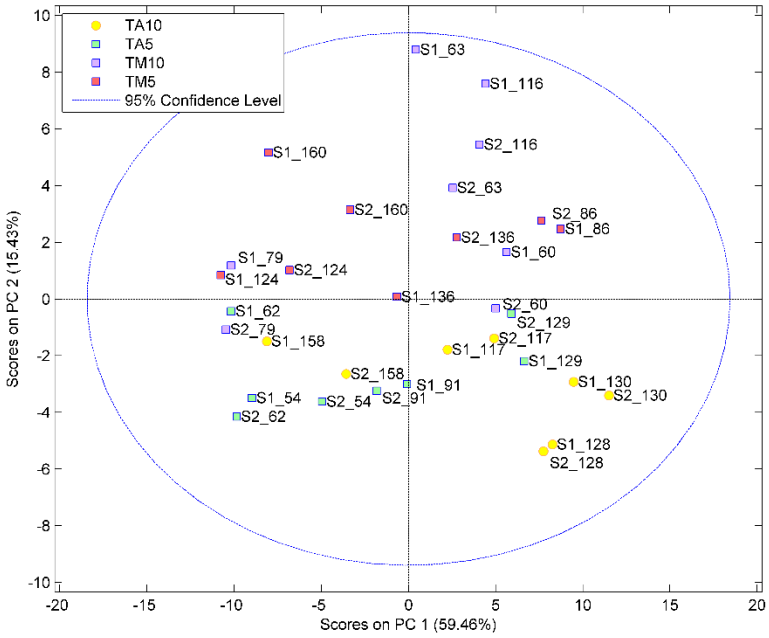

Figure 8: PCA results of the artificially aged coupons

8.5 Conclusions

In this paper we addressed the role of Paraloid® concentration in a two layer brush application method for acrylic coatings formulated with 5% w/w AEDTA or MPT sustainable corrosion inhibitors on quaternary bronze with *Verde Messina* patina. This highly reactive foundry patinated surface gives rise to a pretty wide spread in surface properties as systematically characterised by NdT, thus a proper attention should be paid to properly choose the groups of mock-ups for effectiveness comparison. Colour, thickness and EIS measurements proved valuable for an overall characterisation of aesthetic and chemical-physical evolution of surface properties upon coating application.

Treatments containing AEDTA, applied to patinated bronze (TA10 and TA5) provided slightly higher corrosion resistance with respect to the ones containing MPT (TM10 and TM5), along with a bit higher ΔE*, which aligns with previous results. From an aesthetic point of view, the slight darkening of the surface remained within an acceptable range. Both AEDTA and MPT-based treatments do

not show meaningful differences on the measured properties between applying a 10% w/w Paraloid® solution twice or a first layer with Paraloid® at 5% w/w and the second at 10% w/w.

After the thermo-hygrometric ageing, all the treatments proved to be stable: no colour changes or chemical modifications in the FTIR spectra were observed. However, the Principal Component Analysis revealed that treatments applied as 5% w/w Paraloid® solutions as a first layer were more stable than double-layer coatings with 10% w/w Paraloid®. In conclusion, TA5 resulted in the preferable treatment among the tested ones, as its performances are comparable to TA10 while using a smaller amount of Paraloid®. Future steps of the research include testing weathering performances in an urban marine environment to assess the efficacy of the coatings in more complex and realistic conditions.

8.6 References

[1] E. Bernardi, C. Chiavari, B. Lenza, C. Martini, L. Morselli, F. Ospitali, L. Robbiola, The atmospheric corrosion of quaternary bronzes: The leaching action of acid rain, Corros Sci 51 (2009) 159–170. https://doi.org/10.1016/j.corsci.2008.10.008.

[2] C. Petiti, L. Toniolo, L. Berti, S. Goidanich, Artistic and Laboratory Patinas on Copper and Bronze Surfaces, Applied Sciences (Switzerland) 13 (2023). https://doi.org/10.3390/app132111873.

[3] H. Otmačić Ćurković, T. Kosec, K. Marušić, A. Legat, An electrochemical impedance study of the corrosion protection of artificially formed patinas on recent bronze, Electrochim Acta 83 (2012) 28–39. https://doi.org/https://doi.org/10.1016/j.electacta.2012.07.094.

[4] B. Salvadori, A. Cagnini, M. Galeotti, S. Porcinai, S. Goidanich, A. Vicenzo, C. Celi, P. Frediani, L. Rosi, M. Frediani, G. Giuntoli, L. Brambilla, R. Beltrami, S. Trasatti, Traditional and innovative protective coatings for outdoor bronze: Application and performance comparison, J Appl Polym Sci 135 (2018). https://doi.org/10.1002/app.46011.

[5] E. Cano, D. Lafuente, Corrosion inhibitors for the preservation of metallic heritage artefacts, in: Corrosion and Conservation of Cultural Heritage Metallic Artefacts, Elsevier Ltd, 2013: pp. 570–594. https://doi.org/10.1533/9781782421573.5.570.

[6] A. Balbo, C. Chiavari, C. Martini, C. Monticelli, Effectiveness of corrosion inhibitor films for the conservation of bronzes and gilded bronzes, Corros Sci 59 (2012) 204–212. https://doi.org/10.1016/j.corsci.2012.03.003.

[7] M.T. Molina, E. Cano, B. Ramírez-Barat, Protective coatings for metallic heritage conservation: A review, J Cult Herit 62 (2023) 99–113. https://doi.org/10.1016/j.culher.2023.05.019.

[8] M.P. Casaletto, V. Figà, A. Privitera, A. Mazzaglia, A. Scala, R. Zagami, Sustainable corrosion inhibition of Copper-based alloys by smart β-Cyclodextrin/Benzotriazole complexes, in: Proceedings of the 5th European Cyclodextrin Conference, Lisbon, Portugal, 2017: pp. 3–6.

[9] M.P. Casaletto, C. Cirrincione, A. Privitera, V. Basilissi, A sustainable approach to the conservation of bronze artworks by smart nanostructured coatings, in: Metal 2016, Proceedings of the Interim Meeting of the ICOM-CC Metal Working Group, International Council of Museums Paris, France, 2016: pp. 144–152.

[10] M.T. Molina, E. Cano, B. Ramírez-Barat, Testing protective coatings for metal conservation: the influence of the application method, Herit Sci 11 (2023). https://doi.org/10.1186/s40494-023-00937-0.

[11] G. Masi, J. Esvan, C. Josse, C. Chiavari, E. Bernardi, C. Martini, M.C. Bignozzi, N. Gartner, T. Kosec, L. Robbiola, Characterization of typical patinas simulating bronze corrosion in outdoor conditions, Mater Chem Phys 200 (2017) 308–321. https://doi.org/10.1016/j.matchemphys.2017.07.091.

[12] P. Letardi, Testing New Coatings for Outdoor Bronze Monuments: A Methodological Overview, Coatings 11 (2021). https://doi.org/10.3390/coatings.

[13] G. Pellis, B. Giussani, P. Letardi, T. Poli, P. Rizzi, B. Salvadori, A. Sansonetti, D. Scalarone, Improvement in the sustainability and stability of acrylic protective coatings for outdoor bronze artworks, Polym Degrad Stab 218 (2023). https://doi.org/10.1016/j.polymdegradstab.2023.110575.

[14] H. Otmacic Curkovic, T. Kosec, K. Marušić, A. Legat, An electrochemical impedance study of the corrosion protection of artificially formed patinas on recent bronze, Electrochim Acta 83 (2012) 28–39. https://doi.org/10.1016/j.electacta.2012.07.094.

[15] E. Cano, A. Crespo, D. Lafuente, B. Ramirez Barat, A novel gel polymer electrolyte cell for in-situ application of corrosion electrochemical techniques, Electrochem Commun 41 (2014) 16–19. https://doi.org/10.1016/j.elecom.2014.01.016.

[16] A. Timoncini, E. Brattich, E. Bernardi, C. Chiavari, L. Tositti, Safeguarding outdoor cultural heritage materials in an ever-changing troposphere: Challenges and new guidelines for artificial ageing test, J Cult Herit 59 (2023) 190–201. https://doi.org/10.1016/j.culher.2022.12.003.

[17] H. Otmacic Curkovic, D. Mikic, L. Bera, E. Kovacevic, M. Marcelja, Electrochemical characterization of bronze exposed to outdoor atmosphere, Chem Biochem Eng Q 35 (2021) 165–176. https://doi.org/10.15255/CABEQ.2021.1926.

[18] L.B. Brostoff, Coating strategies for the protection of outdoor bronze art and ornamentation, Universiteit van Amsterdam Amsterdam, Netherlands, 2003.

[19] P. Letardi, Laboratory and field tests on patinas and protective coating systems for outdoor bronze monuments, in: METAL 2004. Proc. Interim Meeting ICOM-CC Metal WG, Camberra, Australia, 2004.

[20] B. Ramírez Barat, E. Cano, In Situ Electrochemical Impedance Spectroscopy Measurements and their Interpretation for the Diagnostic of Metallic Cultural Heritage: A Review, ChemElectroChem 5 (2018) 2698–2716. https://doi.org/10.1002/celc.201800844.

[21] R.F. Witzel, R.W. Burnham, J.W. Onley, Threshold and suprathreshold perceptual color differences, J Opt Soc Am 63 (1973) 615–625. https://doi.org/10.1364/JOSA.63.000615.

Chapter 9

Conclusions

An innovative non-hazardous protective coating for outdoor bronze artworks has been successfully formulated, along with a new system for encapsulating corrosion inhibitors that ensures long-lasting permanence over time. Additionally, a novel and easy-to-interpret chemometric approach has been developed to monitor and study the evolution of coatings.

The multi-analytical approach adopted throughout the research allowed a comprehensive study of the most relevant physical-chemical properties of the newly formulated coatings: transparency, absence of colour, homogeneity and integrity of the film, reversibility and stability.

The results obtained showed that Paraloid® B44 is stable under solar ageing. The 2-amino-5-ethyl-1,3,4-thiadiazol- (AEDTA) corrosion inhibitor emerged as a promising option, since it does not alter the colour of the coating over time and remains stable. When applied to polished bronze mock-ups, it tends to concentrate on the bronze surface and persist in the coating longer than other inhibitors, such as 5-mercapto-1-phenyltetrazole (MPT) and benzotriazole (BTA). Additionally, it was found that Tinuvin® 312 is more stable than Tinuvin® 5050. Therefore, the coating composed of Paraloid® B44 modified with AEDTA and Tinuvin® 312 demonstrated superior performance in terms of chemical and physical properties.

Due to the extensive dataset, a chemometric analysis was conducted and a straightforward methodology with a novel perspective on data analysis was developed, which confirmed the experimental findings obtained.

After that, attention was addressed to the problem of inhibitor retention in the coating. After literature review, cyclodextrins were selected as promising nanocontainers for anticorrosion inhibitors. The results showed that the permanence of the complexed AEDTA was enhanced, and the corrosion inhibitor lasted longer within the coating compared to free AEDTA and BTA.

Selected coatings were applied on bronze patinated coupons that reproduce reactive patinas on quaternary Cu-Sn-Zn-Pb bronze. A study of the application method and an evaluation of surface changes after the coating application were carried out. Protective performances were assessed through Electrochemical Impedance Spectroscopy. Results showed that all the coatings provide protection to the bronze substrate, with the best application method involving a more diluted first layer followed by a more concentrated second layer of Paraloid® B44. Before exposure to outdoor weathering, a thermo-hygrometric artificial ageing was conducted to verify that the coating properties remained unchanged after the application. Once again, the most promising coating was the one containing AEDTA and Tinuvin® 312.

The results from this research laid the groundwork for the InCARE (Innovative Multi-Analytical Characterisation of the Influence of Patina-Coating Interaction on Anti-Corrosive Properties) project. Specifically, the selection of the protective treatment and its application method were crucial to initiate studies on the stability and effectiveness of coatings exposed to outdoor weathering.

As highlighted in the introduction, the interaction with the atmosphere is complex, and various factors can influence the degradation of metallic Cultural Heritage. Artificial ageing was useful to study the stability of the coating under different exposure conditions and to select the most promising formulations and application method. Still, it is not able to reproduce the combined effect of all the degradation agents that act in a real environment, such as particulate matter (PM) or precipitation, and their synergistic action. For this reason, a selection of the coatings developed during my PhD have been applied to bronze-patinated mock-ups and exposed in a marine urban environment at GEMS (Genoa Experimental Marine Station) in December 2024. During the InCARE project, laboratory and especially portable techniques will be used to study the influence of the patina-coating interaction on the effectiveness of protective treatments. This will also allow the definition of effective evaluation protocols for anti-corrosion treatments on outdoor bronze artworks.

Some aspects were only partially explored during my PhD and require further investigation, particularly the detailed characterization of the interface between the patina and the coating. Nanoscale techniques, such as X-ray Photoemission Spectroscopy (XPS) and Focused Ion Beam Scanning Electron Microscopy (FIB-SEM), could provide interesting information. XPS would allow the analysis of chemical reactions occurring on surfaces, while FIB-SEM would provide in an in-

depth examination of the interface, thus addressing crucial issues such as the coating penetration, the detection of corrosion products, as well as the coating thickness and patina depth.

Appendix - Extra Activities and Collaborations

- **CAPuS Project**

Before beginning my PhD project, I won a scholarship within the Key Action 2 (Knowledge Alliances) of the **Erasmus+** Programme, **Conservation of Art in Public Spaces** (**CAPuS**) project. This project aimed to develop guidelines and protocols for the protection and conservation of contemporary public art, and to develop training opportunities for students and professional conservators alike.

This multidisciplinary project resulted in the publication of two papers during my first and second year of PhD, in collaboration with the "Centro Conservazione e Restauro la Venaria Reale" and the University of Vigo.

"A multi-analytical approach for precise identification of alkyd spray paints and for a better understanding of their ageing behaviour in graffiti and urban artworks" Pellis G., Bertasa M., Ricci C., Scarcella A., Croveri P., Poli T., Scalarone D.- Journal of Analytical and Applied Pyrolysis, vol 65, 2022 DOI: https://doi.org/10.1016/j.jaap.2022.105576

"Efficacy of Colour Protectors in Urban Art Paintings under Different Conditions: From a Real mural to the Laboratory" Alonso E., Rivas T., Pozo-Antonio J.S., Pellis G., Scalarone D. *Heritage*, Vol 6 (4), 2023 DOI: https://doi.org/10.3390/heritage6040185

- **Be-Archaeo Project**

During the beginning of the second year of the PhD I had the opportunity to take part to the EU funded 2020 Horizon Call **Beyond Archaeology (Be-Archaeo)** project. This project dealt with the archaeological excavation of the Tobiotsuka Kofun (Soja city in Okayama Prefecture) and challenging studies of other Kofun burial mounds and related archaeological material in ancient Kibi and Izumo area

(present Okayama and Shimane Prefectures, Japan), focusing on the rituals, the regional relationships and the formation of ancient state in Japan.

Thanks to this project, I attended the Okayama University, Japan from September to November 2022. My task was to characterize archaeological metals found during excavations using Optical Microscopy, X-ray fluorescence, and Tomography. This experience enriched my understanding of metal objects found in burial contexts, as well as the various corrosion processes that occur over time. I also gained expertise in employing the techniques previously mentioned, which further contributed to my background on non-invasive characterization of metal sherds.